Classical and Quantal Chaos in the Diamagnetic Kepler Problem

Hiroshi HASEGAWA, Marko ROBNIK* and Günter WUNNER**

Department of Physics, Kyoto University, Kyoto 606
**Institute for Theoretical Physics, University of California*
Santa Barbara, California 93106
***Lehrstuhl für Theoretische Astrophysik, Universität Tübingen*
D-7400 Tübingen

(Received December 12, 1988)

We review the studies of quantum systems of the hydrogen atom in a magnetic field in the language of "chaos" (both in the classical dynamical and the quantum mechanical sense) up to 1988 with an emphasis on 1) a clarification of Solov'ev's discovery of the approximate constant of motion in terms of the normal-form analysis, 2) features of numerical computations of spectra in comparison with experimental optical spectra in the chaotic regime, and 3) the rôle of unstable periodic orbits in the quasi-Landau resonances and their relation to "chaotic" eigenfunctions.

Contents

§ I. Introduction

The idea that the hydrogen atom in a uniform, static magnetic field would provide a prototype object of physical studies which may elucidate richness of chaotic dynamics, both in the classical and quantal regimes and also in the correspondence between them, occurred in several investigations around 1980 (representative works: Edmonds and Pullen,[1] Robnik,[2),2a)] Reinhardt and Farrelly,[3] Harada and Hasegawa.[4] It can be observed that behind this idea existed a motivation of analogy to the pioneering work by Hénon and Heiles[5] on classical nonlinear oscillators in 1964, which demonstrated for the first time the existence of regular and stochastic motions.[6]

The idea occurred, however, not abruptly: During the period between 1964 and 1980 the investigation of the diamagnetic hydrogen atom by means of its classical trajectories took place having a potential importance for this later development. The first significant contribution in this direction was the semiclassical quantization formula of the two-dimensional Kepler motion, ignoring the third motion along the magnetic field (or taking it into account adiabatically), which was proposed by Edmonds[8] for an interpretation of the quasi-Landau resonances, according to his own naming (Garton-Tomkins resonance discovered in 1969 for Ba and Sr[7]), and was led from the prior work by Hasegawa[9] in solid state physics. The new development towards chaos was inevitable in as much as it became indispensable to take into account the full three-dimensional aspect of the problem. It was necessitated, as a matter of experimental fact, from progress of spectroscopy in highly excited diamagnetic Rydberg atoms[10),11)] in search for the possible hidden dynamical symmetry which stimulated the first successful result by Solov'ev.[12] This success brought out a great significance of the theory of near-integrable dynamics, known as the KAM (Kolmogorov-Arnold-Moser) theory on invariant tori,[6] in that it indeed provided a prototype example of the normal form analysis by Robnik[13] showing how to construct such an invariant structure of the trajectories in phase space.

The above discovery of the symmetry in the weak-diamagnetic Kepler system was further supplemented by the purely quantum mechanical computation of the energy eigenvalues and eigenfunctions reported by Clark and Taylor[14),14a)] with thousands of Sturmian basis functions:[15] Their result showed the optical spectral profiles computed, demonstrating how the regularly structured quadratic Zeeman spectrum changes to irregularity which can be identified with "quantum" chaos. But, on the other hand also, a limitation was manifested because of their inability to fill the energy scale completely, leaving an interval of $40\,\mathrm{cm}^{-1}$ down from the ionization threshold just blank. The computations were taken up anew by the Tübingen group,[16] who used a different set of orthonormal complete basis functions and increased the number of basis functions up to 2×10^5, which enabled them to fill a substantial part of the above gap of the essential chaos, pushing the boundary of the theoretical computations up to the field-free ionization threshold $E=0$. By this improvement, they were able to complete the so-called correspondence diagram in the wavelength spectroscopy for astrophysical use[17] (a gauge for polarized optical radia-

tion from white dwarfs) and also to compare the computed spectra with finer experimental ones available since 1986—above all, with the one reported by the Bielefeld group[18] for the first time on the hydrogen atom. An emphasis of such fine computations must be laid, however, on the contribution to a statistical aspect, or fluctuation aspect, of the spectra in the framework of random matrix theory from the quantum chaos viewpoint.[19]

Since many things are thus involved for our review purpose, even if restricted to the recent developments, we must now fix the idea of constitution of this article with a length limited, and we choose the following subject matters: § II. Generalities of chaos in Hamilton dynamics, § III. Surface of section analyses in the diamagnetic Kepler problem, § IV. Transition from regular to chaotic spectra, and § V. Current topics.

We begin in § II with a brief review of the classic work of Hénon and Heiles as an elementary example of chaos and an explanation of the dynamical and deterministic origin of chaos with a focus on the almost integrable system as described by the KAM theory. We will also survey the basic ideas and problems of quantum chaos, and deal with the semiclassical quantization of such systems (Gutzwiller's version, in spite of its potential importance for the problem has to be dispensed with owing to a limitation of space). In particular, § II. 4 is devoted to the theory of the Birkhoff-Gustavson normal form, its classical development and a quantization method applicable to the regime of well-defined tori.

Section III, the central part of the present article, aims at a thorough treatment of the classical problem of surfaces of section, where the subjects are divided into a) magnetic-field scaling, b) analytic description of the invariant tori, c) presentation of the surfaces of section—both analytically and numerically and d) a feature of instability by means of computing Liapunov exponents. In § IV, we present our specific results on quantum (optical) spectra in comparison with the observed ones, discuss energy-level statistics, and examine a proposed interpolation formula of the level-spacings distribution which connects the Poisson and the GOE (Wigner) case. By the name of *current topics* we select, in § V, four subjects which are being investigated intensively both experimentally and theoretically: the structures of the quantum spectra in the classically *regular* regime—experiments by the Orsay group which substantiated the torus quantization of Solov'ev—, the interpretation of the appearance of resonances in the spectra in the classically *chaotic* regime in terms of unstable periodic orbits—in the wake of experiments by the Bielefeld group—, the *visualization* of eigenfunctions in the chaotic regime, and, in particular, the problem of "scarring" of the wavefunctions along unstable periodic orbits.

Still, one more subsection is devoted to a summarizing discussion and orientation about quantum chaos in the diamagnetic Kepler problem, which concludes the present review.

§ II. Generalities of chaos in Hamilton systems

II.1. *Basic concepts and examples*

It is one of the most important discoveries in classical mechanics and in science

in general that there exist simple, nonlinear and deterministic systems, which display chaotic behaviour, and whose motion cannot be predicted, not even in principle. *Simple* means that the underlying system has only a few degrees of freedom N, e.g. $N=2$. *Deterministic* means that the laws of motion are locally perfectly well known; they are given by the velocity vector field in the phase space. The evolution in time is described by ordinary differential equations, and in this way the past and the future of the given systems are uniquely determined by the initial conditions (present state). The motion as a function of time is obtained by finding the integral curves of the velocity vector field, i.e., by solving the differential equations. This is always possible for sufficiently short times, at worst by numerical integration; and yet for sufficiently long times the motion can be unpredictable. The reason for such chaotic motion is the instability of orbits which can separate exponentially. Thus the motion displays *sensitive dependence on initial conditions.* One consequence is that the number of correctly given digits of coordinates in phase space decreases linearly in time. Therefore our prediction of the state of the system will be completely wrong after a *finite* time. Thus the finite precision in measuring the initial state translates into logarithmically small times of the validity of our predictions. The exponential instability can lead to the type of motion which is as random as the outcomes of the coin tossing. In fact, there is a whole hierarchy of chaotic systems extending from the Bernoulli systems (most chaotic), mixing systems, ergodic systems, to the almost integrable systems (KAM systems). An ergodic system is defined by the property that it comes arbitrarily close to almost any point in the phase space as time goes on, infinitely often for almost all initial conditions. ("Almost all" means that the exceptions have measure zero.)

Regular motion results if the orbits "live" on a smooth manifold in phase space, and if they wind quasiperiodically or periodically without selfcrossing. This can occur in systems which possess global and smooth integrals of motion. The invariant manifolds on which the orbits "live" are the level sets of such constants of motion.

Typical systems display a transition from regular motion to the ergodic or ergodic-like regime of irregular motion as one of the system's parameters is varied. A classic example is the Hénon-Heiles system (Hénon and Heiles[5]) of two degrees of freedom defined by the Hamiltonian

$$H=\frac{1}{2}(p_x^2+p_y^2)+\frac{1}{2}(x^2+y^2)+x^2y-\frac{1}{3}y^3\,. \tag{II·1}$$

The Hamilton equations

$$\dot{x}=p_x\,,\qquad \dot{y}=p_y\,,\qquad \dot{p}_x=-x-2xy\,,\qquad \dot{p}_y=-y-x^2+y^2\,, \tag{II·2}$$

can easily be integrated numerically. Each orbit lies, of course, on the energy surface $H(x, p_x, y, p_y)=E=$constant. To reveal the geometry of orbits one introduces the Surface of Section (SOS) defined by

$$p_y=p_y(E;p_x, x, y)\,,\qquad y=0\,,\qquad p_y>0\,. \tag{II·3}$$

The *Poincaré map* on the SOS is simply defined by the image of an initial point on the

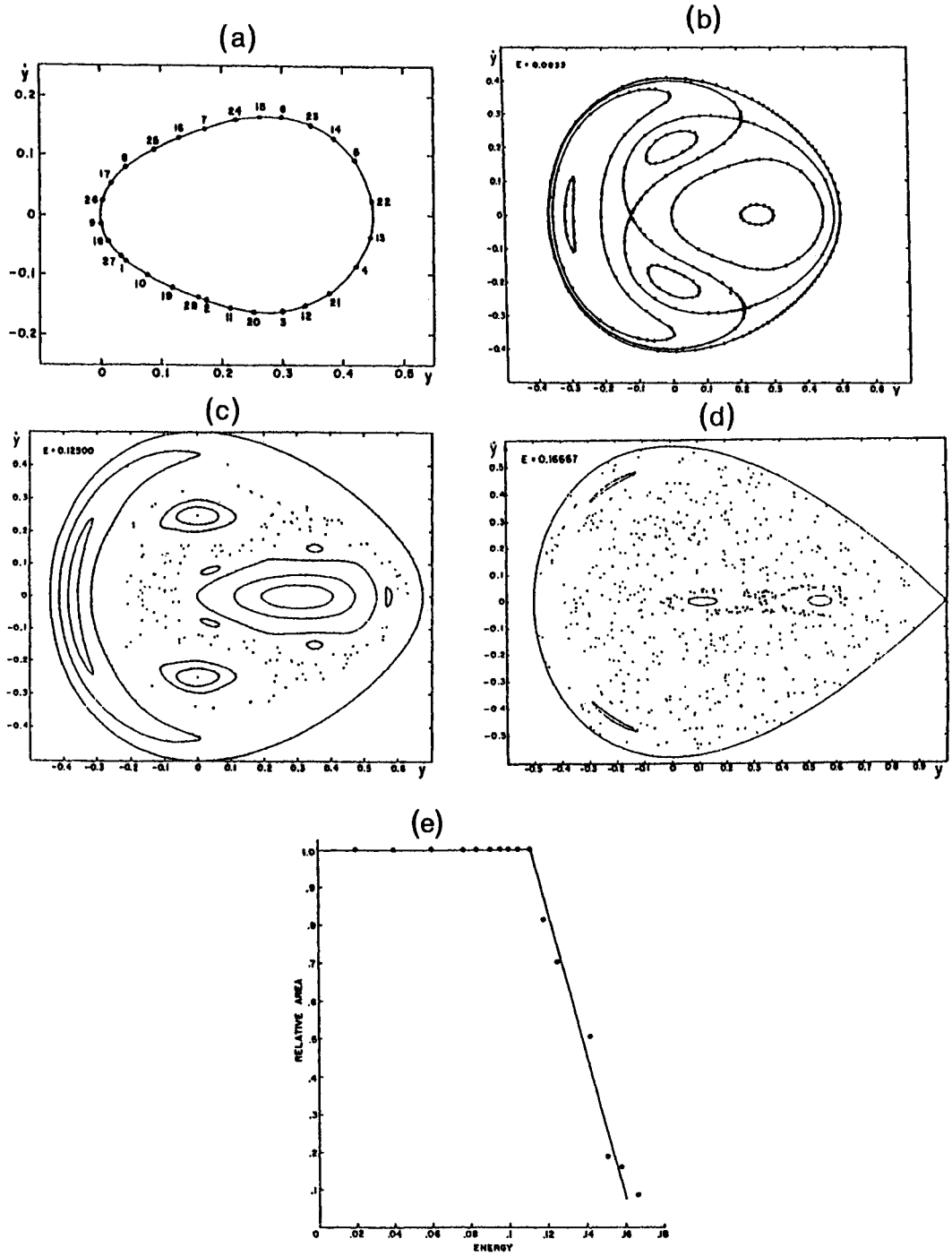

Fig. II-1. The Poincaré mappings on the SOS for the Hénon-Heiles system at different energies. In (e) the relative area of the regular regions versus the energy is plotted, displaying the sharp but nevertheless continuous stochastic transition. (Taken from Hénon and Heiles.[5])

SOS under the time evolution: Pick up an initial point on SOS, let it evolve in time until it returns to SOS; its crossing point with the SOS is defined as the image. As is well known the Poincaré map on the SOS is *area preserving*. If every orbit is bound to cross the SOS, then the Poincaré map contains complete information about the asymptotic behaviour of the orbits in phase space, and its study is thereby nicely reduced to the study of a two-dimensional area preserving map. As an orbit will repeatedly cross the SOS it will thus generate an (infinite) sequence of discrete points. These points can be well organized in the sense that they fill a smooth curve (invariant curve). This happens if there is an independent (of energy) integral of motion $A(x, p_x, y, p_y)$ restricting the orbits to a smooth invariant surface in phase space, which has the topology of a two-dimensional torus, so it is termed *invariant torus*. Figure II-1 shows that at low energies E most of the orbits do lie on invariant tori, whereas with energy increasing there are first some bifurcations of invariant curves appearing in the SOS, followed by a rapid increase of the area of chaotic (irregular) regions on the SOS. At high energy E the SOS has the appearance of an ergodic system. The chaotic motion in such irregular regions displays sensitive dependence on initial conditions. The chaotic orbits do not lie on a smooth invariant curve, and in fact seem to fill two-dimensional regions in the sense that they come arbitrarily close to any point in the region.

If one doubts the genuineness of such chaotic behaviour and suspects that the numerical noise (e.g., rounding-off errors and their propagation) is the actual source of chaos rather than some inherent dynamical properties, then the following study of an area preserving mapping (Rannou[20]) is a highly instructive proof of the deterministic dynamical origin of chaos. The *standard mapping* is defined by

$$x'=x+y \pmod{2\pi}, \qquad y'=y-a\sin x' \pmod{2\pi}, \qquad a=1.3. \tag{II·4}$$

A straightforward calculation of the Jacobi determinant shows that the mapping is area preserving, for the determinant is equal to unity. Its portrait (Fig. II-2(a)) shows generic aspects: Regions of regular motion are coexistent with the regions of irregular motion. Here the dynamics is defined by the iteration of the map. (There is nothing arbitrary about the study of area preserving maps, since every area preserving map can be associated with a Hamiltonian system). One can convince oneself that the two morphological types of orbit, the regular one and the irregular one, are indeed dynamical properties rather than being a consequence of external (numerical rounding-off) perturbations, by looking at the discrete analogy of the continuous standard mapping (II·4), namely,

$$x'=x+y \pmod{m}, \qquad y'=y-\left[a\frac{m}{2\pi}\sin\frac{2\pi x'}{m}\right] \pmod{m}, \qquad a=1.3, \tag{II·5}$$

which is a one-to-one mapping of a discrete grid of $m\times m$ points onto itself. The square brackets denote the rounding to the nearest integer. Since the mapping is one-to-one every point returns to itself no later than after m^2 iterations. Thus every orbit is a periodic orbit. Since the arithmetic is integer and exact there is no numerical noise. Nevertheless the orbits fall into two classes: The regular periodic

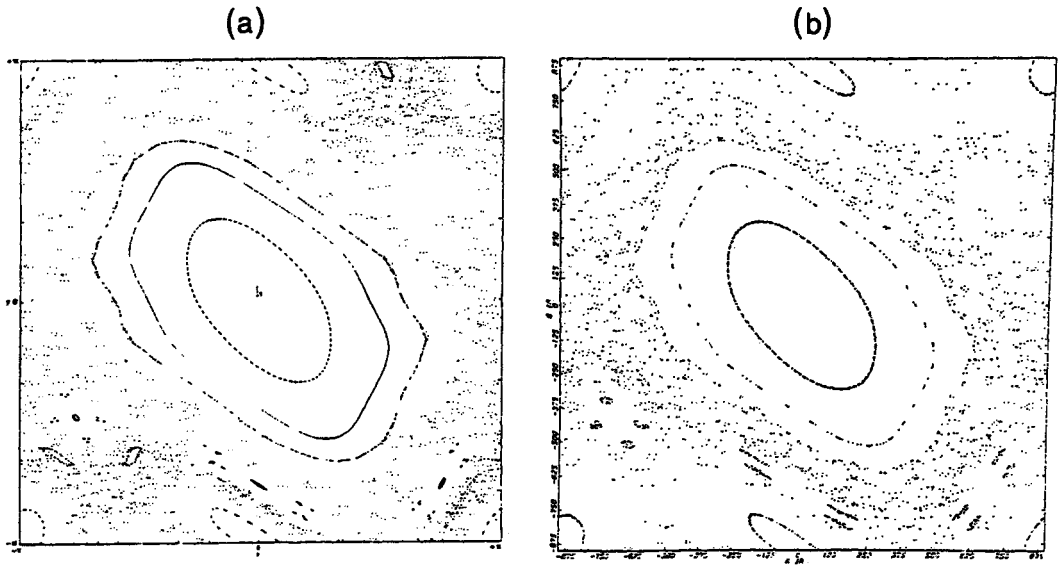

Fig. II-2. The phase portrait of the continuous (a) and of the discrete (b) standard mapping according to Rannou.[20] See text. (Taken from Hénon.[20a])

orbits seem to lie on a smooth curve and tend to fill it in the limit of large m, $m\to\infty$. The irregular periodic orbits seem to fill a two-dimensional region and do so in the ergodic sense in the limit of large m. This is shown in Fig. II-2(b) for $m=1800$ as a persuasive evidence for the dynamical and deterministic origin of chaotic behaviour. The irregular periodic orbits have periods of order m^2 in accordance with their ergodic-like behaviour within the chaotic region, whilst the regular periodic orbits have periods of order m, which is a consequence of the fact that they lie on smooth curves whose lengths scale linearly with m.

There are other exact models of nonlinear systems displaying chaotic behaviour. Without the precise definition of such an exact model of chaos, namely, Smale's horseshoe map,[21),22)] we would like to emphasize the importance of this system for the understanding of the origin of chaos: It is a repetition of the stretching and of the folding operations which gives rise to the exponential divergence of nearby trajectories. But we will not go into details. Instead, in the following subsections we will concentrate predominantly on the almost integrable motion in the regime described by the Kolmogorov-Arnold-Moser (KAM) theory, and shall review some less known methods such as the Birkhoff-Gustavson normal form[13),23)] for our purpose.

Before doing so let us briefly review the fundamental aspects of quantum chaos. The World is quantum mechanical in nature and as soon as we begin to study phenomena at the molecular, atomic or even nuclear level classical mechanics must be replaced by quantum mechanics. *The problem of quantum chaos* may be stated as follows. Are there any quantum phenomena such that, *firstly,* the name chaos is appropriate for them, and, *secondly,* they are related to the classical chaos of the corresponding classical Hamilton systems? The answer is definitely positive (Berry,[24)] Robnik,[2),25)] Bohigas and Giannoni,[19)] Casati et al.,[26)] Bohigas and Weidenmüller[27)]).

In classical chaos there are two major aspects. *The nonstationary aspects* concern the transient behaviour of classical dynamics, and embody such properties as sensitive dependence on initial conditions (positive Liapunov exponents). One should bear in mind that the spectrum of the evolution operator (the Liouville operator) is continuous in the case of chaotic motion, whilst it is discrete if the motion is regular, i.e., periodic or generally almost-periodic. *The stationary aspects* of classical chaos are defined by the asymptotic behaviour (dynamical properties for infinite times) and embody such properties as the geometry of the topologically transitive invariant sets, i.e., such sets that cannot be further decomposed into smaller invariant sets, and their bifurcations.

In quantum chaos, too, we have to distinguish between these two major aspects. In the dynamical *nonstationary* problem of evolving quantum states we encounter the difficulty that as long as purely bound systems are studied the spectrum of the evolution operator (Hamilton operator) is *always* discrete, and the evolution of the quantum states therefore is always almost-periodic. There is no sensitive dependence on initial conditions (any meaningful definition of Liapunov exponents in quantum mechanics would result in the conclusion that they are always exactly zero), no decay of correlations and the power spectrum of the autocorrelation functions is discrete. Nevertheless, it has been found that quite generally for times smaller than the so-called *break time* $t=\hbar/$(mean-level-spacing) the agreement with classical chaotic behaviour is good or at least satisfactory, but ultimately for times larger than the break time the discreteness of the spectrum shows up in the almost-periodic behaviour. Important systems in regard of this nonstationary aspect of quantum chaos are the kicked rotator and the hydrogen atom in microwaves, especially the question of microwave ionization of the atoms in highly excited states (Rydberg atoms) where the semiclassical and classical pictures become relevant and useful (de Broglie wavelength is small compared to the typical dimensions of the electronic motion). (See Casati et al.[26] and the references therein.)

The *stationary* problem in quantum chaos is concerned with the solutions of the stationary Schrödinger equation and corresponds to the stationary problem of classical chaos. The theoretical, computational and experimental work in studying *the properties of the energy spectra* (and of other observables) has led to the firmly established conclusion that the spectra of classically integrable quantum Hamilton systems generically exhibit Poisson statistics, while the classically ergodic systems exhibit the statistical properties of random matrix theories. The latter statement is the subject of the conjecture originally due to Berry[24] and Bohigas et al.[28] Theoretical arguments in support of the conjecture go back to the ideas by Dyson[29] and were further developed by Pechukas,[30] Yukawa[31] and recently by Wilkinson.[32] The role of antiunitary symmetries for the level statistics in classically ergodic systems has been explained by Robnik[33]: If there is an antiunitary symmetry (such as time reversal symmetry), then the Gaussian Orthogonal Ensemble statistics of random matrix theories applies, whereas the Gaussian Unitary Ensemble statistics applies if there is no such symmetry. Numerical evidence has been given by Bohigas, Giannoni and Schmit,[28] Seligman and Verbaarschot,[34] Berry and Robnik.[35] The mixed cases of generic systems (KAM-systems) have been studied by Robnik,[36] Berry and

Robnik,[37] Seligman et al., [38),39] Robnik,[40] Wintgen and Friedrich,[41] Hasegawa et al., [42] (also Wunner et al.[87]).

A surprise in the above research of quantum chaos was the finding that the statistics of random matrix theory apply not only to the spectra of sufficiently complex systems with many coupled degrees of freedom (ignorance motivated the statistical approach in the early development for nuclear levels) but also to relatively simple systems having a few degrees of freedom, provided that their classical dynamics is ergodic (knowledge of the statistical properties of the classical motion motivates the approach). Recent development of the formulation by Pechukas, Yukawa and others elucidate this question further (cf. Hasegawa[95]): By regarding the perturbations of a Hamilton matrix for a regular quantum system as the source of chaos for this system developing in a course of dynamics, i.e., by treating the perturbation parameter as *time* of dynamics, they show the way of introducing a natural ensemble of the Hamiltonian matrices obeying the same dynamics.

The problem of *the properties of the eigenfunctions* of (quantum systems whose classical counterparts are) classically chaotic systems has been the subject of increasing interest in recent years (Heller,[43),45] Robnik,[36] Heller et al.,[44] Robnik[22),46),47]). Briefly, the eigenfunction of a classically ergodic system is predicted to be roughly a superposition of a Gaussian random function and of the scars of the classically periodic orbits—regions of enhanced probability density. The first firm computational evidence and a theory of scars was given by Heller.[43] Since the existence of scars, e.g., in atomic systems has important observational consequences, we shall discuss this problem in the last section.

The hydrogen atom in a strong magnetic field is one of the current central topics in atomic physics (cf. Taylor [48]). It has been shown to be a classically chaotic system[1)~4] displaying a transition from the (almost) integrable motion at low energies and/or magnetic field strength to the ergodic-like behaviour at high energies and/or field strength. It is regarded as a paradigm of quantum chaos due to its elementarity and experimental importance, in the course which started in 1982 at the Aussois meeting.*) The progress since then was enormous calling for a review of the status, which is our motivation for writing the present article. The very recent experimental achievements in this regard emphasize the necessity for review and discussion.

II.2. *Integrable and almost integrable systems—KAM theory***)

The classical Kepler problem is a good textbook example of an integrable system. Owing to its supersymmetry there are many more integrals of motion than needed for integrability. By *integrable* we mean that there are at least N(N=the number of freedoms) global, analytical, single-valued and independent integrals of motion, being in involution, i.e., such that all Poisson brackets vanish. By the important theorem stated explicitly by Arnold[49] the integrability implies that each invariant surface in phase space (of $2N$ dimensions) must have the topology of the N-

*) The first statement that the irregular levels in the classically ergodic-like region computed by Clark and Taylor[14] can be identified with *quantum chaos* (in the sense of the stationary problem) was given by Robnik[2] at that meeting, and then by Harada and Hasegawa[4] on a quantitative basis (see Fig. II-5).

**) This is an extended version of a brief review offered in Robnik.[2]

dimensional torus (sphere with $N-1$ handles), the so-called *invariant torus*.

The phase space of an integrable system is thus filled everywhere with invariant tori. In absence of perturbations the motion is confined to an invariant torus, which justifies the attribute "stable system". It is then possible to use the topologically most natural canonically conjugate variables, namely, the action-angle variables. The actions I_j, $1\leq j\leq N$, are defined as the integrals $I_j=(1/2\pi)\int_{C_j}\boldsymbol{p}\cdot d\boldsymbol{q}$ along the irreducible circuits C_j on the torus (these are loops, which for topological reasons cannot be shrunk to a point by a continuous transformation), hereafter called "irreducible (or elementary) cycle". They label a given torus, while the position of a phase point on the torus is specified by the angles Θ_j, $1\leq j\leq N$, canonically conjugate to the actions I_j. The angle Θ_j changes by 2π along the closed irreducible cycle C_j. The Hamiltonian reads $H=H(\boldsymbol{I})$, so that the angles are cyclic variables by construction. The equations of motion

$$\dot{\boldsymbol{I}}=-\frac{\partial H}{\partial\boldsymbol{\Theta}}=0\,,\qquad \dot{\boldsymbol{\Theta}}=\frac{\partial H}{\partial\boldsymbol{I}}=\boldsymbol{\omega}(\boldsymbol{I})=\text{constant}\,, \tag{II·6}$$

can immediately be integrated to yield : $I_j=$constant, $\Theta_j=\omega_j t+$constant, showing that the motion on an invariant torus is quasiperiodic. A torus is called rational (also resonant) or irrational according to whether the frequencies $\omega_j=\partial H/\partial I_j$ are rationally connected or not. In the resonant case the motion is periodic.

Incidentally, for the Kepler problem all tori are resonant, since all frequencies depend only on the value of the total energy, and are thus equal, as is well known. Let us look more closely at the Kepler problem. The Hamilton function in spherical coordinates can be written

$$H=\frac{\boldsymbol{p}^2}{2m}+\frac{C}{r}=\frac{1}{2m}\left(p_r{}^2+\frac{p_\theta{}^2}{r^2}+\frac{p_\varphi{}^2}{r^2\sin^2\theta}\right)+\frac{C}{r}\,,\qquad C<0\,. \tag{II·7}$$

We have three actions

$$I_r=\frac{1}{2\pi}\oint p_r dr\,, \tag{II·8}$$

$$I_\theta=\frac{1}{2\pi}\oint p_\theta d\theta\,, \tag{II·9}$$

$$I_\varphi=\frac{1}{2\pi}\oint p_\varphi d\varphi\,. \tag{II·10}$$

The action I_φ is equal to the z-component of the angular momentum. The angular momentum $\boldsymbol{L}=\boldsymbol{r}\times\boldsymbol{p}$ is a constant of motion, and so is $\boldsymbol{L}^2$,

$$L^2=\boldsymbol{L}^2=p_\theta{}^2+\frac{p_\varphi{}^2}{\sin^2\theta}=\text{constant}\,. \tag{II·11}$$

From this follows

$$I_\theta=\frac{1}{2\pi}\oint d\theta\sqrt{L^2-\frac{p_\varphi{}^2}{\sin^2\theta}}\,. \tag{II·12}$$

This integral can be calculated conveniently using the substitution

$$z^2=\frac{L^2\sin^2\theta-p_\varphi^2}{\cos^2\theta}. \tag{II·13}$$

The integral (II·12) consists of four equal contributions $\int_0^\infty dz\cdots$, since $z=0$ corresponds to the turning point, whilst $z=\infty$ corresponds to $\theta=\pi/2$. The result is simple,

$$I_\theta=L-p_\varphi. \tag{II·14}$$

Finally, we calculate

$$I_r=\frac{1}{\pi}\int_{r_{\min}}^{r_{\max}}\frac{dr}{r}\sqrt{2mHr^2-L^2-Cr}=-\left\{L+\frac{C}{2\sqrt{-2mH}}\right\}. \tag{II·15}$$

The new Hamilton function

$$H=-\frac{C^2}{8m(I_r+I_\theta+I_\varphi)^2} \tag{II·16}$$

is degenerate in the sense that all three frequencies

$$\omega_{\text{Kepler}}=\omega_r=\frac{\partial H}{\partial I_r}=\omega_\theta=\frac{\partial H}{\partial I_\theta}=\omega_\varphi=\frac{\partial H}{\partial I_\varphi} \tag{II·17}$$

are equal, as has been claimed. Thus on each torus we have 1:1:1 resonance and consequently all orbits are periodic. This degeneracy is a consequence of the supersymmetry of the Kepler problem. We will show that there exists another conserved vector, namely, the so-called *Runge-Lenz vector*

$$\boldsymbol{A}=\boldsymbol{p}\times\boldsymbol{L}+mC\frac{\boldsymbol{r}}{r}. \tag{II·18}$$

Using $\dot{\boldsymbol{r}}=\boldsymbol{p}$ and $\boldsymbol{p}=C\boldsymbol{r}/r^3$ one shows

$$\frac{d\boldsymbol{A}}{dt}=0. \tag{II·19}$$

The Runge-Lenz vector has also the following three properties:

$$\boldsymbol{A}\cdot\boldsymbol{L}=0, \tag{II·20}$$

$$A^2=m^2C^2+2mHL^2, \tag{II·21}$$

$$\boldsymbol{r}\cdot\boldsymbol{A}=L^2+mCr. \tag{II·22}$$

Since $\boldsymbol{A}$ is perpendicular to $\boldsymbol{L}$, it lies in the orbital plane. We can use it as the reference line $\varphi=0$. Then one has trivially $\boldsymbol{r}\cdot\boldsymbol{A}=rA\cos\varphi$, which must be equal to (II·22) whence the elliptic orbits

$$r=\frac{L^2/mC}{1-(A/mC)\cos\varphi} \tag{II·23}$$

are derived without even solving a single integral.

The degeneracy of the Kepler problem is also reflected in the fact that the

periodic orbits can be embedded in different systems of tori. The problem is separable in two different coordinate systems (classically and quantum mechanically!), namely, the spherical coordinates and the parabolic cylindrical coordinates. If one is dealing with the perturbations of the Kepler problem, then the first job is to find out which tori are the unperturbed tori when the perturbation asymptotically vanishes. An important example is provided by the central object of our study in this work, namely the hydrogen atom in a strong magnetic field (the Diamagnetic Kepler Problem, DKP). It has been shown that this system is not integrable[1)~4)] and that at low energies and at low magnetic fields most of the Kepler tori do survive the diamagnetic perturbation, and that they can be described by the third choice of coordinates, namely, the elliptic cylindrical coordinates, which answers the question of the unperturbed tori as discussed in § III.2.

What happens to tori of an integrable system under a small perturbation has been a long-standing and most important question of classical mechanics. Some people like Landau thought that all systems are integrable, but that we are in almost all cases just unable to find the integrals. The opposite extreme was favoured by Fermi, who believed that integrable systems are exceptions (which is correct), and become ergodic when slightly perturbed (which is incorrect).

As a surprise came, then, a partial answer due to Kolmogorov, Arnold and Moser (*KAM Theorem*): All tori of the unperturbed integrable system $H_0(\boldsymbol{I})$ outside the resonant gaps survive a perturbation $H_0(\boldsymbol{I}) \to H_0 + \varepsilon V$. The resonant gaps are centered around the rational tori, and their width is determined by the inequality

$$\left|\sum_{j=1}^{j=N} k_j \omega_j\right| < K(\varepsilon)\left(\sum_{j=1}^{j=N} |k_j|\right)^{-a}, \qquad \text{(II·24)}$$

where $K(\varepsilon)$ is some constant vanishing when $\varepsilon \to 0$, being the same for all tori, while k_j are integer numbers. The volume of each gap is small with ε, and summing up the volumes of all gaps we still reach the same conclusion, since the series is convergent ($a > N-1$). This is the basis of the condensed formulations of the KAM theorem, such as "most tori survive", or "all sufficiently irrational invariant tori survive", although they may be slightly distorted (see Fig. II-3).

However, the KAM Theorem says nothing about the motion within the resonant gaps. No general predictions can be given, but there are examples for the persistence of even the rational invariant tori as demonstrated in the Hénon-Heiles system.[5)] But usually tori within the resonant gaps are destructed, resulting in a hierarchy of smaller and smaller tori embedded in the chaotic region.

It is difficult to predict what happens when a perturbation is applied. One indispensable concept and tool in such an analysis is the Poincaré mapping on the Surface of Section (SOS). When each orbit of given energy passes through the SOS, then the Poincaré mapping will give full information on the stability of motion. For example, when $N=2$, the irrational invariant tori will appear as a curve consisting of periodic points. Simple periodic orbits correspond to fixed points, while a chain of n periodic points is called n-cycle, and each point of the n-cycle is a fixed point of the n-th iterate of the Poincaré mapping. One important property of the Poincaré mapping is that it is area preserving, a direct consequence of the symplectic nature of

the Hamiltonian systems.

The stability analysis of the periodic orbits is then reduced to the stability analysis of the Poincaré mapping and of its iterates, i.e., the stability of the fixed points of some area preserving mapping T. A fixed point x_0 of an area preserving mapping T is said to be stable if for each neighbourhood U of x_0 there exists a subneighbourhood $V \subseteq U$ such that all iterates $T^k(V)$ lie in U. Putting the coordinate origin to x_0 and linearizing T, we find that its linear part M is a 2×2 unimodular matrix with constant real coefficients. Its eigenvalues are thus either complex conjugates λ, λ^* on the unit circle, or reciprocals λ, $1/\lambda$ on the real axis. They are determined by

$$\lambda^2-\lambda\mathrm{Tr}(M)+1=0\,. \qquad \text{(II·25)}$$

In the former case M describes elliptic rotation, the discrete motion being confined to ellipses ; x_0 is called an elliptic fixed point of T. In the latter case we have hyperbolic rotation, the motion being confined to hyperbolae on the same or interchanging branches, depending on whether the eigenvalues are positive or negative, respectively. A hyperbolic fixed point of T is unstable, and nearby orbits separate exponentially. An elliptic fixed point is stable (and the nearby orbits separate linearly) except in cases of low order resonances, i.e., in cases that the rotation angle of M is $2\pi/m$, $m=1, 2, 3, 4$, where the linear stability analysis is not sufficient.

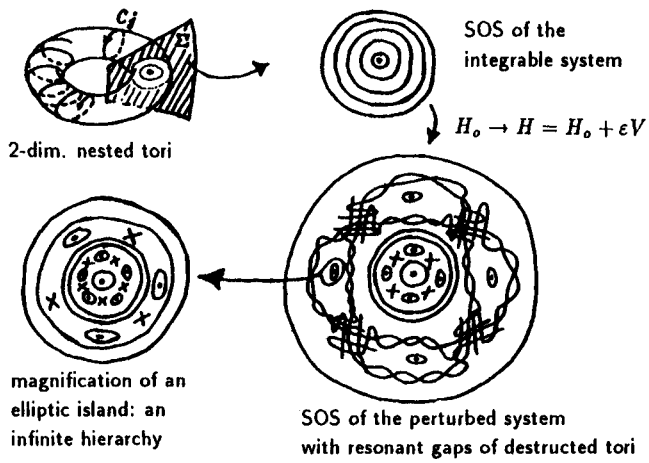

Fig. II-3. The scenario of the KAM theorem. (Taken from Robnik.[2])

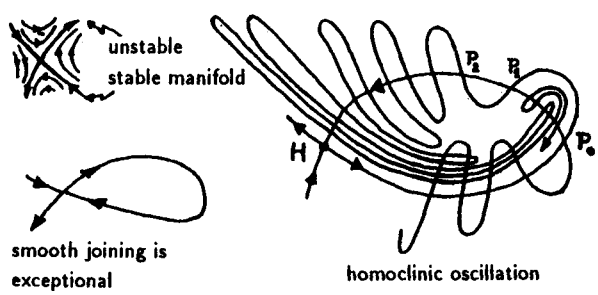

Fig. II-4. The homoclinic points. (Taken from Robnik.[2])

The stable elliptic islands surrounding the elliptic fixed points within the otherwise chaotic resonant gaps are sketched in Fig. II-3. How they come about upon a small perturbation of an integrable system is explained by the *Poincaré-Birkhoff theorem*: When an area preserving mapping has a simple closed invariant curve consisting of fixed points, then due to the KAM Theorem and the area preserving property, an even number of these fixed points is shown to survive a small perturbation. Half of them are elliptic, and the others are hyperbolic. The almost self-similar infinite hierarchy is explained by the fact that all considerations above are valid for any iterate of the Poincaré mapping.

It remains to understand how the chaotic motion can arise. This is connected with the hyperbolic points. All that has been done so far is the linearization around a hyperbolic fixed point. We shall concentrate on the asymptotes of the hyperbolae and the motion on them. We call them incoming or outgoing strand, according to whether M acts as a contraction or expansion, respectively (Fig. II-4). Actually, these linear parts can be extended into the nonlinear region of T, and are then called stable and unstable manifold, respectively. Now, the most important thing is how they meet each other. If they join smoothly, nothing special happens. But such a smooth joining is exceptional, since they will generically (i.e., in almost all cases) meet transversally at a point which is not a fixed point. When they do so, they will do it infinitely many times, as a little reflection shows. Moreover, due to the area preserving property of the mapping the amplitude of the oscillations will become larger and larger, so that an extremely complex motion arises, which has little in common with the regular integrable behaviour. Such an oscillatory motion is called homoclinic oscillation. It is a prototype of chaotic motion. Indeed, it can be shown that no smooth integral of motion exists for homoclinic oscillation (by embedding Smale's horseshoe mapping). We see that hyperbolicity+transversality imply chaotic motion. Since both occur in almost all cases upon a perturbation, we get a feeling that the type of motion within the resonant gaps, as shown in Fig. II-3, is of the generic type.

We can now understand the nature of the extreme of completely unstable systems, as opposed to the stable integrable systems: They must be full of hyperbolic periodic orbits. Indeed, an ergodic system can be and must be full of periodic hyperbolic orbits. They are dense in the phase space and their measure is zero. In a certain sense the periodic orbits, being all unstable, span the flow of even an ergodic system. This fact is not less surprising than the approximation of the real numbers by the rationals.

However, a generic Hamilton system is neither integrable nor ergodic, both extremes being exceptional. (We consider only systems with a few degrees of freedom. It should be noted that the ergodic systems are less exceptional than the integrable ones, since they are structurally stable: A small perturbation does not change the two fundamental properties, hyperbolicity and transversality). To be specific, a typical system displays all features of an integrable system at low energies. At some critical energy a rather sharp (but not discontinuous) transition, the so-called stochastic transition occurs: The invariant tori are observed to disappear rapidly as the energy is increasing, and the motion becomes irregular almost everywhere on the

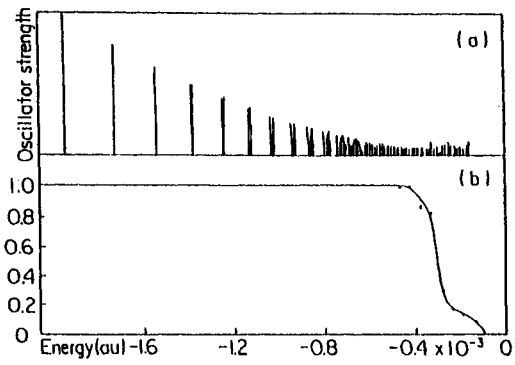

Fig. II-5. (a) The oscillator strengths for $\Delta m=0$ transitions from the ground state to the excited states of the diamagnetic H atom after Clark and Taylor.[14] (b) The relative area of the regular regions versus the energy. The hump near the chaotic boundary reflects the "remnant tori". (Taken from Harada and Hasegawa,[4] cf. Ref. 65).)

energy surface. When the motion is numerically integrated the best way to observe the transition from the regular to the irregular motion is by means of Poincaré mappings. But it is quite difficult to predict the critical energy. In § II. 1 we have discussed the classic example of Hénon and Heiles.[5] The case for the diamagnetic Kepler system is shown in Fig. II-5 according to Harada and Hasegawa[4] (see Fig. III-8 for a more precise result) where the transition is found to be not sharp.

II.3. *Semiclassical approach to quantization*

By the semiclassical quantization we mean in general methods of approximation that yield in a direct way approximate solutions to the Schrödinger equation that are correct in the leading term of $\hbar$, and become asymptotically exact as $\hbar \to 0$.

In the rare cases that a system is integrable we have the well-defined and well-known quantization conditions initiated by Einstein[50] and rigorously developed by Maslov and Fedoryuk.[51] The method is known under the names: tori quantization, topological quantization, Maslov quantization, Einstein quantization, Einstein-Brillouin-Keller (EBK) quantization, ···. It is just the quantization of the classical action,

$$I_j=\left(m_j+\frac{\alpha_j}{4}\right)\hbar\,, \tag{II·26}$$

where $m_j=0, 1, 2, 3, \cdots$, while α_j is the number of caustics encountered in the configuration space upon traversing the irreducible cycle C_j (the integration path to obtain the action I_j), and is called *Maslov index*. (See Fig. III-4 as an example: Both paths γ_α and γ_β have index 2). The (semiclassical) spectrum is then given by

$$E_m=H(\boldsymbol{I}_m)\,, \tag{II·27}$$

i.e., it is nothing but the value of the Hamiltonian taken at the quantized values of the classical actions (II·26).

It is easy to derive this.[22] First one should appreciate the little known fact that *in the semiclassical limit* when $\hbar \to 0$ the quantization (here meaning the association of classical variables and the quantal operators in disregard of product-ordering) commutes with the classical canonical transformations: Thus we can work in any coordinate system in the classical phase space without spoiling the semiclassical

validity of the results (see, e.g., Robnik[13),22)]).

Therefore we can work in the most natural coordinate system of an integrable system, namely, with actions and angles, which are the natural coordinates on the invariant tori filling the entire phase space. Therefore we use the prescription

$$\boldsymbol{I}=-i\hbar\frac{\partial}{\partial\boldsymbol{\Theta}}. \tag{II·28}$$

Since the Hamiltonian is by construction the function of the actions alone (i.e., the angles are cyclic variables) $H=H(\boldsymbol{I})$, so that $\boldsymbol{I}=$constant, one has trivially the result for the wave functions

$$\psi=\frac{1}{(2\pi)^{N/2}}\exp\left\{\frac{i}{\hbar}(\boldsymbol{I}\cdot\boldsymbol{\Theta}-Et)\right\}. \tag{II·29}$$

The above solution is the eigenfunction of the Hamiltonian (in the semi-classical approximation) if it satisfies the uniqueness requirement (single-valuedness), which implies

$$\boldsymbol{I}=\boldsymbol{I}_m=\boldsymbol{m}\hbar\,,\qquad m_j=0,\,1,\,2,\,3,\,\cdots, \tag{II·30}$$

so that the energy spectrum is

$$E_m=H(\boldsymbol{I}_m). \tag{II·31}$$

Now this is not yet the Maslov result (II·26), for it differs from the latter by the constant Maslov index terms; nevertheless its leading behaviour at high quantum numbers is correct!

To obtain the Maslov result (II·26) we have to go over into the common configuration space. We replace the exponent of the wave function (II·29) such that

$$\boldsymbol{I}\cdot\boldsymbol{\Theta}\rightarrow\text{classical action}=\int_{\text{on torus}}\boldsymbol{p}\cdot d\boldsymbol{q}=S(\boldsymbol{q},\boldsymbol{I}),$$

where the definition of the action and angle variables assures to write

$$\boldsymbol{I}\cdot\boldsymbol{\Theta}=S(\boldsymbol{q},\boldsymbol{I})\qquad \mod\left[\begin{array}{l}\text{periodic functions of }\boldsymbol{\Theta}\\ \text{with period }2\pi\text{ for every }\Theta_j\end{array}\right]. \tag{II·32}$$

Recall that $S(\boldsymbol{q},\boldsymbol{I})$ is the generating function, $\boldsymbol{\Theta}=\partial S/\partial\boldsymbol{I}$, whence

$$d^N\boldsymbol{\Theta}=\left|\mathrm{Det}\frac{\partial^2 S}{\partial\boldsymbol{I}\partial\boldsymbol{q}}\right|d^N\boldsymbol{q}. \tag{II·33}$$

Thus finally projecting (II·29) onto the q-space we obtain

$$\psi(\boldsymbol{q})=\frac{1}{(2\pi)^{N/2}}\sqrt{\left|\mathrm{Det}\frac{\partial^2 S}{\partial\boldsymbol{I}\partial\boldsymbol{q}}\right|}\exp\left\{\frac{i}{\hbar}(S(\boldsymbol{q},\boldsymbol{I})-Et)\right\}. \tag{II·34}$$

Strictly speaking, Eq. (II·32) is correct only for closed loops as only then the canonical invariance of the action integral $\int\boldsymbol{p}\cdot d\boldsymbol{q}$ is guaranteed, which in fact underlies the definition of the action-angle variables. Nevertheless, as *a rule of replacement* in going over from the $(\boldsymbol{q},\boldsymbol{p})$-representation to the $(\boldsymbol{I},\boldsymbol{\Theta})$-representation, Eq. (II·32) is certainly correct, and yields the correct torus quantization, as we will now show.

The requirement of single-valuedness must be satisfied again, so that by virtue of (II·32)

$$\frac{1}{\hbar}\Delta_j S-\alpha_j\frac{\pi}{2}=2\pi m_j\,, \tag{II·35}$$

where α_j is the Maslov index which stems from the pre-exponential of $\psi(\boldsymbol{q})$ and $\Delta_j S$ is the change of the action around the irreducible cycle C_j, and by definition is equal to $2\pi I_j$. Thus the condition (II·35) is the Maslov condition (II·26), and the resulting energy spectrum is given by the Maslov formula (II·27). The eigenfunctions are given by (II·34) evaluated at the quantized actions as given by (II·26, 27).

The morphology of the eigenfunctions will be discussed in § V.4.

II.4. *Birkhoff-Gustavson method of constructing invariant tori and a method of quantizing the normal form*

Suppose we are studying the motion of a classical Hamilton system near an equilibrium point. The system may have an arbitrary number N of degrees of freedom. Then, to the lowest approximation the motion is described by N uncoupled (one-dimensional) harmonic oscillators. However, they become coupled if the higher-order (anharmonic) terms in the Taylor expansion of the potential are taken into account. As a result of the coupling the system becomes non-integrable in almost all cases; in fact, being a generic system, it is neither integrable nor ergodic but shows a stochastic transition at the critical energy, such as in the Hénon-Heiles system. Above the critical energy which marks the sharp but nevertheless continuous stochastic transition the motion is chaotic on the entire energy surface (in phase space), but below that energy the motion has all features of regular integrable motion in the sense of the KAM regime of small perturbations, where the invariant tori still exist almost everywhere in the phase space the excluded stochastic gaps having the volume of order of a perturbation parameter.

We have then the difficult problem to predict analytically the KAM invariant tori, or equivalently, to construct the approximate integrals of motion. One of the possible methods is to calculate the normal form of the classical Hamiltonian. This was originally developed by Birkhoff for the nonresonant cases (no commensurability conditions for the frequencies of the harmonic oscillators), and consists of a series of canonical transformations, which are polynomial functions of coordinates and momenta. The algorithm is such that after $s-2$ transformations the new Hamiltonian is in normal form to degree s. By definition, this means that all monomials of order s in the power expansion of the Hamiltonian commute (Poisson brackets vanish) with the (unchanged) harmonic part of the Hamiltonian. In fact, all normal terms are just polynomials of the N actions. This formal procedure can be extended *ad infinitum* ($s\to\infty$), whereby one obtains a power expansion of the Hamiltonian as a function of the actions. Each of the N actions, when expressed in terms of the original coordinates and momenta, is itself a power expansion of an integral of motion. However, the series diverges: If the convergence radius of the series were non-zero, then the system would be rigorously integrable in some region of phase space, since the integrals of motion would be analytic there. But according

to the KAM Theorem a generic system is non-integrable, and we have thin gaps of irregular chaotic motion as described in § II.2, unless the system is accidentally rigorously integrable. The convergence radius of such series can generally never be made non-zero, whatsoever the method we use. Hence the name formal integral of motion.

Birkhoff's algorithm was generalized by Gustavson[23] to the resonant cases (see also Arnold[49]). The divergence difficulties of course still exist. But one should observe that while the infinite series has no rigorous meaning, the Hamiltonian in normal form *truncated* after the degree s is a rigorously integrable system that is close to the original system in the following sense: Its invariant tori are close approximations to the KAM invariant tori of the actual system, if they really exist. This fact can be used for the torus quantization. The method of calculating the normal form has been further developed by Robnik,[13] where also a new method of quantizing the normal form in an algebraic way has been proposed and tested on some systems such as Hénon-Heiles systems and the hydrogen atom in a magnetic field (Robnik and Schrüfer[52]), with success for low-lying levels. For the quantization of highly excited Rydberg states it is more practical to resort to the torus quantization.

The truncated normal Hamiltonian is also useful in the dynamical sense—in the sense of adiabatic invariants. Namely for sufficiently short times its trajectories follow closely those of the exact KAM system, whilst the asymptotic behaviour is not correctly described except for the motion on the exact KAM-tori. The quality of the approximations offered by the normal form Hamiltonian is the better the closer we are to the equilibrium point, i.e., the smaller the coupling between the N harmonic oscillators, i.e., the smaller the energy. Clearly, above the critical energy where the stochastic transition occurs, these formal integrals of motion lose their meaning completely, as the large scale invariant tori no longer exist. The only practical value might be in approximating the "cantori"*) —if they are strongly pronounced— and the adiabatic invariants and thereby the motion for short times if the chaos is not too strong (see an example provided by Hasegawa et al.[65] for the hydrogen atom).

Consider a Hamiltonian with N degrees of freedom in the form

$$H(x, y)=\sum_{j=2}^{\infty} H^{(j)}(x, y)\,, \tag{II·36}$$

where $x=(x_1, x_2, \cdots, x_N)$ are the coordinates, $y=(y_1, y_2, \cdots, y_N)$ the momenta, and

$$H_0(x, y)=H^{(2)}(x, y)=\sum_{k=1}^{N} \frac{\omega_k}{2}(x_k{}^2+y_k{}^2) \tag{II·37}$$

is the harmonic part of (II·36), with ω_k, $1\leq k\leq N$, being the oscillation frequencies. Each term $H^{(j)}$ in (II·36) is assumed to be a homogeneous polynomial of degree j, i.e.,

$$H^{(j)}(x, y)=\sum_{|k|+|l|=j} h_{kl}x^k y^l\,, \tag{II·38}$$

where h_{kl} are real constants, and we use the multi-indices like $k=(k_1, k_2, \cdots, k_N)$ with

*) A *cantorus* (plural *cantori*) has been defined and introduced by Aubry and by Percival in 1978/79 as the remnant of a broken invariant torus, being itself an invariant set but having the topology of the Cantor set rather than that of a smooth manifold (see MacKay et al.[121] and the references therein).

the definitions

$$|k|=|k_1|+|k_2|+\cdots+|k_n|\,, \qquad x^k\equiv {x_1}^{k_1}{x_2}^{k_2}\cdots {x_N}^{k_N}\,.$$

We say that there is an *rth-fold resonance* at the equilibrium point $(x, y)=(0, 0)$, if there are r linearly independent commensurability conditions between the frequencies, i.e.,

$$\sum_{k=1}^{N} a_{jk}\omega_k=0\,, \tag{II·39}$$

where $j=1, 2, \cdots, r$, and the rank of the real matrix a_{jk} equals r. The equilibrium point is said to be non-resonant if there are no rational connections (II·39).

We now define the normal form. The Hamiltonian (II·36) is in normal form to degree s if

$$D_{(x,y)}H^{(j)}(x, y)=0 \tag{II·40}$$

for $2\leq j\leq s$, where the partial differential operator

$$D_{(x,y)}\equiv\{H_0, \cdot\}=\sum_{k=1}^{N}\omega_k\left(x_k\frac{\partial}{\partial y_k}-y_k\frac{\partial}{\partial x_k}\right), \tag{II·41}$$

so that (II·40) is just the Poisson bracket $\{H_0, H^{(j)}\}$.

It is useful to introduce the quantities

$$\tau_k\equiv\frac{1}{2}({x_k}^2+{y_k}^2)\,, \qquad 1\leq k\leq N\,. \tag{II·42}$$

The following theorem is the main result of Gustavson.[23]

Theorem (*Gustavson*). If the Hamiltonian (II·36) is in normal form to all orders ($s=\infty$), and is represented by a formal series, then:

(a) For an rth-fold resonance we have $N-r$ independent formal integrals of the motion,

$$I_l=\sum_{k=1}^{N}\mu_{lk}\tau_k\,, \tag{II·43}$$

where μ_{lk}, $1\leq l\leq N-r$, are the independent solutions of the commensurability conditions (II·39), i.e.,

$$\sum_{k=1}^{N} a_{ik}\mu_{lk}=0\,, \qquad 1\leq i\leq r\,.$$

In this case the Hamiltonian (II·36) is itself an integral independent of the I_k's.

(b) In the non-resonant case we have N independent integrals $\tau_1, \tau_2, \cdots, \tau_N$, and the Hamiltonian (II·36) becomes a function of them, i.e.,

$$H=H(\tau_1, \tau_2, \cdots, \tau_N)\,. \tag{II·44}$$

Given a Hamilton system with the quadratic kinetic+potential energy, we can always shift the energy scale, shift and rotate the coordinate axes x_k, and stretch the coordinates and momenta in such a way that the Hamiltonian appears in the form

$$H(x, y)=H_0+\sum_{j=3}^{\infty} U^{(j)}(x)\,, \tag{II·45}$$

where

$$H_0=\sum_{k=1}^{N}\omega_k\tau_k \tag{II·45a}$$

is the harmonic part, while $U^{(j)}(x)$ are just the homogeneous polynomials of degree j arising from the Taylor expansion of the potential $U=U(x)$ around the equilibrium point $x=0$. The Hamiltonian (II·45) is thus a special case of (II·36): The anharmonic terms depend only on the coordinates x. Note that (II·45) is an even function of momenta.

The question now is whether the Hamiltonian (II·45) can be brought to the normal form by a canonical transformation $(x, y)\mapsto(q, p)$, so that $H(x, y)\mapsto\tilde{H}(q, p)$, where $q=(q_1, q_2, \cdots, q_N)$, $p=(p_1, p_2, \cdots, p_N)$ are new coordinates and momenta, respectively, and $\tilde{H}(q, p)$ is the normal form Hamiltonian. The answer is positive by theorem 1 in Gustavson's work.*)

Let $H(x, y)$ from (II·36) be in normal form to degree $s-1$. Then there exists a generating function

$$G^{(s)}(x, p)=xp+W^{(s)}(x, p)\,, \tag{II·46}$$

where $W^{(s)}(x, p)$ is a homogeneous polynomial of degree s, such that after the canonical transformation

$$q=x+\frac{\partial W^{(s)}(x, p)}{\partial p}\,,\qquad y=p+\frac{\partial W^{(s)}(x, p)}{\partial x}\,, \tag{II·47}$$

the new Hamiltonian $H(q, p)$ is in normal form up to degree s. To show this consider first the equality

$$H\left(x, p+\frac{\partial W^{(s)}}{\partial x}\right)=\tilde{H}\left(x+\frac{\partial W^{(s)}}{\partial p}, p\right). \tag{II·48}$$

From the power expansion of these expressions we see

$$H^{(j)}(\xi, \eta)=\tilde{H}^{(j)}(\xi, \eta)\,,\qquad 2\leq j\leq s-1\,, \tag{II·49}$$

where (ξ, η) stands for the arguments of the functions. In other words, those terms which are already in normal form are not affected by the transformation. The homogeneous polynomial $W^{(s)}(x, p)$ determining the generating function can be chosen in such a way that

$$\{H_0, \tilde{H}^{(s)}\}=D_{(q,p)}\tilde{H}^{(s)}(q, p)=0\,,$$

i.e., that $\tilde{H}$ is in normal form up to degree s. This can be seen by equating the terms of order s in (II·48), whence

*) Gustavson's result[23] on the formal integrals was summarized in his two theorems 1 and 2; the existence of the canonical transformation which brings the Hamiltonian into the normal form in every order, and the assurance of the $N-r$ formal integrals in case of the rth-fold resonance. This latter theorem is in our exposition in the text *Theorem* (a) and (b).

$$D_{(x,p)}W^{(s)}(x,p)=H^{(s)}(x,p)-\tilde{H}^{(s)}(x,p)\,. \tag{II·50}$$

By definition $H^{(s)}$ must be in the kernel of the partial differential operator $D_{(x,p)}$. Now since D is a linear operator, it allows a unique decomposition of the space of polynomials into a direct sum of the kernel $\mathcal{N}$ and the range $\mathcal{R}$. Accordingly, each polynomial can be uniquely decomposed into a sum of its $\mathcal{N}$-component and $\mathcal{R}$-component. To solve (II·50) we take $\tilde{H}^{(s)}$ to be the $\mathcal{N}$-component of an arbitrary additive polynomial from $\mathcal{N}$. To make $W^{(s)}$ unique we require, following Gustavson, that $W^{(s)}$ is in the range $\mathcal{R}$ of D.

Having obtained the solution for $\tilde{H}^{(s)}$ and $W^{(s)}$ we can calculate the remaining terms of the new Hamiltonian $\tilde{H}$ in the power expansion of (II·48). It turns out that for each $i=2, 3, 4,\cdots$

$$\tilde{H}^{(i)}(x,p)=H^{(i)}(x,p)+\sum\frac{1}{j!}\left[\frac{\partial^{|j|}H^{l}}{\partial p^{j}}\left(\frac{\partial W^{(s)}}{\partial x}\right)^{j}-\frac{\partial^{|j|}\tilde{H}^{l}}{\partial x^{j}}\left(\frac{\partial W^{(s)}}{\partial p}\right)^{j}\right], \tag{II·51}$$

where the summation over j is restricted by the conditions

$$l+|j|(s-2)=i\,,\qquad 1\leq|j|\leq l<i\,,\qquad l\geq 2\,,\qquad s\geq 3\,, \tag{II·51a}$$

and we use the multi-index notations

$$\begin{aligned}&j!\equiv j_1!\,j_2!\cdots j_N!\,,\\&\partial^{|j|}H^{(l)}/\partial p^{j}\equiv\partial^{|j|}H^{(l)}(x,p)/\partial p_1{}^{j_1}\partial p_2{}^{j_2}\cdots\partial p_N{}^{j_N}\,,\\&(\partial W^{(s)}/\partial x)^{j}\equiv(\partial W^{(s)}/\partial x_1)^{j_1}\cdots(\partial W^{(s)}/\partial x_N)^{j_N}\,.\end{aligned} \tag{II·51b}$$

One can see that for $i<s$ we get indeed (II·49), while for $i=s$ we recover Eq. (II·50). All terms $\tilde{H}^{(j)}$, $j>s$, can be then calculated successively by the formula (II·51).

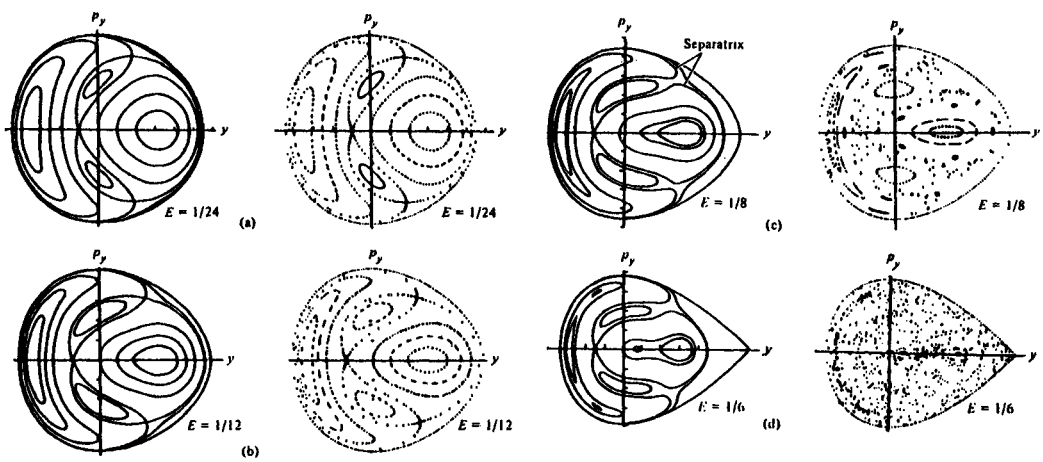

Fig. II-6. Comparison between the contours of the integral of motion (left) obtained by the Birkhoff-Gustavson procedure with the numerical ("exact") invariant curves (right) of the Hénon-Heiles system. (Taken from Lichtenberg and Lieberman.[6])

By the assumption $H^{(2)}(x, y)$ is already in normal form. Consequently, by a series of successive canonical transformations generated by $G^{(3)}$, $G^{(4)}$, $\cdots$, $G^{(s)}$, $\cdots$, we can calculate the normal form to an arbitrary degree.

The success of the Birkhoff-Gustavson procedure in approximating the rigorously existing KAM invariant tori is clearly demonstrated by the original work of Gustavson[23] on the Hénon-Heiles system with one-fold resonance of two degrees of freedom ($N=2, r=1$) (see Fig. II-6). Its lowest-order, nontrivial normal form involves polynomials up to fourth order in x and p, amenable to analytic treatment. By this we mean that, within this order of the normal form Hamiltonian and the other constant of the motion, the invariant tori can be traced by algebraic curves subject up to a quartic equation with which action integrations can be performed. The situation is the same for the diamagnetic Kepler problem, which is the basis of the torus quantization in § III and clarifies Solov'ev's procedure.[12]

The structure of the normal form has been further studied by Robnik.[13] The fact that the normal form can be always presented as in (II·61) is an important property of the normal form and a prerequisite for quantizing it. We will now review that work.

The following proposition can be easily proven.

Proposition (Robnik[13]) : If the Hamiltonian (II·36) is an even function of momenta, i.e., $H(x, y)=H(x, -y)$, and is assumed in normal form up to degree $s-1$, then the Hamiltonian $\tilde{H}(q, p)$ obtained according to the transformation (II·45 through II·51) is also an even function of momenta, i.e.,

$$\tilde{H}(q, p)=\tilde{H}(q, -p)\,.$$

A consequence is that for the Hamilton system (II·45), which has the usual form kinetic+potential energy, we find the result that its normal form to any degree s is an even function of momenta. This will be used later on.

In order to study the structure of the general normal form we now make a *non*-canonical transformation to the *complex* variables

$$z_k=\frac{\sqrt{2}}{2}(x_k+iy_k)\,, \qquad 1\leq k\leq N\,, \tag{II·52}$$

so that the coordinates and the momenta are

$$x_k=\frac{\sqrt{2}}{2}(z_k+z_k^*)\,, \qquad y_k=-\frac{i\sqrt{2}}{2}(z_k-z_k^*)\,, \tag{II·53}$$

where z_k^* is the complex conjugate of z. We see from (II·53) that $\tau_k=z_kz_k^*$ and with $\theta_k=\arg z_k$, we obtain

$$z_k=\sqrt{\tau_k}\,e^{i\theta_k}\,, \qquad 1\leq k\leq N\,. \tag{II·54}$$

It can be easily seen that the operator $D_{(x,y)}$ from (II·41) becomes

$$D=\sum_{k=1}^{N}\omega_k\frac{\partial}{\partial\theta_k}\,. \tag{II·55}$$

By definition the normal form (II·36) contains only polynomials from the kernel

$\mathcal{N}$ of the operator D. A basis of $\mathcal{N}$ can be most easily determined by using the complex variables (II·52). Inserting (II·53) into the normal form (II·36) yields the power series in complex variables z_k, z_k^*. But since (II·45) is an even function of momenta, so is its normal form (II·36), and all coefficients in the series are real. Since the series $H(x, y)$ is real-valued we conclude that if $z^m z^{*n}$ occurs in the formal series, then its complex conjugate $z^{*m} z^n$ must do so with the same real coefficients. Here we used again the multi-index notation $z=(z_1, z_2, \cdots, z_N)$, $m=(m_1, m_2, \cdots, m_N)$, etc.

The monomials $z^m z^{*n}$ in the kernel $\mathcal{N}$ of the operator D given in (II·55) are determined by

$$Dz^m z^{*n}=0\,,$$

whence

$$D=\sum_{k=1}^{N}\omega_k\frac{\partial}{\partial\theta_k}\,. \tag{II·56}$$

This condition implies that m_k-n_k, $1\leq k\leq N$, must be a linear combination of the rows of the commensurability matrix a_{lk}, $1\leq l\leq r$, given in (II·39). To simplify the expressions we assume that each row vector $(a_{l1}, \cdots, a_{ln})=a_l$ has integer components without a common factor. From (II·56) we obtain

$$m-n=\sum_{l=1}^{r}\gamma_l a_l\,, \tag{II·57}$$

where γ_l are non-negative numbers. Note that the integer vectors a_l can have negative components. It is not very convenient to write

$$z^m z^{*n}=\tau^n z^{\sum_{l=1}^{r}\gamma_l a_l}$$

because negative powers of z can appear in the second factor. Instead, we introduce the resonant monomials

$$K_l=\tau^{|a_l|/2}\exp(i\textstyle\sum_{k=1}^{N}a_{lk}\theta_k)=U_1^{|a_{l1}|}U_2^{|a_{l2}|}\cdots U_N^{|a_{lN}|}\,, \tag{II·58}$$

where

$$U_k=\begin{cases}z_k\,, & \text{if} \quad a_{lk}\geq 0\\ z_k^*\,, & \text{if} \quad a_{lk}<0\end{cases}\,. \tag{II·59}$$

It can be easily seen that $DK_l=0$, i.e., K_l, $1\leq l\leq r$, are constants of the motion of the harmonic part $H_0=\sum_{k=1}^{N}\omega_k\tau_k$. Writing

$$\gamma=(\gamma_1, \gamma_2, \cdots, \gamma_r) \qquad \text{and} \qquad K=(K_1, K_2, \cdots, K_r)\,, \tag{II·60}$$

we obtain the most general expression (Robnik[13])

$$H(x, y)=\sum_{\gamma}f_\gamma(\tau)(K^\gamma+K^{*\gamma}) \tag{II·61}$$

for the normal form (II·36), where $f_\gamma(\tau)$ is a real polynomial. The summation runs over all non-negative integers $\gamma=(\gamma_1, \cdots, \gamma_N)$ and $K^\gamma=K_1^{\gamma_1}K_2^{\gamma_2}\cdots K_N^{\gamma_N}$, etc. We see that the normal form is generally a function of the variables $\tau=(\tau_1, \tau_2, \cdots, \tau_N)$ defined

in (II·42) and $K=(K_1, K_2, \cdots, K_N)$, as defined in (II·58 through II·60). In the non-resonant case $r=0$, and H depends only on τ, which are thus the action variables.

In the same paper (Robnik[13]) the general fourth-degree normal form has been calculated for Hamilton systems with two degrees of freedom, which was still possible without using the computer algebra. The Hamiltonian is assumed in the form

$$\begin{aligned} H&=\omega_1\tau_1+\omega_2\tau_2+U^{(3)}(x_1, x_2)+U^{(4)}(x_1, x_2)\,,\\ U^{(3)}&=ax_1{}^3+bx_1{}^2x_2+cx_1x_2{}^2+dx_2{}^3\,,\\ U^{(4)}&=Ax_1{}^4+Bx_1{}^3x_2+Cx_1{}^2x_2{}^2+Dx_1x_2{}^3+Ex_2{}^4\,, \end{aligned} \tag{II·62}$$

where it is assumed $\omega_1/\omega_2\neq 1/2, 2$. Its fourth-degree normal form can be cast in the standard form (II·61), namely,

$$\begin{aligned} H=&\omega_1\tau_1+\omega_2\tau_2+g_{20}\tau_1{}^2+g_{11}\tau_1\tau_2+g_{02}\tau_2{}^2\\ &+(\gamma_1\tau_1+\gamma_2\tau_2)(K+K^*)+\gamma_3(K^2+K^{*2})\,, \end{aligned} \tag{II·63}$$

where

$$K=z_1z_2{}^*=\frac{1}{2}[(x_1x_2+p_1p_2)+i(p_1x_2+x_1p_2)]\,. \tag{II·64}$$

The $\omega_1/\omega_2=1$ resonance is the only one affecting the fourth-order normal form ($\omega_1/\omega_2\neq 1/2, 2$ has been excluded by the assumption — see (II·62). This would change already the third-order normal form). In this case γ_1, γ_2 and γ_3 (which should not be confused with the summation index γ in (II·61)) have to be determined with $\omega_1=\omega_2=\omega$, while in all other cases $\gamma_1=\gamma_2=\gamma_3=0$. The easiest way of finding the coefficients of normal form (II·63) is to use the complex variables. We distinguish between two cases. In all cases the third-degree term $\tilde{H}^{(3)}_{(x,p)}$ vanishes, while the fourth-degree term is written in the form

$$\tilde{H}^{(4)}(x, y)=\sum_{k+l+m+n=4} h(klmn)x_1{}^kx_2{}^ly_1{}^my_2{}^n\,. \tag{II·65}$$

The nonvanishing coefficients $h(klmn)$ are listed in Table II-1. There are 19 non-zero and 16 vanishing coefficients.

(a) *The non-resonant case and the higher-order resonances* ($\omega_1/\omega_2\neq 1/2, 2, 1$)
The result is

$$\begin{aligned} g_{20}&=\frac{3}{2}h(4000)+\frac{1}{2}h(2020)+\frac{3}{2}h(0040)\,,\\ g_{11}&=h(2200)+h(2002)+h(0220)+h(0022)\,,\\ g_{02}&=\frac{3}{2}h(0400)+\frac{1}{2}h(0202)+\frac{3}{2}h(0004)\,,\\ \gamma_1&=\gamma_2=\gamma_3=0\,. \end{aligned} \tag{II·66}$$

(b) *The lowest-order resonance* $\omega_1=\omega_2=1$.
The result can be given in a more explicit form

$$g_{20}=\frac{3}{2}\left(A-\frac{5}{2}a^2-\frac{5}{18}b^2\right),$$

$$g_{11}=C-\frac{2}{3}(b^2+c^2)-3(ac+bd)\,,$$

$$g_{02}=\frac{3}{2}\left(E-\frac{5}{2}d^2-\frac{5}{18}c^2\right),$$

$$\gamma_1=\frac{3}{4}\left(B-\frac{10}{3}b\left(a+\frac{1}{3}c\right)\right),$$

$$\gamma_2=\frac{3}{4}\left(D-\frac{10}{3}c\left(d+\frac{1}{3}b\right)\right),$$

$$\gamma_3=\frac{1}{4}(C-2(b^2+c^2)+ac+bd)\,. \qquad \text{(II·67)}$$

The Hénon-Heiles system is the special case of (II·62) when $\omega_1=\omega_2=1$ and $b=\lambda$, $d=\lambda\eta$, whilst all other coefficients of $U^{(3)}$ and of $U^{(4)}$ vanish. The result follows directly from (II·67),

$$g_{20}=-\frac{5}{12}\lambda^2\,,\qquad g_{11}=-\frac{2}{3}\lambda^2\left(1+\frac{9}{2}\eta\right),\qquad g_{02}=-\frac{15}{4}\lambda^2\eta^2\,, \qquad \text{(II·68a)}$$

$$\gamma_1=\gamma_2=0\,,\qquad \gamma_3=-\frac{1}{2}\lambda^2\left(1-\frac{1}{2}\eta\right). \qquad \text{(II·68b)}$$

Table II-1. The nonvanishing coefficients $h(klmn)$ determining the fourth-degree normal form as given in Eqs. (II·65) and (II·66).

$h(4000)=A-\frac{1}{2}(\omega_1 v_5^2+\omega_2 v_7^2)$	$v_1=2a/3\omega_1$
$h(0400)=-\frac{1}{2}(\omega_1 v_8^2+\omega_2 v_6^2)$	$v_2=2d/3\omega_2$
$h(0040)=-\frac{1}{2}(9\omega_1 v_1^2+\omega_2 v_9^2)$	$v_3=b/2\omega_1(1-\omega_2^2/4\omega_1^2)$
$h(0004)=E-\frac{1}{2}(\omega_1 v_{10}^2+9\omega_2 v_2^2)$	$v_4=c/2\omega_2(1-\omega_1^2/4\omega_2^2)$
$h(3100)=B-(\omega_1 v_3 v_5+\omega_2 v_4 v_7)$	$v_5=a/\omega_1$
$h(0031)=-(6\omega_1 v_1 v_9+2\omega_2 v_9 v_{10})$	$v_6=d/\omega_2$
$h(0013)=-2(\omega_1 v_9 v_{10}+3\omega_2 v_2 v_{10})$	$v_7=(\omega_1/\omega_2-\omega_2/2\omega_1)v_3$
$h(1300)=D-(\omega_1 v_3 v_8+\omega_2 v_4 v_6)$	$v_8=(\omega_2/\omega_1-\omega_1/2\omega_2)v_4$
$h(2200)=C-\frac{1}{2}(\omega_1 v_3^2+2\omega_1 v_5 v_8+\omega_2 v_4^2+2\omega_2 v_7 v_6)$	$v_9=\omega_1 v_3/\omega_2$
$h(2020)=\frac{1}{2}(4\omega_1 v_5^2+\omega_2 v_3^2-6\omega_1 v_1 v_5-2\omega_2 v_7 v_9)$	$v_{10}=\omega_2 v_4/\omega_1$
$h(2002)=\frac{1}{2}(4\omega_1 v_7^2+\omega_2 v_4^2-2\omega_1 v_5 v_{10}-6\omega_2 v_2 v_7)$	
$h(0220)=\frac{1}{2}(\omega_1 v_3^2+4\omega_2 v_8^2-6\omega_1 v_1 v_8-2\omega_2 v_6 v_9)$	
$h(0202)=\frac{1}{2}(\omega_1 v_4^2+4\omega_2 v_6^2-2\omega_1 v_8 v_{10}-6\omega_2 v_2 v_6)$	
$h(0022)=-(2\omega_1 v_9^2+3\omega_1 v_1 v_{10}+2\omega_2 v_{10}^2+3\omega_2 v_2 v_9)$	
$h(2011)=4\omega_1 v_5 v_7+\omega_2 v_3 v_4-2\omega_1 v_5 v_9-2\omega_2 v_7 v_{10}$	
$h(1102)=2\omega_1 v_4 v_7+2\omega_2 v_4 v_6-\omega_1 v_3 v_{10}-3\omega_2 v_2 v_4$	
$h(1120)=2\omega_1 v_3 v_5+2\omega_2 v_3 v_8-3\omega_1 v_1 v_3-\omega_2 v_4 v_9$	
$h(0211)=\omega_1 v_3 v_4+4\omega_2 v_8 v_6-2\omega_1 v_8 v_9-2\omega_2 v_6 v_{10}$	
$h(1111)=2\omega_1 v_3 v_7+2\omega_1 v_4 v_5+2\omega_2 v_3 v_6+2\omega_2 v_4 v_8-2\omega_1 v_3 v_9-2\omega_2 v_4 v_{10}$	

A method of quantization has been developed in the same paper (Robnik[13]). When it comes to quantizing the normal form one faces all the questions connected to the non-existence of a canonically invariant quantization scheme: The association between the classical variables and the quantum operators cannot be made invariant against the classical canonical transformations, so it does matter in which systems of classical variables one works. For the discussion the reader is referred to the original paper. Here we just summarize the final result of that theory, in the form of the following quantization prescription for the Hamilton operator corresponding to the normal Hamiltonian (II·61),

$$\hat{H}=\sum_{\gamma} f_{\gamma}(\hat{\tau})(\hat{K}^{\gamma}+\hat{K}^{*\gamma}), \tag{II·69}$$

where

$$\hat{\tau}_j=\hat{z}_j^{\dagger}\hat{z}_j+\frac{1}{2}\hbar \tag{II·70}$$

and

$$\hat{K}_l=\hat{U}_1^{|a_{l1}|}\hat{U}_2^{|a_{l2}|}\cdots\hat{U}_N^{|a_{lN}|}, \qquad \hat{U}_k=\begin{cases}\hat{z}_k, & \text{if} \quad a_{lk}\geq 0,\\ \hat{z}_k^{\dagger}, & \text{if} \quad a_{lk}<0,\end{cases} \tag{II·71}$$

and $\hat{z}_k$ and $\hat{z}_k^{\dagger}$ are annihilation and creation operators. Their action on the eigenstates of the harmonic operator $\hat{H}_0$ corresponding to the Hamiltonian $\hat{H}_0$ defined in (II·37) is

$$\hat{z}_k|n_1,\cdots,n_k,\cdots,n_N\rangle=\sqrt{\hbar n_k}\,|n_1,\cdots,n_k-1,\cdots,n_N\rangle, \tag{II·72a}$$

$$\hat{z}_k^{\dagger}|n_1,\cdots,n_k,\cdots,n_N\rangle=\sqrt{\hbar(n_k+1)}\,|n_1,\cdots,n_k+1,\cdots,n_N\rangle. \tag{II·72b}$$

The quality of this approximation is the same as in the semiclassical theories. The power of the method is the simple final result, which together with the use of Table II-1 enables one to immediately write down the spectrum of an arbitrary Hamiltonian of the form (II·62), etc. and of the more general ones ($N>2$) once the normal form has been calculated. In cases that there is no resonance the result is particularly simple: Each operator given in (II·70) is simply replaced by the number $(n_k+1/2)\hbar\omega_k$, because in such cases (II·69) does not depend on the operators $\hat{K}$ and is diagonal in the harmonic basis.

Example : Consider the Hamiltonian (II·62) with c and C being nonzero, while all other coefficients are assumed to vanish; the frequencies ω_1 and ω_2 are not in a low-order resonance, i.e., $\omega_1/\omega_2\neq 1/2,\ 2,\ 1$. Then the energy spectrum obtained by quantizing the normal form according to the method just described is given by

$$E_{n_1n_2}=\left(n_1+\frac{1}{2}\right)\hbar\omega_1+\left(n_2+\frac{1}{2}\right)\hbar\omega_2+\hbar^2\left[\left(n_1+\frac{1}{2}\right)\left(n_2+\frac{1}{2}\right)\times\right.$$
$$\left.\left(C+\frac{2\omega_2c^2}{\omega_1^2-4\omega_2^2}\right)-\left(n^2+\frac{1}{2}\right)^2\frac{c^2}{4\omega_1}\left(\frac{3\omega_1^2-8\omega_2^2}{\omega_1^2-4\omega_2^2}\right)\right] \quad n_1,\ n_2=0,\ 1,\ 2,\cdots. \tag{II·73}$$

This must be compared with the result of the exact nondegenerate quantum perturba-

tion theory, which differs from (II·73) only by a constant (i.e., independent of the quantum numbers) of order $\hbar^2$, namely,

$$E_{n_1 n_2}(\text{Robnik}) - E_{n_1 n_2}(\text{perturbation theory}) = \frac{3}{16} \frac{c^2 \hbar^2 \omega_1}{(\omega_1^2 - 4\omega_2^2)}, \qquad \text{(II·74)}$$

which emphasizes the high quality of the method especially at high quantum numbers, where the constant term (II·74) becomes negligible.

Another example, a case of the typical resonance $\omega_1/\omega_2=1$, is given by the Hénon-Heiles system, as discussed in detail in Robnik.[13] It was shown there that the present method gives the best result of all the available semiclassical procedures, at least for low-lying levels. This very method has been applied also to the diamagnetic hydrogen atom by Robnik and Schrüfer.[52] It is further dealt with in § III.2 in a satisfactory analytic representation which resolves the problem of the "unperturbed tori" to survive the diamagnetic perturbation.

§ III. Surface of section analyses in DKP

III. 1. *Scaling properties of diamagnetic Kepler systems*

A classical nonrelativistic Hamiltonian for atoms in a uniform magnetic field $\boldsymbol{B}$ satisfies a remarkable scaling property as regards the magnetic field strength. Namely, let its strength be measured in the unit

$$B_0 = m_e^2 e^3 c \hbar^{-3} = 2.35 \times 10^9 \text{ gauss}$$

(electronic Bohr magneton $\times B_0$ = Rydberg energy)

and be denoted by

$$\gamma \equiv B/B_0 . \qquad \text{(III·1)}$$

Express such a Hamiltonian function in terms of a set of cartesian coordinates $\{x_i\}$ and their momenta $\{p_i\}$ as well as of the parameter γ as $H(\{p_i\}, \{x_i\}\,;\,\gamma)$. Then

$$H(\{\gamma^{-1/3} p_i\}, \{\gamma^{2/3} x_i\}\,;\,\gamma=1) = \gamma^{-2/3} H(\{p_i\}, \{x_i\}\,;\,\gamma) . \qquad \text{(III·2)}$$

It says that the scaling of the coordinate and momentum variables by $\gamma^{-2/3}$ and $\gamma^{1/3}$, respectively, results in a scaling of the energy variable by $\gamma^{2/3}$ (thereby, all other subsidiary parameters, i.e., masses and charges being fixed).*)

One can immediately infer that another scaling exists: A scaling of the time variable consistent to the above, which must be by γ^{-1}. Its correctness can be seen indeed from two simple dimensional analyses; (a) $[time]\times[energy]=[action]$ and (b)$[time]\times$[momentum]=[mass]$\times$[length]. One accordingly infers the existence of

*) There are several other scaling relations proposed; Surmelian and O'Connell,[56] Wunner and Ruder[57] (charge and mass scaling), and Robnik[2a] (p_φ-scaling, where p_φ is the value of the angular momentum component parallel to $\boldsymbol{B}$). The last one is equivalent to (III·2), provided $p_\varphi \neq 0$.

a *moving unit system* related to this scaling —moving according to a variation of the field strength— which is useful for discussing dynamics, spectroscopy and so forth of diamagnetic atoms, because the scaling eliminates the variation. Such a unit system should be particularly useful for the spectroscopy near ionization threshold, because it utilizes the scaling by γ (i.e., the magnetic field strength) on the frequency domain that conforms to a choice of the familiar cyclotron frequency eB/m_ec.

The scaling equality (III·2) and hence the existence of the field-eliminating unit system mentioned above for diamagnetic atoms has been recognized very limitedly in spite of its basic character (the equality is not indicated in any established text-books of quantum mechanics to our knowledge), the utility now starting to be known gradually. We shall discuss some of this feature below and also in § V. The first explicit use of such a unit system was made, without mentioning the equality (III·2) however, by Gajewski :[53] He noted that a characteristic length l can be introduced by which, together with the cyclotron frequency, the classical equation of motion for the diamagnetic Kepler motion can be made B-independent. This length is given by

$$l=(m_ec^2B^{-2})^{1/3}=0.93\times10^{-2}B^{-2/3}\ \text{cm}$$
$$=[\text{Bohr radius}]\times\gamma^{-2/3}\,. \tag{III·3}$$

Let us write down the simplest diamagnetic Kepler Hamiltonian in the cylindrical coordinates (ρ, φ, z) to examine the scaling:

$$H=\frac{1}{2m_e}\left(p_\rho{}^2+\frac{p_\varphi{}^2}{\rho^2}+p_z{}^2\right)+\frac{e^2B^2}{8m_ec^2}\rho^2-\frac{e^2}{\sqrt{\rho^2+z^2}}+\frac{ep_\varphi}{2m_ec}B$$
$$\equiv H(p_\rho, p_z, \rho, z\,;\, p_\varphi, \gamma)\,,\qquad \gamma=B/B_0\,(\text{cf. III·1})\,. \tag{III·4}$$

In this representation, the scaling equality can be easily seen to become

$$H(\gamma^{-1/3}p_\rho, \gamma^{-1/3}p_z, \gamma^{2/3}\rho, \gamma^{2/3}z\,;\,\gamma^{1/3}p_\varphi, \gamma=1)$$
$$=\gamma^{-2/3}H(p_\rho, p_z, \rho, z\,;\,p_\varphi, \gamma)\,, \tag{III·5}$$

and, by the choice of Gajewski's unit (III·3) for length together with the unit $\gamma^{2/3}$ for energy, the Hamiltonian (III·4) becomes*)

$$\tilde{H}=\frac{1}{2}\left(\tilde{p}_\rho{}^2+\frac{\tilde{p}_\varphi{}^2}{\tilde{\rho}^2}+\tilde{p}_z{}^2\right)+\frac{1}{8}\tilde{\rho}^2-\frac{1}{\sqrt{\tilde{\rho}^2+\tilde{z}^2}}+\frac{\tilde{p}_\varphi}{2}\,, \tag{III·6}$$

where

$$(\tilde{\rho}, \tilde{z})=\gamma^{2/3}(\rho, z)\,, \tag{III·6a}$$

$$(\tilde{p}_\rho, \tilde{p}_z)=\gamma^{-1/3}(p_\rho, p_z) \tag{III·6b}$$

and

$$\tilde{p}_\varphi=\gamma^{1/3}p_\varphi\,. \tag{III·6c}$$

*) Another choice of the unit, i.e., $2l$ for length and $2m_ec/eB$ for time, leads to the following expression: $\tilde{H}=1/2(\tilde{p}_\rho{}^2+\tilde{p}_\varphi{}^2/\tilde{\rho}^2+\tilde{p}_z{}^2+\tilde{\rho}^2-1/\tilde{r}+2\tilde{p}_\varphi)$, which has been adopted by several authors.[62]

Also, the scaling of the Hamiltonian $H \to \tilde{H} = \gamma^{2/3} H$ implies that the scaled energy $\varepsilon \equiv \tilde{E}$ is related to the unscaled one as

$$E(=E(\gamma)) = \gamma^{2/3} \varepsilon \,. \tag{III·6d}$$

It suggests that the "determination of all the energies" for the fixed system (III·6) would suffice to solve the (quantum mechanical) spectral problem of an arbitrary diamagnetic Kepler system (III·4). It is too optimistic to think so, and before drawing any conclusion about such a possibility one must specify what is meant by the *determination*.

Within the context of classical mechanics, the determination of all the energies means to express the Hamiltonian as a function of the action variables, the number of which is equal to the degrees of freedom of the Hamiltonian: As to the explicit diamagnetic Kepler system (III·4) which is of two degrees of freedom after setting p_φ =const (=m; a constant of the motion), it means to find a canonical transformation

$$(p_\rho, p_z\,;\, \rho, z) \to (J_1, J_2\,;\, \varphi_1, \varphi_2)$$

with

$$H = H(J_1, J_2\,;\, p_\varphi = m, \gamma) \,. \tag{III·7}$$

In a strict sense this requires the integrability, and since the Hamiltonian (III·4) is not separable (verifiable *a posteriori* by the existence of chaos) the required integrability is satisfied only in the context of KAM theory and practically by the Birkhoff-Gustavson method as discussed in § II. It is then possible to apply the general scaling law (III·2) to such a transformed Hamiltonian in the following form:

$$\begin{aligned} &H(\gamma^{1/3} J_1, \gamma^{1/3} J_2\,;\, \gamma^{1/3} m, \gamma = 1) \\ &\quad = \gamma^{-2/3} H(J_1, J_2\,;\, m, \gamma) \,. \end{aligned} \tag{III·8}$$

An explicit derivation of this relation from (III·2)[54] is based on the existence of a set of well-defined two-dimensional two-tori parametrized by an assumed third constant of motion, imbedded in the four-dimensional phase space $(\rho, z\,;\, p_\rho, p_z)$ filling its allowed region, which assures two independent action variables J_1 and J_2. A full discussion of such a structure will be given in § III. 2. Here we show an extent of details for the special case of a *two-dimensional model* to bring out the utility of the scaling law.

A two-dimensional diamagnetic Kepler system is defined by setting $z=0$ and p_z $=0$ in the Hamiltonian (III·4):

$$H(p_\rho, \rho\,;\, p_\varphi, \gamma) = \frac{1}{2m_e}\left(p_\rho^2 + \frac{p_\varphi^2}{\rho^2}\right) + \frac{\gamma^2 e^2}{8a_B^3}\rho^2 - \frac{e^2}{\rho} + \frac{e^2}{2a_B} m\gamma \,, \tag{III·9}$$

where a_B is the Bohr radius given by $\hbar^2/m_e e^2$. Historically, this model played an important role for an understanding of the resonance peaks of optical spectra near the first ionization threshold of Ca and Sr atoms, also of alkali atoms, called now Garton-Tomkins resonances.[7] The scaling equality for this case reads:

$$E(\gamma^{1/3} J\,;\, \gamma^{1/3} m, \gamma = 1) = \gamma^{-2/3} E(J\,;\, m, \gamma) \,, \tag{III·10}$$

where the single action variable J is explicitly given in terms of E (constant value of the Hamiltonian) as well as m by

$$J=\frac{1}{\pi}\int_{\rho_1}^{\rho_2}\left[2\left(E'+\frac{1}{\rho}\right)-\frac{m^2}{\rho^2}-\frac{\gamma^2}{4}\rho^2\right]^{1/2}d\rho\,,\qquad E'=E-\frac{m}{2}\gamma\,. \tag{III·11}$$

Here, atomic units ($m_e=e=\hbar=1$) are used for simplicity. We note that one is dealing with a purely periodic motion, the period of which is calculated by

$$T=2\pi\frac{dJ}{dE'}=2\int_{\rho_1}^{\rho_2}\left[2\left(E'+\frac{1}{\rho}\right)-\frac{m^2}{\rho^2}-\frac{\gamma^2}{4}\rho^2\right]^{-1/2}d\rho\,. \tag{III·12}$$

The classical turning points ρ_1 and ρ_2 of such a periodic motion in these integrals are the two real zeroes of the square root there. For $m=0$, $\rho_1=0$ and the integration is made from 0 to $\rho_0(=\rho_2)$.

Hasegawa et al.[54] obtained the scaling law in the form of a scaling of the energy and the magnetic field strength individually with respect to the action variable J: There exists a universal function which relates the scaled energy to the scaled field for the two-dimensional model (III·9). For $m=0$, this scaling law reads

$$\epsilon=f(\beta)\,,\qquad \text{where}\qquad \epsilon=J^2E\qquad \text{and}\qquad \beta=J^3\gamma\,, \tag{III·13}$$

which is to realize Feneuille's conjecture[55] explicitly. To outline this result, it suffices to note a factoring of the square root of the action integrand in (III·11):

$$2\left(E+\frac{1}{\rho}\right)-\frac{\gamma^2}{4}\rho^2=\frac{1}{\rho_0}\frac{1-x}{x}(1+u(x+x^2))\,,\qquad x\equiv\frac{\rho}{\rho_0}\,,$$

where ρ_0 is the unique positive zero of the left-hand side in the above equation, and

$$u=\left(\frac{\rho_0}{2}\right)^3\gamma^2\quad\left(\text{or }\gamma=\left(\frac{2}{\rho_0}\right)^{2/3}u^{1/2}\right),\qquad E=\frac{1}{\rho_0}(-1+u)\qquad 0\le u<\infty$$

$$J=\left(\frac{\rho_0}{2}\right)^{1/2}\frac{2}{\pi}\int_0^1\left[\frac{1-x}{x}(1+u(x+x^2))\right]^{1/2}dx\,.$$

These establish a parameter representation of ϵ and β as follows:

$$\epsilon=\frac{u-1}{2}\{\Phi(u)\}^2\equiv G(u)\,, \tag{III·14a}$$

$$\beta=u^{1/2}\{\Phi(u)\}^3\equiv F(u)\,, \tag{III·14b}$$

where

$$\Phi(u)=\frac{2}{\pi}\int_0^1\left[\frac{1-x}{x}(1+u(x+x^2))\right]^{1/2}dx\,. \tag{III·14c}$$

Thus, Feneuille's universal function f in (III·13) is given by $f(x)=G\circ F^{-1}(x)$. We note that the form (III·13) implies the previous form (III·10) with $m=0$, and vice versa. This can be seen by identifying $E(J\,;\gamma)=J^{-2}f(J^3\gamma)$ so that both scaling laws are identical.

As to the formula of period T(III·12) for $m=0$, one can get

$$\frac{dJ}{dE}=\frac{2}{\gamma\pi}\int_0^1\left[\frac{ux}{(1-x)(1+u(x+x^2))}\right]^{1/2}dx\,, \tag{III·15}$$

which shows that the scaling of time is by γ^{-1}. From the parameter representation of energy (III·14a), the ionization threshold $E=0$ can be seen to correspond to $u=1$, for which the above integral yields

$$\frac{2}{\pi}\int_0^1\left[\frac{x}{1-x^3}\right]^{1/2}dx=\frac{2}{3\pi}\int_0^1\xi^{1/2-1}(1-\xi)^{1/2-1}d\xi=\frac{2}{3}\,,$$

showing that

$$\frac{2\pi}{T}=\frac{3}{2}\gamma\,, \tag{III·16}$$

i.e., the Garton-Tomkins frequency.[58]

The extension of these analyses to $m\neq0$ cases is more intricate but still feasible to an extent to show the scaling law[54] as well as to compute the resonance frequency.[59] Experimental situations often require $m\neq0$ analyses but, fortunately, only with its small integer values. Optical spectra near ionization threshold represent the situation of considerably high principal quantum number n, $\gamma^{1/3}n\approx1$, which satisfies, in the present terminology, $J\gg|m|$. Under such circumstances, the corrections to the formulas discussed so far due to $m\neq0$ can be often ignored. One of good examples to show that the correction is indeed small was provided by the n vs $\gamma^{-1/3}$ plot of the Garton-Tomkins peaks in Cs atoms given by Gay, Delande and Biraben[60),60a)] with a comparison of the plot to a theoretical prediction, as shown in Fig. III-1. We note that this prediction can be deduced fully from (III·14), as outlined below.

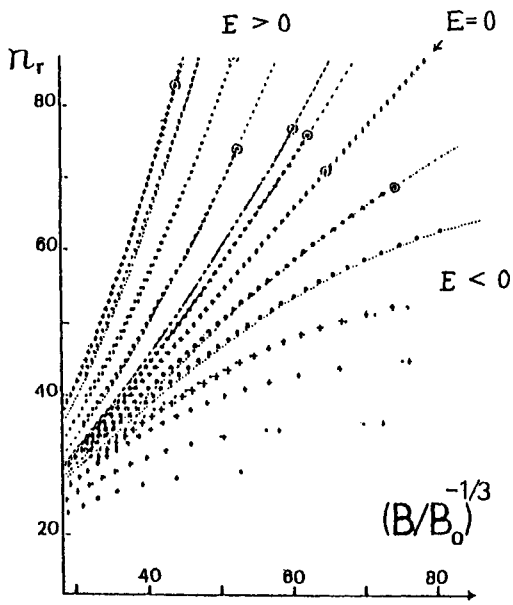

Fig. III-1. Experimental and theoretical plots of the radial quantum number against $(B/B_c)^{-1/3}$ $(=\gamma^{-1/3})$ at various energies for the dominant series of the spectrum of Cs (after Gay et al.[60]) Theoretical points expressed by crosses and broken curves were computed by the formula (III·11) with $m=3.5$ ($|m|=3$ is the actual Cs experimental value), but can be well reproduced by (III·17) (unpublished work by S. Adachi).

The above-mentioned n vs $\gamma^{-1/3}$ plot in Fig. III·1, if $m=0$ allowed, must be deduced by converting (III-14a, b) into a relation of J vs $\gamma^{1/3}$, in which the energy E is regarded as a parameter: $J=\Psi(\gamma^{-1/3};E)$. Note that for high values of the principal quantum number n the continuous variable J may be set just equal to n. We show that the function Ψ can be constructed explicitly as follows:

$$J=\gamma^{-1/3}[1+\phi(2E\gamma^{-2/3})]^{1/6}\Phi[1+\phi(2E\gamma^{-2/3})]\,, \tag{III·17}$$

where $\phi(x)$ is a real root of

$$\phi^3-x^3\phi-x^3=0\,. \tag{III·17a}$$

Since the latter equation shows $\phi(0)=0$, which corresponds to the ionization threshold $E=0$, the J vs $\gamma^{-1/3}$ curve represents a straight line:

$$J=\gamma^{-1/3}\Phi(1)=\gamma^{-1/3}\times 1.159\cdots\,. \tag{III·17b}$$

$$\left(\Phi(1)=\frac{2}{\pi}\int_0^1\left[\frac{1-x^3}{x}\right]^{1/2}dx=\frac{2}{3\pi}B\left(\frac{3}{2},\frac{1}{6}\right)\text{ where }B(x,y)\text{ is the beta function}\right).$$

More in detail, since the function $\Phi(u)$ is a very smooth, increasing function of u for $0\leq u\leq 4$; with $\Phi(0)=1$ and $\Phi(4)=1.5$,[54] the demonstrated feature for $E\gtrless 0$ in Fig. III-1 can be seen easily by noting $\phi(x)\gtrless 0$ for $x\gtrless 0$. Finally, (III·17) and (III·17a) can be deduced from (a) $J=\gamma^{-1/3}u^{1/6}\phi(u)$ by rewriting (III·14b), and from (b) $(u-1)^3-x^3u=0$ with $x=2E\gamma^{-2/3}$, as is obtained easily by the elimination of Φ from the two parameter representations (III·14a, b).

In § V.3 we shall see another interesting application of the scaling laws for the more general class of resonances near the ionization threshold, which has been studied by the Bielefeld group:[61] The resonances can be classified according to groups of (unstable) periodic orbits indexed by the single integers 1, 2,$\cdots$, the first one ((I_1)) corresponding just to the two-dimensional model (planar periodic orbit) and the rest (I_2), $(I_3)\cdots$ to those of generally three-dimensional structure (non-planar ones), for which the two equivalent relations between E, J and γ hold such that (III·17) or (III·13) can be extended. In particular, Feneuille's scaling relation (III·13) can be extended in terms of a set of universal functions from $f(=G\circ F^{-1})\equiv f_1$ to f_2, f_3 and so forth with a simplified construction of the f-functions (see §§ III. 3, 4 and V.2, 3).

III. 2. *Analytic description of invariant tori in the weak diamagnetic limit*

Our concern in this subsection will be the diamagnetic Kepler system (III·4) with the field-dependent term as a perturbation to lowest order. Hence throughout this subsection atomic units are used to write

$$H=\frac{1}{2}\left(p_\rho{}^2+\frac{m^2}{\rho^2}+p_z{}^2\right)+\frac{\gamma^2}{8}\rho^2-\frac{1}{\sqrt{\rho^2+z^2}}\,, \tag{III·18}$$

(the constant Zeeman energy is omitted)

whose structure of invariant tori will serve for analyses of chaos in the sequel.

2.1. Birkhoff-Gustavson normal form to lowest order

We need a special coordinate system by which the Kepler motion can be described as two harmonic oscillators uncoupled when $\gamma=0$. The well-known parabolic coordinate must be relevant and was used to study chaos first by Edmonds and Pullen[1] and then followed by several authors.[3),52),99),100)] Application of the Birkhoff-Gustavson

procedure in terms of this coordinate was first made by Reinhardt and Farrelly,[3] only by a graphical demonstration however, a fully systematic construction that followed is due to Robnik and Schrüfer,[52] who applied a general method of Robnik[13] (see § II. 4).

There are many choices of such parabolic coordinates referring to the starting cylindrical one, but there exists a unique choice that makes the free Kepler motion fully separate: $(\rho, z)\to(u, v)$

$$\rho=uv\,, \qquad p_\rho=\frac{1}{u^2+v^2}(vp_u+up_v)\,, \tag{III·19}$$

$$z=\frac{1}{2}(v^2-u^2)\,, \qquad p_z=\frac{1}{u^2+v^2}(-up_u+vp_v)\,. \tag{type I}$$

The Hamiltonian (III·18) for $\gamma=0$ is then

$$H=\frac{1}{2(u^2+v^2)}\left(p_u{}^2+\frac{m^2}{u^2}+p_v{}^2+\frac{m^2}{v^2}-4\right).$$

Introduce a *regularized* Hamiltonian

$$\mathcal{H}=(u^2+v^2)(H-E)+2\ . \tag{III·20}$$

Then

$$\mathcal{H}=\frac{1}{2}\left(p_u{}^2+(-2E)u^2+\frac{m^2}{u^2}\right)+\frac{1}{2}\left(p_v{}^2+(-2E)v^2+\frac{m^2}{v^2}\right)$$

for $\gamma=0$, and for $\gamma\neq0$ with an additional term

$$+\frac{\gamma^2}{8}u^2v^2(u^2+v^2)\,. \tag{III·21}$$

Note that the regularization by a multiplication of the factor $u^2+v^2(=2r)$ amounts to a change of time.[3] Therefore, for $m=0$, the unperturbed ($\gamma=0$) Hamiltonian with negative energy expresses two uncoupled harmonic oscillators with the same frequency $\omega=(-2E)^{1/2}$: It meets the case of the $\omega_1/\omega_2=1$ resonance for two degrees of freedom in the general formulation,[13] where the normal Hamiltonian admits a formal expansion

$$\sum_{\nu=0}f_\nu(\tau_1, \tau_2)(K^\nu+K^{*\nu})\,, \qquad K=a_1a_2{}^*\,, \qquad \tau_i=a_i{}^*a_i\,, \qquad (i=1,2) \quad \text{(cf. § II. 4)}$$

in terms of the 'annihilation and creation operators' a_i, $a_i{}^*$'s [i.e., $a_i=(1/\sqrt{2})(\omega^{1/2}q_i+i\omega^{-1/2}p_i)$, $a_i{}^*=(1/\sqrt{2})(\omega^{1/2}q_i-i\omega^{-1/2}p_i)$ in the classical sense] associated with the two free oscillators. Robnik and Schrüfer[52] carried out the expansion up to 14-th order, i.e., $O(\gamma^6)$ for (III·21) with $m=0$.*)

*) For general $m\neq0$, the B-G procedure can be extended to a system of four oscillators subject to a constraint, which establishes the full approximate constant of Solov'ev, $\Lambda(\boldsymbol{A})$ (M. Kuwata's result[67]).

As far as the restriction $m=0$ is made, the parabolic coordinate of type I in (III·19) is not a unique choice in view of the $\omega_1/\omega_2=1$ resonance: Any rotated coordinate in the u-v plane may be used, and we may have

$$\rho=\frac{1}{2}(U^2-V^2), \qquad p_\rho=\frac{1}{U^2+V^2}(Up_U-Vp_V), \tag{III·22}$$

$$z=UV, \qquad p_z=\frac{1}{U^2+V^2}(Vp_U+Up_V), \qquad \text{(type II)}$$

This is the rotation of type I coordinate by $\pi/4$:

$$u=\frac{1}{\sqrt{2}}(U-V) \quad \text{and} \quad v=\frac{1}{\sqrt{2}}(U+V), \tag{III·23}$$

by which the centrifugal potential in (III·18) cannot be separated unless $m=0$. If this is the case, however,

$$\mathcal{H}=\frac{1}{2}(p_U{}^2+(-2E)U^2)+\frac{1}{2}(p_V{}^2+(-2E)V^2)$$

for $\gamma=0$, and for $\gamma\neq 0$ with an additional term[3]

$$+\frac{\gamma^2}{32}(U^2-V^2)^2(U^2+V^2). \tag{III·24}$$

It is straightforward to obtain the lowest order, nontrivial normal form of the Hamiltonian; to take a projection of the perturbation part (γ^2-term in (III·21) or in (III·24)) onto the space which is involutive with $\tau_1+\tau_2$ (i.e., whose Poisson bracket vanishes with $\tau_1+\tau_2$). Let us introduce a parameter n defined by

$$n\equiv(-2E)^{-1/2}. \tag{III·25}$$

Then the unperturbed Hamiltonian is written in common as

$$\mathcal{H}^{(2)}=n^{-1}(\tau_1+\tau_2) \qquad \text{in both types of coordinate}, \tag{III·26}$$

and the perturbation as $\mathcal{H}^{(6)}$; a sextet polynomial of the a's and the a^*'s written in each coordinate. The results of the normalization to such a lowest order can now be written as

$$\frac{1}{2}n\mathcal{H}^{(6)}_{\text{normal}}=\frac{1}{2}(\tau_1+\tau_2)$$

$$+\frac{\gamma^2}{32}n^4(\tau_1+\tau_2)(3\tau_1\tau_2+K^2+K^{*2}) \tag{III·27a}$$

or

$$+\frac{\gamma^2}{32}n^4(\tau_1+\tau_2)\left(\frac{5}{4}(\tau_1+\tau_2)^2-\frac{9}{2}\tau_1\tau_2-\frac{K^2+K^{*2}}{4}\right) \tag{III·27b}$$

for the Hamiltonian in type I (III·21), and in type II (III·24) coordinate, respectively.

The relation between the regularized Hamiltonian $\mathcal{H}$ and the original H in

(III·20) indicates that $H=E$ implies $\mathcal{H}=2$, which, in turn, requires

$$\frac{1}{2}n\mathcal{H}_{\text{normal}}=n=\frac{1}{2}(\tau_1+\tau_2) \quad \text{to lowest order} \tag{III·28·0}$$

$$=\frac{1}{2}n\mathcal{H}^{(6)}_{\text{normal}} \quad \text{to next order} \tag{III·28·1}$$

$$\cdots, \quad \text{etc.}$$

We assume a quantization rule for $\gamma=0$ to be given by

$$n=N \quad \text{(non-zero integers, as can be assured later).} \tag{III·29}$$

A combination of this rule with (III·25) yields, to next order,

$$E=-\frac{1}{2n^2}=-\frac{1}{2N^2}+\frac{\gamma^2}{16}N^2(3\tau_1\tau_2+K^2+K^{*2}) \tag{III·30a}$$

or

$$+\frac{\gamma^2}{16}N^2\left(\frac{5}{4}(\tau_1+\tau_2)^2+\frac{9}{2}\tau_1\tau_2-\frac{K^2+K^{*2}}{4}\right). \tag{III·30b}$$

Clearly, the second term represents the quadratic Zeeman correction which requires an additional rule of quantization due to the $\omega_1/\omega_2=1$ resonance. According to Gustavson (see theorem (a) in § II. 4) there exists another constant of motion different from the energy even in the presence of a resonance, and this will provide a two-dimensional invariant torus embedded in the four-dimensional phase space. We show its detailed structure in terms of a geometric notion, namely, the Runge-Lenz hyperboloid.

2.2. Runge-Lenz hyperboloid of Solov'ev

The possibility of the third constant of motion in the diamagnetic Kepler system (III·4), other than energy E and angular momentum component p_ϕ, was discussed by several authors[63] around 1980. The first successful result due to Solov'ev[12] is expressed in the form

$$\Lambda(\boldsymbol{A})\equiv 4(A_x{}^2+A_y{}^2)-A_z{}^2(=4\boldsymbol{A}^2-5A_z{}^2)=\Lambda\,, \tag{III·31}$$

where A_x, A_y, A_z are the three cartesian components of the Runge-Lenz vector,

$$\boldsymbol{A}=\boldsymbol{p}\times\boldsymbol{L}-\frac{\boldsymbol{r}}{r}\,(\boldsymbol{L}=\boldsymbol{r}\times\boldsymbol{p})=\left(\boldsymbol{p}^2-\frac{1}{r}\right)\boldsymbol{r}-(\boldsymbol{r}\cdot\boldsymbol{p})\boldsymbol{p}\,. \tag{III·31a}$$

It says that the intersection of the energy surface and a manifold formed by (III·31), for a possible real value of Λ, yields the aimed invariant torus. Since $|\boldsymbol{A}|$ $(=\sqrt{1+2EL^2})$ represents the eccentricity of a Kepler ellipse, less than unity for $E<0$, the allowed values of Λ are

$$-1\leq\Lambda\leq 4\,. \tag{III·31b}$$

Solov'ev obtained the form (III·31), which we call the *Runge-Lenz hyperboloid*, from

a consideration of perturbation average discussed by Arnold.[49] Namely, a motion of the vector $\boldsymbol{A}$ around its constant value perturbed by the presence of a weak magnetic field $\boldsymbol{B}$, or any function of the $\mathbf{A}$, is averaged over the period of the Kepler ellipse, which shows*)

$$\lim_{B\to 0}\left\langle\frac{d}{dt}\Lambda(\boldsymbol{A})\right\rangle \Big/ \left\langle\frac{d}{dt}\boldsymbol{A}^2\right\rangle = 0 . \tag{III·32}$$

Here we outline how such an intersection can be located and traced on a plane in the phase space (i.e., a surface of section).[64),65] Also, we aim at its connection to the B-G normal form deduced in (III·30).

We need a convenient representation of the two vectors $\boldsymbol{L}$ (angular momentum) and $\boldsymbol{A}$, namely, the *rotating cylindrical coordinate representation* (RCCR). Suppose a cylindrical coordinate (ρ, φ, z) is given as $x=\rho\cos\varphi$ and $y=\rho\sin\varphi$. Then, any vector $\boldsymbol{V}$ in RCCR is given by a rotation of $\boldsymbol{V}$ represented in (x, y, z) by angle φ around the z-axis so that

$$V_\xi = V_x\cos\varphi + V_y\sin\varphi , \qquad V_\eta = -V_x\sin\varphi + V_y\cos\varphi . \tag{III·33}$$

For example, RCCR of $\boldsymbol{r}(x, y, z)$ and $\boldsymbol{p}(p_x, p_y, p_z)$ are: $\boldsymbol{r}(\rho, 0, z)$ and $\boldsymbol{p}(p_\xi=p_\rho, p_\eta=p_\varphi/\rho, p_z)$. Here, we obtain RCCR of $\boldsymbol{L}$ and $\boldsymbol{A}$ with the result given by

$$\boldsymbol{L}\left\{\begin{array}{l} L_\xi = -\dfrac{z}{\rho}p_\varphi \\ L_\eta = zp_\rho - \rho p_z \\ L_z = p_\varphi \end{array}\right\} \qquad \boldsymbol{A}\left\{\begin{array}{l} A_\xi = -(zp_\rho - \rho p_z)p_z - \dfrac{\rho}{r} + \dfrac{{p_\varphi}^2}{\rho} \\ A_\eta = -\left(p_\rho + \dfrac{z}{\rho}p_z\right)p_\varphi \\ A_z = (zp_\rho - \rho p_z)p_\rho - \dfrac{z}{r} + \dfrac{z{p_\varphi}^2}{\rho^2} \end{array}\right\} ,$$

$$r = \sqrt{\rho^2+z^2} . \tag{III·34}$$

This representation is useful particularly for those motions with p_φ (constant of motion)$=0$, because then the η-component of the three vectors $\boldsymbol{r}$, $\boldsymbol{p}$ and $\boldsymbol{A}$ vanishes while $\boldsymbol{L}$ has its nonvanishing component only for the η-direction, that is to say, the motion is confined in the ξ-z plane. Under this circumstance one can write

$$\Lambda(\boldsymbol{A}) = 4\boldsymbol{A}^2 - 5{A_z}^2 = -\boldsymbol{A}^2 + 5{A_\xi}^2 . \tag{III·35}$$

We shall use the above formula to relate the normal form in (III·30) to $\Lambda(\boldsymbol{A})$ later. First let us obtain SOS $\Sigma(\rho, p_\rho ; z=0)$, generally $p_\varphi\neq 0$, defined by the trace of intersection $H=E$ and $\Lambda(\boldsymbol{A})=\Lambda$ projected onto $z=0$. As can be seen from (III·34), then, $\boldsymbol{L}^2 = \rho^2{p_z}^2 + {p_\varphi}^2$ and

$$\boldsymbol{A}^2 = 1 - n^{-2}(\rho^2{p_z}^2 + {p_\varphi}^2) , \qquad n \text{ in (III·25)} , \qquad {A_z}^2 = \rho^2{p_\rho}^2{p_z}^2 , \tag{III·36}$$

*) For $B\neq 0$, let the *pseudo angular momentum* and the *pseudo Runge-Lenz vector* be defined by $\boldsymbol{L}=\boldsymbol{r}\times\boldsymbol{v}$ and $\boldsymbol{A}=\boldsymbol{v}\times\boldsymbol{L}-(\boldsymbol{r}/r)$, respectively, where $\boldsymbol{v}=\boldsymbol{p}+(\boldsymbol{B}/2)\times\boldsymbol{r}$, and consider $k^2\Lambda(\boldsymbol{A})=(1-k^2)\boldsymbol{A}^2-{A_z}^2$. By the equation of motion, $(d/dt)\boldsymbol{A}^2=-4E(\boldsymbol{r}\cdot\boldsymbol{v})(\boldsymbol{r}\times\boldsymbol{v})B$ and $(d/dt){A_z}^2=-2A_zp_z(\boldsymbol{r}\times\boldsymbol{v})\cdot\boldsymbol{B}$. The unknown parameter k is determined so that $\lim_{B\to 0}\langle(d/dt)\Lambda(\boldsymbol{A})\rangle/\langle(d/dt)\boldsymbol{A}^2\rangle=0$. This procedure is shown to give $k^2=(1/5)$ (equivalent to (III·32)) (Refs. 64)).

which simplify the remaining manipulation. The result can be shown to be a quadratic equation for ρ with coefficients rational function of p_ρ:

$$\rho^2-\frac{2n^2}{n^2p^2+1}\rho+\frac{n^4(k^2\Lambda'+m^2p^2)}{(n^2p^2+1)(n^2p^2+k'^2)}=0 \tag{III·37}$$

with notational convention

$$p\equiv p_\rho\,,\qquad m=p_\varphi \tag{III·37a}$$

and

$$\Lambda'\equiv\frac{k'^2}{k^2}-\Lambda\,;\qquad k^2=\frac{1}{5}\,,\qquad k'^2=1-k^2=\frac{4}{5}\,. \tag{III·37b}$$

This defines an algebraic function $p=p(\rho)$ and hence the associated action integral $\int p(\rho)d\rho$ in terms of the so-called *Abel integral*. The nontrivial part of this integral, we show, is of the form

$$j=\frac{1}{\pi}\int\left[1-\frac{n^2p^2+1}{n^2p^2+k'^2}(k^2\Lambda'+m^2p^2)\right]^{1/2}\frac{n^2dp}{n^2p^2+1}\,, \tag{III·38a}$$

$$=\frac{1}{\pi}\int\left[n^2k^2(1+\Lambda)+m^2-n^2k^2\mathrm{sn}^2(\zeta,k)-\frac{m^2}{\mathrm{sn}^2(\zeta,k)}\right]^{1/2}d\zeta \tag{III·38b}$$

by the transformation $p\to\zeta$:

$$p=n^{-1}\mathrm{cn}(\zeta,k)/\mathrm{sn}(\zeta,k)\,,\qquad dp=[n^{-1}\mathrm{dn}(\zeta,k)/\mathrm{sn}^2(\zeta,k)]d\zeta\,.$$

Further, by a so-called Gauss transformation of *Jacobi's elliptic function with modulus* k to that with k^{-1}, i.e., $k\mathrm{sn}(k^{-1}u,k)=\mathrm{sn}(u,k^{-1})$, and by setting $\mathrm{sn}(u,k^{-1})=\sin\vartheta$, the above action integral becomes

$$j=\frac{1}{\pi}\int\left[n^2\left(1+\frac{\Lambda}{1-k^{-2}\sin^2\vartheta}\right)-\frac{m^2}{\sin^2\vartheta}\right]^{1/2}d\vartheta\,. \tag{III·38c}$$

This is precisely the action integral Solov'ev obtained,[12),*)] provided a proper specification is made of the range of integration.

2.3. SOS $\Sigma(\xi, p_\xi\,;\, z=0)$ and SOS $\Sigma(z, p_z\,;\, \xi=0)$ for $m=0$

For $m=0$, the surface of section $z=0$ implied by (III·37) is not bounded in the ρ-p_ρ plane in the limit $\rho\to0$, which is due to the absence of the centrifugal potential. The dependence of ρ vs p_ρ is drawn schematically in Fig. III-2, where the geometrical meaning of the action integral (III·38a) is indicated. If the two branches of the root of (III·37) are denoted by $\rho_\pm$, one can write

$$j=\frac{1}{2\pi}\int(\rho_+-\rho_-)dp\,,\qquad \text{whereas}\qquad J=\frac{1}{2\pi}\int_{-\infty}^{\infty}(\rho_++\rho_-)dp=n, \tag{III·39}$$

*) Solov'ev obtained this result by identifying the integration variable ϑ with the polar angle of the $\boldsymbol{A}$-vector, and its proper conjugate momentum with $L_\perp\equiv[L^2-L_z^2/\sin^2\vartheta]^{1/2}$ which seemed difficult to prove. A proof has been provided by Pinard based on a geometrical construction (private communication). H. H. thanks Professor J. Pinard for his kind communication, and withdraws with apology the author's premature statement.[66)] See also § V.1.

which shows the existence of another action variable $J: J=n$ (defined by (III·25)) implies the Rydberg spectrum $E=(-1/2)J^{-2}$, if the quantization $J=1, 2, \cdots$ is allowed (as can be justified by means of a contour integration and the Maslov-index argument given in the last part of the next subsection 2.4).

The unbounded SOS can be avoided by going over to the parabolic coordinate representation (type II): From (III·22), the section $z=0$ corresponds to $V=0$ ($\rho>0$), or $U=0$ ($\rho<0$)—negative ρ should be allowed to interprete that ρ represents the rotating cylindrical coordinate ξ, and for this reason the notation $\Sigma(\xi, p_\xi; z=0)$ is adopted. Similarly, from (III·19) the section $\xi=0$ corresponds to $u=0$ ($z>0$), or v

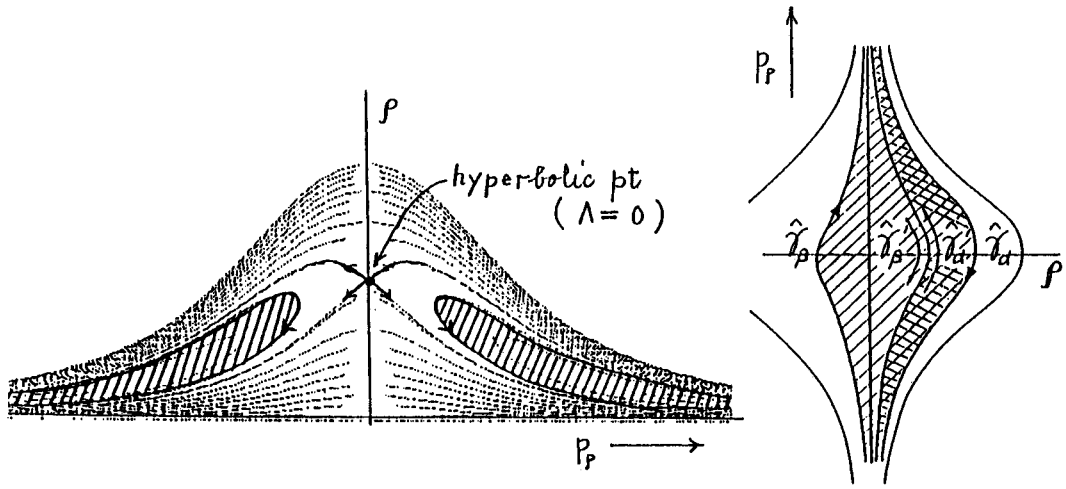

Fig. III-2. Analytic curves ρ vs p_ρ for the case $m=0$ in (III·37) which represents the surface of section $z=0$ of the invariant tori in the weak diamagnetic limit parametrized by $\Lambda\in(-1, 4]$ of the Runge-Lenz hyperboloidal value ($\Lambda=4$, the outermost contour; $\Lambda=0$, the unique separatrix line which separates the two regions of the motions). The shaded area represents the action integral j(III·38a, $m=0$) for a $\Lambda(<0)$. It can be extended to case $\Lambda>0$ (see the separate figure which indicates $J=n$ as well as j (doubly shaded area) for $\Lambda>0$).

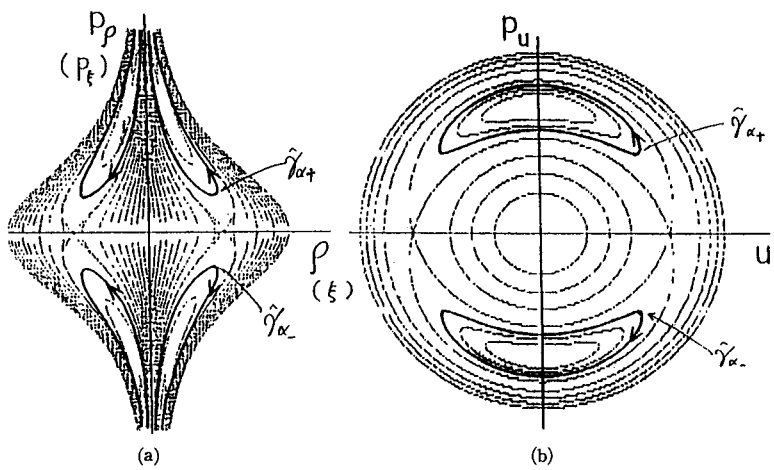

Fig. III-3. Graph presentations of the surface of section (a) $\Sigma(\xi, p_\xi;\ z=0)$ and its map onto (b) $\Sigma(q_U, p_U;\ V=0)$. Their duals $\Sigma(z, p_z;\ \xi=0)$ and $\Sigma(q_v, p_v;\ u=0)$ have similar structures.

$=0$ ($z<0$), which yields SOS $\Sigma(z, p_z\,;\,\xi=0)$.

An invariant torus for a given set of values (n, Λ) can be given by a quartic equation for the four canonical variables (q_i, p_i), $i=u, v$ (type I) or U, V (type II), intersected by the energy surface, as follows:

$$5\tau_u\tau_v-(q_vp_u-q_up_v)^2=n^2(1+\Lambda)\,,\qquad \tau_u+\tau_v=2n\,, \tag{III·40a}$$

$$5\tau_U\tau_V-\frac{1}{4}(q_Vp_U-q_Up_V)^2=n^2(4-\Lambda)\,,\qquad \tau_U+\tau_V=2n\,, \tag{III·40b}$$

where

$$\tau_i\equiv\frac{1}{2}(q_i^2+p_i^2)\,,\qquad i=u,\ v\quad\text{and}\quad U,\ V\,. \tag{III·40c}$$

Projecting the first manifold onto $u=0$, and the second onto $V=0$, we get

$$\begin{aligned}&\text{I}\quad \Sigma(q_v, p_v\,;\,u=0):\ (4n^2-p_v^2-q_v^2)(5p_v^2+q_v^2)=4n^2(1+\Lambda)\,,\\ &\text{II}\quad \Sigma(q_U, p_U\,;\,V=0):\ (4n^2-p_U^2-q_U^2)(5p_U^2+q_U^2)=4n^2(4-\Lambda)\,.\end{aligned} \tag{III·41}$$

Each SOS corresponds to

$$\begin{aligned}&\text{I}\quad \Sigma(z, p_z\,;\,\xi=0):\quad z^2-\frac{2n^2}{n^2p_z^2+1}z+\frac{n^2(k^2+k^2\Lambda)}{(n^2p_z^2+1)(n^2p_z^2+k^2)}=0\,,\\ &\text{II}\quad \Sigma(\xi, p_\xi\,;\,z=0):\quad \xi^2-\frac{2n^2}{n^2p_\xi^2+1}\xi+\frac{n^2(k'^2-k^2\Lambda)}{(n^2p_\xi^2+1)(n^2p_\xi^2+k'^2)}=0\,,\\ &\qquad\qquad k^2=\frac{1}{5}\,,\qquad k'^2=\frac{4}{5}\qquad\text{cf. (III·37).}\end{aligned} \tag{III·42}$$

A computer-graphic drawing of SOS $\Sigma(\xi, p_\xi\,;\,z=0)$ and its correspondent $\Sigma(q_Up_U\,;\,V=0)$ is shown in Fig. III-3.

Two key formulas to deduce the above result are given by

$$\tau_u\tau_v=n^2(1-A_z^2)\,,\qquad \tau_U\tau_V=n^2(1-A_\xi^2) \tag{III·43}$$

and

$$(q_vp_u-q_up_v)^2=(q_Vp_U-q_Up_V)^2=4\boldsymbol{L}^2\,. \tag{III·44}$$

Also, a combination of these with (III·35) yields

$$\begin{aligned}K^2+K^{*2}&\equiv\frac{1}{4}(q_u+ip_u)^2(q_u-ip_v)^2+\text{c.c.}\\ &=2\tau_u\tau_v-\boldsymbol{L}^2(\text{type I, similarly for type II})\,,\end{aligned} \tag{III·45}$$

establishing the invariant expression for the normal form (III·30) as

$$E=-\frac{1}{2N^2}+\frac{\gamma^2}{16}N^2(1+\Lambda(\boldsymbol{A}))\,. \tag{III·46}$$

This is subject to a further quantization by the action integrals below.

2.4. Action integrals for $m=0$: dual structure and analyticity

We start from

$$\text{I}\quad j_\xi=\frac{2n}{\pi}\int_0^{\theta_0^*}\sqrt{\frac{k'^2-k^2\Lambda-k'^2\sin^2\theta^*}{1-k'^2\sin^2\theta^*}}d\theta^*\,, \tag{III·47a}$$

where $\theta_0^*=\frac{\pi}{2}$ for $-1<\Lambda<0$, $=\sin^{-1}\sqrt{1-\frac{k^2}{k'^2}\Lambda}$ for $0<\Lambda$,

$$\text{II}\quad j_z=\frac{2n}{\pi}\int_0^{\theta_0}\sqrt{\frac{k^2+k^2\Lambda-k^2\sin^2\theta}{1-k^2\sin^2\theta}}d\theta\,, \tag{III·47b}$$

where $\theta_0=\sin^{-1}\sqrt{1+\Lambda}$ for $-1<\Lambda<0$, $\frac{\pi}{2}$ for $0<\Lambda$.

The latter integral is the special case $m=0$ of (III·38a), whose geometrical meaning on SOS $\Sigma(\xi, p_\xi; z=0)$ has been illustrated (see Fig. III-2). A remarkable *dual structure* can be seen to exist between these action integrals: Namely,

$$j_\xi \rightleftarrows j_z \quad \text{by the interchange of the modulus}$$
$$\text{of elliptic functions}\quad k^2\rightleftarrows k'^2 \quad\text{and}\quad k^2\Lambda\rightleftarrows -k^2\Lambda\,. \tag{III·48}$$

Obviously, this duality stems from the invariance of the Kepler Hamiltonian by the interchange $\xi\rightleftarrows z$ for $m=0$ as well as the antisymmetry of the Runge-Lenz hyperbola (III·35) —this is reexpressed as

$$k^2\Lambda(\boldsymbol{A})=k'^2\boldsymbol{A}^2-A_z{}^2=-k^2\boldsymbol{A}^2+A_\xi{}^2\,. \tag{III·35′}$$

What is more important for physics, particularly for spectroscopy, is the identity

$$j_\xi+j_z=J(=n)\,. \tag{III·49}$$

The significance of the duality and this sum rule in spectroscopy will be discussed in § V.1.

Our concern here is to explore a deeper origin of the above feature, namely, the *analyticity* of the two-dimensional two-torus for the (weakly perturbed) Kepler motion: The torus can be parametrized by a single complex variable ζ, the conjugate momentum of which, p_ζ, is given in terms of doubly periodic analytic functions on the complex ζ-plane, i.e., elliptic functions. Thus the two-dimensional two-torus under consideration must be a Riemann surface of $p_\zeta=p(\zeta)$ with one 'hole' structure (Fig. III·4, see a detail in Ref.67)). Consequently, both action integrals are identified to be a Cauchy integral of a complex analytic function along two elementary cycles on the ζ-plane:

$$j_{z,\xi}=\frac{1}{2\pi}\int_{\gamma_\alpha,\ \gamma_\beta}p(\zeta)d\zeta(=j_{\alpha,\beta})\,, \tag{III·50}$$

$$p(\zeta)=n[k^2(1+\Lambda)-k^2\mathrm{sn}^2(\zeta, k)]^{1/2}\,, \tag{III·50a}$$

where α and β are related to ζ by $\zeta=\alpha+i\beta+\text{const}$ (the elliptic cylindrical coordinate to parametrize the Fock hypersphere[68),69)]), and $\gamma_{\alpha,\beta}$ are two segments parallel to α and

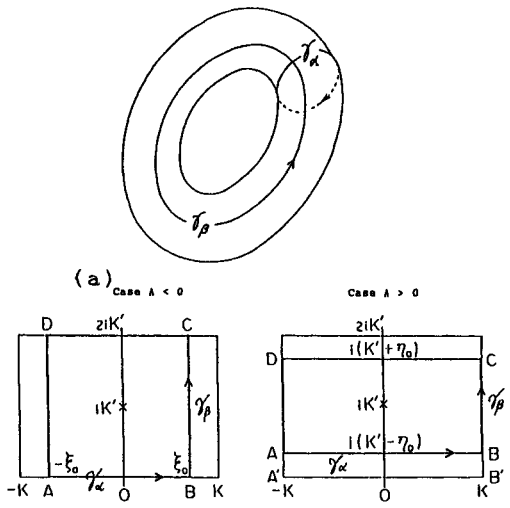

Fig. III-4. Schematics of a two-dimensional two-torus of Hamiltonian systems with two degrees of freedom for which the weak diamagnetic Kepler system is a representative. (a) The Riemann surface of the analytic function $\wp(\zeta)$ of the complex coordinate $\zeta=\alpha+i\beta+$const on which the above torus structure is represented; case $m=0$ and $\Lambda\gtrless 0$. Two elementary cycles γ_α and γ_β are those along which two action integrals are defined in terms of two elliptic integrations involving K and K' (the complete elliptic integrals of the 1st kind with modulus k and the complementary modulus $k'=\sqrt{1-k^2}$).

β which define the double periods to characterize the two elementary cycles. This means that the two action integrals j_z and j_ξ, individually defined as the one on each surface of section, are actually a counterpart of the other of the two action integrals on the one identical torus. An appendix to this subsection (at the end of § III) summarizes the matter of the elliptic cylindrical coordinate relevant here.

Consider a contour integral of the analytic function $\wp(\zeta)$ along a double combination of $\gamma_\alpha+\gamma_\beta$ which encircles a rectangular portion (a parallelogram) $\overline{ABCDA}$ on the (Riemann surface of) ζ-plane in Fig. III-4(a). Since $\wp(\zeta)$ is single-valued and regular in this portion except at one point $\zeta=i\cdot K'$, which is a simple pole of $\wp(\zeta)$ with residue $i\cdot n$, this contour integral yields the value n; a proof of the sum rule (III·49), which we may call the "Rydberg speciality".[64),66)] Futhermore, since this contour integration can be regarded as along a complex trajectory in the phase space with four caustics, the resulting Maslov index α in the quantization rule, $\int pdq=2\pi(N+\alpha/4)$, must be 4. This justifies the primitive quantization rule (III·29).

III. 3. *Surfaces of section in general diamagnetic strength*

The analytic description of the foregoing section can no longer be used once one gets into regimes where the Lorentz force and the Coulomb force acting on the electron become of comparable size. To determine trajectories, and thus SOS in this more general, nonseparable situation, one is forced to resort to solving numerically the equations of motion. In doing so one can make use of the scaling properties discussed in § III.1, which imply that, except for a similarity transformation, the classical dynamics of a hydrogen atom in a uniform magnetic field depends solely on the value of the scaled energy

$$\varepsilon=\frac{E}{\gamma^{2/3}}, \qquad \text{(III·51)}$$

and *not* on energy and magnetic field strength individually (cf. III·6). That is, to exploit the whole of classical dynamics it suffices to determine trajectories and

surfaces of section as functions of one single parameter, the scaled energy ε. Furthermore, the scaled angular momentum $\tilde{p}_\varphi = \gamma^{1/3} p_\varphi$ remains negligibly small under laboratory conditions and can be ignored in what follows (corresponding to $m=0$).

Trajectories can be determined, e.g., using the cylindrical coordinates, in which case the equations of motion are governed by the (scaled) Hamiltonian (III·6). A feature of that Hamiltonian is its singularity at $\tilde{r}(=(\tilde{\rho}^2+\tilde{z}^2)^{1/2})=0$, which can be removed by introducing the parabolic coordinates u, v defined in Eq. (III·19) and the rescaled time τ given by

$$dt = 2\tilde{r}\,d\tau = (u^2+v^2)d\tau\,. \tag{III·52}$$

The equations of motion generated by the Hamiltonian (III·6) at fixed scaled energy ε are then found to be equivalent to the equations of motion generated by the Hamiltonian

$$h = \frac{1}{2}(p_u{}^2+p_v{}^2) - \varepsilon(u^2+v^2) + \frac{1}{8}u^2v^2(u^2+v^2) \tag{III·53}$$

at the fixed "energy" 2.

Although there is clearly a one-to-one correspondence between the solutions of the equations of motion in cylindrical and parabolic coordinates (III·19), it is useful to consider some qualitative aspects in detail. Near the origin $\tilde{\rho}=0$, $\tilde{z}=0$ (or $u=0$, $v=0$) the motion of the electron in cylindrical coordinates is dominated by the Coulomb force and, for $\varepsilon<0$, corresponds to Kepler ellipses which reduce to straight lines reflected at the origin for vanishing angular momentum. In the parabolic coordinates such a straight-line limit of a Kepler ellipse will not be reflected at the origin but will continue, e.g., from the u, $v>0$ quadrant to the u, $v<0$ quadrant,

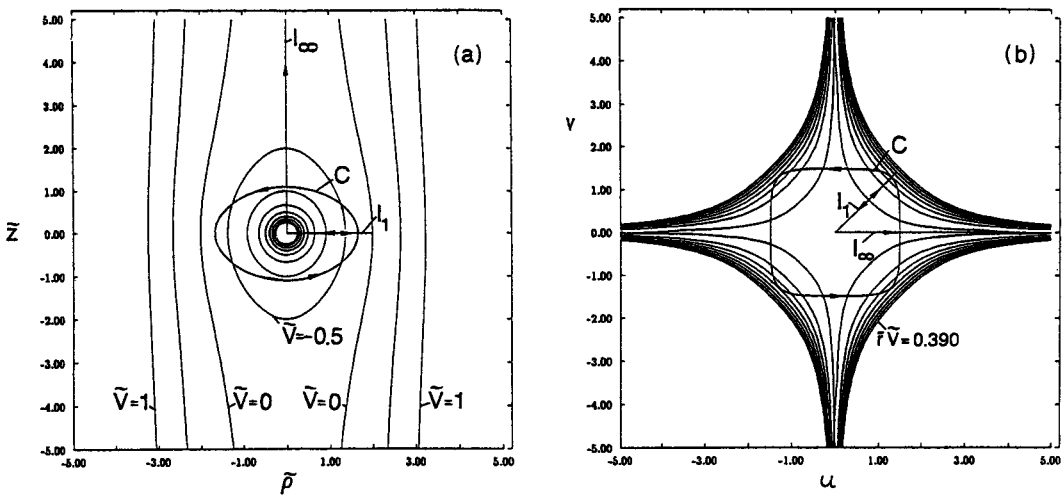

Fig. III-5. The three periodic orbits I_1, I_∞, C at the zero-field threshold $\varepsilon=0$ in (a) the cylindrical $\tilde{\rho}-\tilde{z}$ representation and (b) the regularized $u-v$ representation. Also shown are, in Fig. III-5(a), the lines of constant potential $\tilde{V}=\tilde{V}_{\text{dia}}+\tilde{V}_{\text{Coulomb}}=\tilde{\rho}^2/8-(\tilde{\rho}^2+\tilde{z}^2)^{-1/2}$, decreasing from $\tilde{V}=1$ in steps of 0.5 to $\tilde{V}=-4$ (innermost contour), and, in Fig. III-5(b), the lines of constant $\tilde{r}\tilde{V}$, decreasing from $\tilde{r}\tilde{V}=0.390$ in steps of 0.195 to -0.975.

because the potential is regular at $v=u=0$.

In order to illustrate the differences in the two representations Fig. III-5 shows, in both coordinate systems, the straight-line orbits perpendicular (I_1) and parallel (I_∞) to the field as well as the almost circular orbit (C) which reduces to an exact circle (in both representations) in the field-free limit. We note that in the other set of the parabolic coordinates introduced in § III.2, U, V(III·23) (obtained from u, v by a rotation by $\pi/4$), the orbits I_1 and I_∞ interchange their meaning in that I_1 runs along a coordinate axis (U) while I_∞ runs along a bisectrix of a quadrant. The orbits I_1 and I_∞ are in fact limiting cases of a whole family of curved periodic orbits $\{I_\nu\}_{1<\nu<\infty}$ (see Fig. III-6) of the diamagnetic Kepler problem that pass through the origin. These have recently gained importance in the interpretation of long-range modulations in the photoabsorption spectra of magnetic Rydberg atoms[18),70),71)] (see also § V.2).

As an example, SOS's $\Sigma(\rho, p_\rho; z=0)$ are shown in Fig. III-7 for a magnetic field strength of 6 Tesla and decreasing binding energy of the electron with respect to the field-free ionization threshold (this was first presented by Harada and Hasegawa[4)] and simulated analytically [65),*)]). In these SOS the orbit I_1 corresponds to the right-hand limiting contour of the kinematically allowed region, while the p_ρ-axis corresponds to I_∞. Furthermore, the orbit C is represented by the hyperbolic point visible in the panel for $-132\ \mathrm{cm}^{-1}$. As the energy is decreased the regular structures present in the (regular) weak-diamagnetic case are gradually destroyed. In particular it is seen that irregularity first sets in around the hyperbolic point, and below $\sim -24\ \mathrm{cm}^{-1}$ no regular orbits can be recognized in the surfaces of section $\Sigma(\rho, p_\rho; z=0)$ any more. In Fig. III-8 the breakdown of regularity is quantified by plotting the area fraction of regular orbits as a function of energy for $B=6$ Tesla. By the scaling relation (III·5) Fig. III-8 is universal, and not restricted to that set of parameters. Converting the absolute to scaled energies one arrives at the ε scale shown at the top horizontal axis

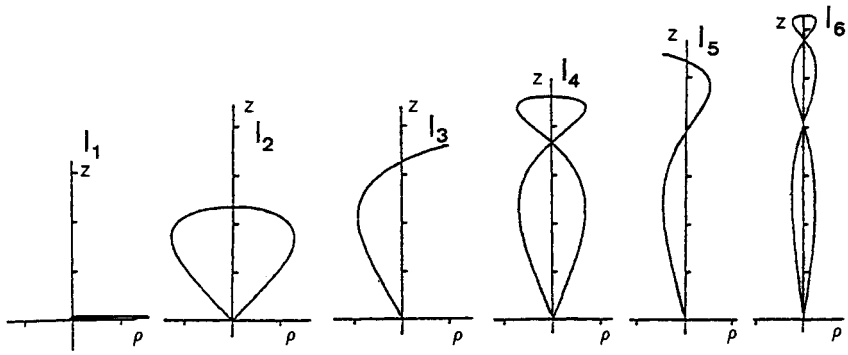

Fig. III-6. Leading members of the family of classical periodic orbits $\{I_\nu\}_{1<\nu<\infty}$ at $E=0$. The first member I_1 is the straight-line orbit perpendicular to the direction of the magnetic field, the limiting case I_∞ corresponds to the straight-line orbit parallel to the field. (From Ref. 115).)

*) The analytic simulation of $\Sigma(\rho, p_\rho; z=0)$ performed in Ref. 65) is by taking into account the diamagnetic part beyond the first order perturbation and hence some higher-order effects of ε, exhibiting an essential hyperbolicity of the tori to remain on the average.

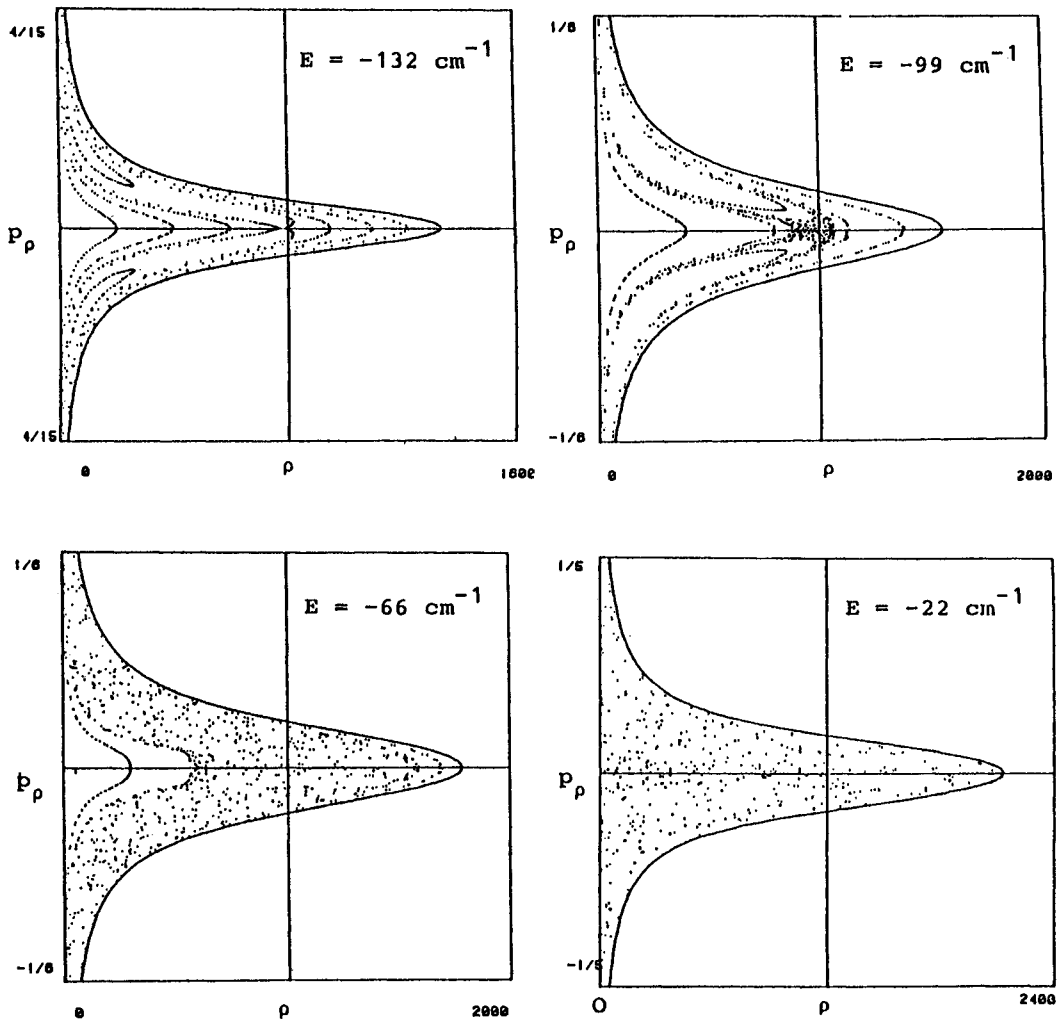

Fig. III-7. Poincaré surfaces of section of classical motion $\Sigma(\rho, p_\rho; z=0)$ at different energies and for $B=6$ Tesla, $m=0$. Note that chaos grows around the hyperbolic point, and finally fills most of phase space at $-22\,\mathrm{cm}^{-1}$.

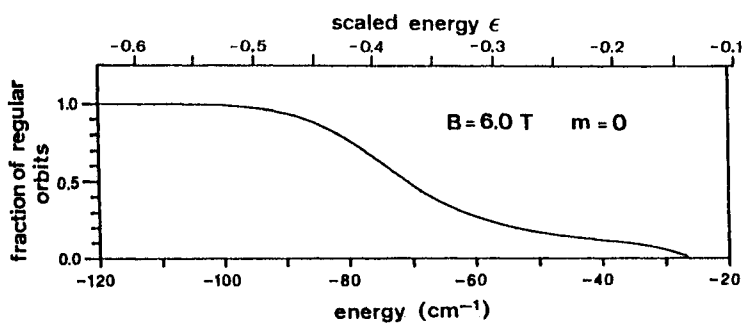

Fig. III-8. Area fraction of the surfaces of section $\Sigma(\rho, p_\rho; z=0)$ which is filled by regular orbits as a function of scaled energy (top horizontal scale), or in explicit spectroscopic units for a magnetic field strength of 6 Tesla. Note the transition from regularity to irregularity between $\epsilon \sim -0.48$ and -0.125.

of Fig. III-8.

As a second example of SOS at increasing diamagnetic strength Fig. III-9 shows a sequence of SOS's $\Sigma(v, p_v; u=0)$. From (III·19) it follows that this corresponds to $\rho=0$ ($z\geq 0$). The diamagnetic term does not contribute in this case in (III·53), and by rescaling the v coordinate, $v^*=v\sqrt{2(-\varepsilon)}$, the limiting contours ($p_u=0$) become circles of radius 2. The SOS's show the results obtained for orbits starting at the origin and by varying the starting angle ϑ with respect to the B direction. From the starting condition $p_v=\pm 2\sin(\vartheta/2)$ one recognizes that the orbit I_1 is represented, in the regular and near-regular panels, by the two elliptic points $p_v=\pm\sqrt{2}$ on the p_v axis, while the orbit I_∞ along the direction of the magnetic field is represented by the outermost circle. The separatrix visible in the regular and near-regular regime separates the phase space in two different parts characterized by librating and rotating motion (cf. Delos et al.[72] and § V.1). As an alternative, Fig. III-10 shows SOS's $\Sigma(V, P_V; U=0)$ (i.e., $z=0$) for decreasing scaled energy. The limiting contours ($P_U=0$) are in this case given by a third-degree equation in V^2. As discussed before, the orbits I_1 and I_∞ interchange their meaning with respect to the SOS's $\Sigma(v, p_v; u=0)$ and thus also with respect to the positions of the elliptic points.

Figures III-9 and III-10 again display the breakdown of regularity as the scaled energy is decreased. It is seen that as one intrudes into the chaotic regime, other elliptic points are born and subsequently evanesce, indicative of other periodic orbits which eventually become unstable (a feature just as described in § II.2), and that

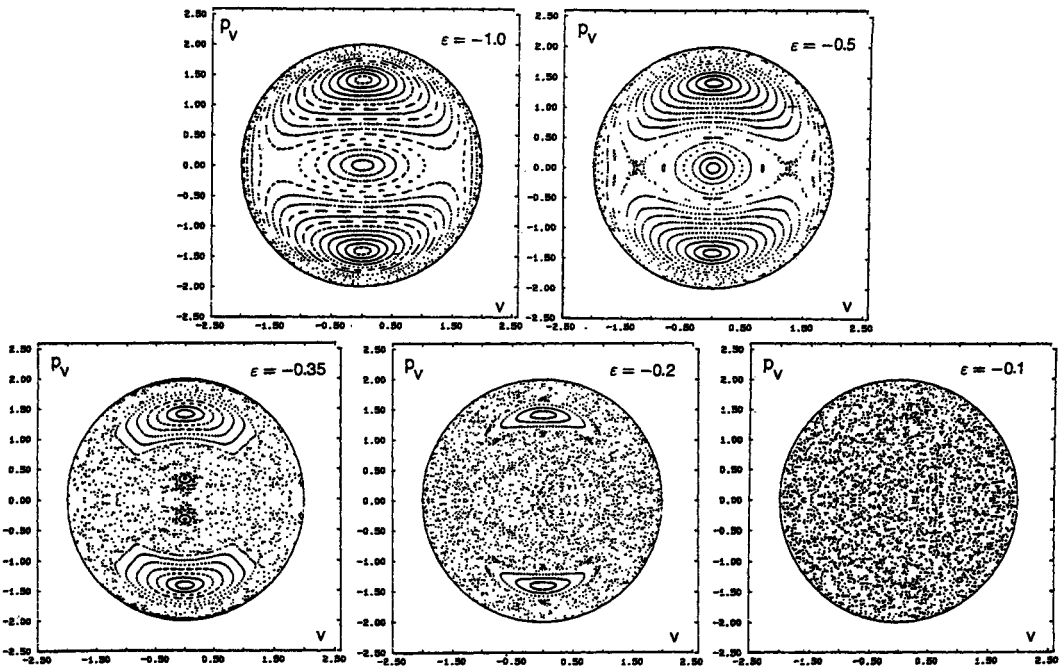

Fig. III-9. Poincaré surfaces of section $\Sigma(v, p_v; u=0)$ at different scaled energies (corresponding to increasing diamagnetic strength). The elliptic fixed point at the origin corresponds to the straight-line orbit I_∞, the other two fixed points to the straight-line orbit I_1.

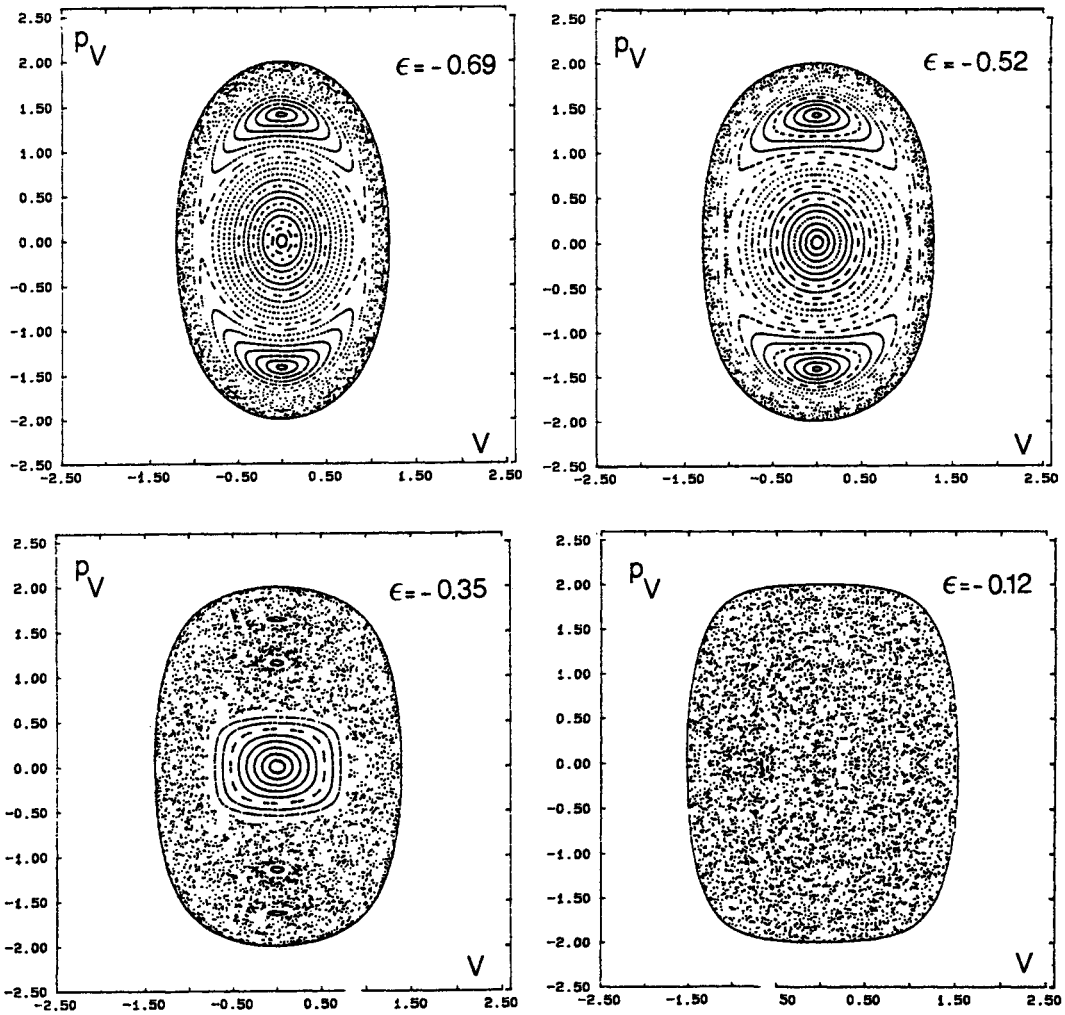

Fig. III-10. Poincaré surfaces of section $\Sigma(V, p_V; U=0)$ (i.e., $z=0$) at different scaled energies. The connection of the elliptic fixed points to the straight-line orbits is interchanged with respect to Fig. III-9.

apparently the orbit perpendicular to the magnetic field is the last one to finally turn unstable.

In the next subsection we want to examine the transition from stability to instability of trajectories in the diamagnetic Kepler problem in more detail using the concept of Liapunov exponents and, in doing so, pay special attention to these quasi-periodic orbits. The subsection summarizes results presented by us elsewhere (Schweizer et al.[73]) with a supplement.

III. 4. *Stability analyses—Liapunov exponents*

A quantitative measure for the degree of instability of a classical trajectory in the chaotic region is provided by the Liapunov exponent which characterizes, roughly speaking, the velocity at which trajectories in the vicinity of a given trajectory

exponentially separate from that trajectory in phase space. The Liapunov exponent is the same for all phase space points lying on a given classical trajectory. Furthermore, isolated unstable *periodic* trajectories are known to lead to modulations in the quantum mechanical level densities[71] and in observable cross sections,[74),75)] and a quantitative measure of the stability of the orbits is therefore requisite to quantitatively account for observable features in the level density and other spectra.

To introduce the concept of Liapunov exponents we consider the trajectory $\gamma(t)$ starting, at $t=0$, at the phase space point $\gamma(t=0)=(x_1, \cdots, x_N, p_1, \cdots, p_N)$ ($N=2$ in our case) and study the evolution in time of the norm $\|\delta\gamma(t)\|$ of the infinitesimal separation $\delta\gamma$ between the trajectory $\gamma(t)$, which passes through $\gamma(0)$ at $t=0$, and a nearby trajectory which passes through $\gamma(0)+a$ at $t=0$. As shown by Oseledec[76] the limit

$$\lim_{t\to\infty}\frac{1}{t}\ln\|\delta\gamma(t)\|=L(a) \tag{III·54}$$

exists for all non-vanishing displacement vectors a, and the Liapunov exponent (associated with phase space point $\gamma(0)$) is defined as the maximum of the at most $2N$ different values (III·54) corresponding to different directions of the displacement vector. Following Meyer[77] we calculate the stability matrix $M(0, t)$ along the trajectory passing through $\gamma(0)$:

$$M_{ij}(0, t)=\frac{\partial\gamma_i(t)}{\partial\gamma_j(0)}, \tag{III·55}$$

and the Liapunov exponent λ is then the long-time limit of the Liapunov function $\lambda(t)$:

$$\lambda=\lim_{t\to\infty}\lambda(t)\equiv\lim_{t\to\infty}\frac{1}{t}\ln\|M(0, t)\|, \tag{III·56}$$

where $\|M\|$ is a norm[78] (any norm) of the matrix M. As shown by Meyer[77] the limit defined in (III·56), though not the Liapunov function itself, is invariant under canonical transformations. We list a few important properties that follow immediately from (III·55, 56). Using

$$M_{ij}(T, T+t)=\frac{\partial\gamma_i(T+t)}{\partial\gamma_j(T)}, \tag{III·57}$$

we obtain

$$M(0, T+t)=M(T, T+t)M(0, T) \tag{III·58}$$

(chain rule). From the triangle inequality for matrix norms we have

$$\|M(0, T+t)\|\leq\|M(0, T)\|\|M(T, T+t)\|. \tag{III·59}$$

Conversely we can use the relation

$$M(T, T+t)=M(0, T+t)M(0, T)^{-1} \tag{III·60}$$

to deduce the result

$$\|M(T, T+t)\|\leq\|M(0, T+t)\|\|M(0, T)^{-1}\|. \tag{III·61}$$

(Because the flow is Hamiltonian the matrix M is symplectic ;[77] in particular M and M^{-1} have finite norms). From (III·59, 61) it follows that the ratio $\|M(0,\ T+t)\|$ $/\|M(T,\ T+t)\|$ is bounded from above by $\|M(0,\ T)\|$ and from below by the positive number $\|M(0,\ T)^{-1}\|^{-1}$. This means that the Liapunov function $\lambda(t)$ defined with $M(0,\ t)$ and with $M(T,\ t)$ differ only by a bounded function divided by t and hence yield the same Liapunov exponents (III·56) in the limit $t\to\infty$. Thus all points along a given trajectory have the same Liapunov exponent.

The Liapunov exponent becomes particularly easy to calculate for periodic trajectories. If T is the period of a periodic orbit, then $M(0,\ nT)=M(0,\ T)^n$. In the limit $n\to\infty$ we have

$$\|M(0,\ T)^n\|^{1/n}\xrightarrow{n\to\infty}\sigma\,, \tag{III·62}$$

where σ is the maximum absolute value $|m_i|$ of all eigenvalues of $M(0,\ T)$ (see p. 299 of Ref.78)). Hence

$$\lambda=\lim_{n\to\infty}\frac{1}{nT}\ln\|M(0,\ nT)\|=\frac{1}{T}\ln\sigma\,. \tag{III·63}$$

For periodic orbits, the Liapunov exponent can be obtained directly from the maximum (by absolute value) eigenvalue of the stability matrix after *one* period.

We would like to mention that the Liapunov exponent is constant inside one and the same stochastic region, because it contains a dense orbit (topological transitivity). The longest (unstable) periodic orbits are also dense in such a region and their Liapunov exponent asymptotically approaches the value for chaotic orbits.

For the hydrogen atom in a uniform magnetic field the Liapunov exponents are not independent of which Hamiltonian, (III·6)) or (III·53), we use for calculating the trajectories. The reason for this is that the transformation leading from (III·6) to (III·53) is not canonical. The relation between the Liapunov exponents λ_k based on the perturbed Kepler problem (III·6) and the Liapunov exponents λ_s based on the parabolic representation (III·53) can be derived by decomposing the transformation into two steps. In the first step a canonical transformation takes us from the cylindrical coordinates $\tilde{\rho}$, $\tilde{z}$ to the parabolic coordinates u, v as defined by Eq. (III·19). As shown by Meyer[77] such a transformation may lead to a modified Liapunov function $\tilde{\lambda}(t)$—and a modified stability matrix $\tilde{M}(t)$ — but the Liapunov exponent (III·56) defined in the infinite-time limit remains unchanged. In the second step we keep the coordinates and momenta —and hence also the stability matrix— unchanged, but rescale the time according to Eq. (III·52). Hence

$$\lambda_k=\lim_{t\to\infty}\frac{1}{t}\ln\|M(0,\ t)\|=\lim_{t\to\infty}\frac{1}{t}\ln\|\tilde{M}(0,\ t)\| \tag{III·64}$$

but

$$\lambda_s=\lim_{\tau\to\infty}\frac{1}{\tau}\ln\|\tilde{M}(0,\ \tau)\|\,. \tag{III·65}$$

Thus the relation between λ_k and λ_s can be written as

$$\frac{\lambda_s}{\lambda_k}=\lim_{t,\tau\to\infty}\frac{t}{\tau}=\lim_{t,\tau\to\infty}\frac{1}{\tau}\int_{\tau'=0}^{\tau(t)}2\tilde{r}(\tau')d\tau', \tag{III·66}$$

and obviously depends on the trajectory under consideration and, in particular, on the mean value of the radial distance $\tilde{r}=(1/2)(u^2+v^2)$. For periodic orbits Eq. (III·66) simplifies to

$$T_s\lambda_s=T_k\lambda_k, \tag{III·67}$$

where T_k is the period of the orbit in "natural time" t and T_s is *one half* of the corresponding period (that is of *half* a traversal in the u-v plane) in the rescaled time τ.

We now turn to a discussion of results obtained for the Liapunov exponents for the diamagnetic Kepler problem. In generating both the trajectories and the stability matrix it is useful to adopt the Taylor-series expansion method outlined by Meyer.[77] This procedure is suggested by the fact that, as in his problem of quartic oscillators, the potential appearing in the Hamiltonian (III·53) has a very simple polynomial form and hence higher-order derivatives can easily be determined analytically using the equations of motion. In the numerical computations of the trajectories with sufficiently small step sizes of rescaled time τ the elapsing of "physical" time t is followed by simultaneously integrating the relation (III·52).

Table III-1. Scaled energies ε_ν where the orbit I_∞ becomes unstable (with increasing ε) and energies s_ν where stability is regained. The energies i_ν give the onset of instability for the periodic orbits I_2, I_3, ···, I_7.

ν	ε_ν	s_ν	i_ν
2	−0.392	−0.328	−0.295
3	−0.273	−0.238	−0.244
4	−0.216	−0.195	−0.202
5	−0.182	−0.167	−0.174
6	−0.160	−0.150	−0.157
7	−0.142	−0.134	−0.140
8	−0.130	−0.123	—

The simplest periodic orbits are the straight line orbits I_1 perpendicular and I_∞ parallel to the direction of magnetic field. As shown by Wintgen[80] the orbit I_1 is stable up to a scaled energy ε_1, and the product of the Liapunov exponent λ_1 and the period T_1 of the orbit is then accurately proportional to the square

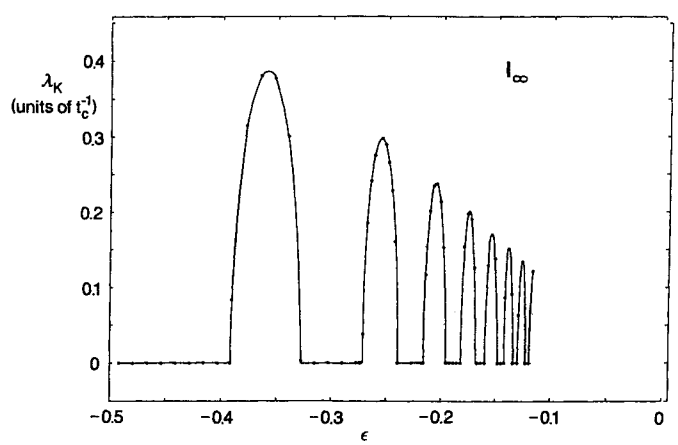

Fig. III-11. Liapunov exponent λ_k for the orbit I_∞ parallel to the magnetic field as a function of scaled energy.

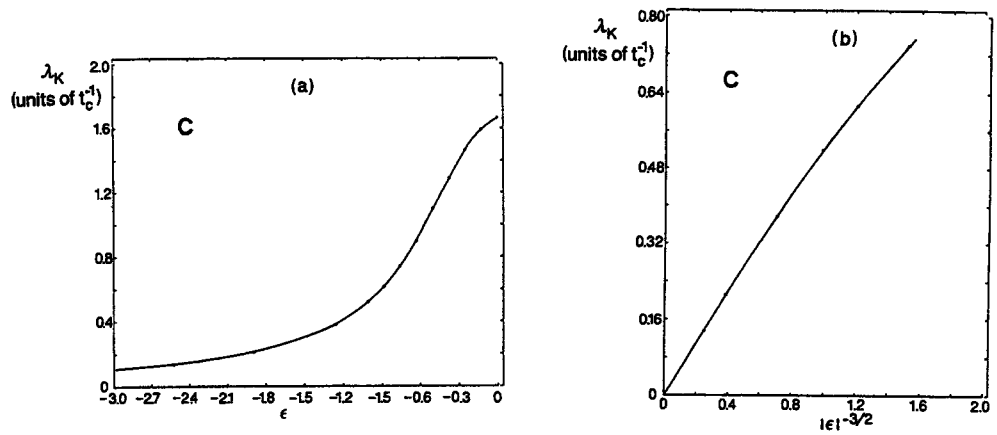

Fig. III-12. Liapunov exponent λ_k of the almost circular orbit as a function (a) of ε and (b) of $|\varepsilon|^{-3/2}$.

root of $\varepsilon-\varepsilon_1$. Present calculations yield $\varepsilon_1=-0.1272$ and

$$\lambda_1^2 T_1^2=13.61(\varepsilon-\varepsilon_1)\,. \tag{III·68}$$

(Note that by the invariance property (III·66) this result is independent of whether the computations are performed in "physical" or rescaled time.) For the periodic orbit I_∞ parallel to the magnetic field, the dependence of the Liapunov exponent on the scaled energy is much more complicated. Up to an energy $\varepsilon_2=-0.392$ the orbit is stable. Then intervals of instability and stability alternate*) and accumulate at the escape threshold $\varepsilon=0$ where the orbit becomes regular. The Liapunov exponent of the orbit I_∞ as a function of ε is displayed in Fig. III-11. The energies ε_2, ε_3, ε_4, $\cdots$ where the orbit becomes unstable, and the points s_2, s_3, s_4, $\cdots$ where it regains stability are given in the first two columns of Table III-1. Also note that the product $\lambda_\infty T_\infty$, which was plotted by Wintgen,[80] increases as a function of ε, while the Liapunov exponent λ_∞ itself, shown in Fig. III-11, decreases as ε tends to the ionization threshold.

As pointed out in Ref.80), and fully clarified in § V.3, the points of onset of instability ε_ν coincide with the "cut-off points" where the periodic orbits I_2, I_3, I_4, $\cdots$ begin to exist (see below), and these cut-off energies can be written as: [61),80)]

$$\varepsilon_\nu=-\frac{1}{2}(\nu-\alpha_\nu)^{-2/3} \tag{III·69}$$

with a weakly ν-dependent and converging set of "defect parameters" α_ν (see § V. 3).

Before we discuss the orbits I_2, I_3, I_4, $\cdots$ we turn our attention to the "almost circular" orbit C, which reduces to a circle in the field-free limit. As shown in the preceding subsection the orbit C corresponds to a hyperbolic fixed point, and can be considered the "germ" for chaos. As a matter of fact, the orbit C is unstable for all finite values of ε, as is also borne out by the explicit calculation of the Liapunov exponent. Figure III-12(a) shows the Liapunov exponent λ_C as a function of ε and

*) This result was first obtained by Sumetskii[79] by linearizing the second-order differential equation of ρ with respect to z and considering its "Bloch-like" solution.

Fig. III-12(b) shows λ_C as a function of $|\varepsilon|^{-3/2}$ for negative energies. Towards the field-free limit $\varepsilon \to -\infty$, λ_C is well reproduced by

$$\lambda_C = 0.55|\varepsilon|^{-3/2} . \qquad \text{(III·70)}$$

Benettin et al.[81)~83)] have studied various types of billiards and calculated Liapunov exponents. For systems which are regular for vanishing value of a non-integrability parameter p and become ergodic for finite values of p, Benettin[83)] finds a universal behaviour of the maximal Liapunov exponent, which for all billiards increases as $\sqrt{p}$ for small p. For a hydrogen atom in a uniform magnetic field it is actually the square, γ^2, of the field strength parameter which appears as the coefficient of the nonintegrable term in the Hamiltonian (III·18). Rewriting Eq. (III·70) as

$$\lambda_C = 0.55|E|^{-3/2}\sqrt{(\gamma^2)} \qquad \text{(III·71)}$$

shows that the hydrogen atom in a uniform magnetic field obeys Benettin's square-root law if we regard γ^2 as the non-integrability parameter for fixed energy E.*)

As mentioned above, the orbits I_2, I_3, ⋯ are born at certain energies where the orbit I_∞ becomes unstable and bifurcates (see below). Liapunov exponents of the orbits I_2, ⋯⋯, I_7 are shown as functions of scaled energy in Fig. III-13. The orbits are born stable but subsequently become unstable at the energies i_2, ⋯, i_7 which are tabulated in the last column of Table III-1. We make a comment on the dependence of Liapunov exponents on representation. Figure III-14 shows the Liapunov exponents λ_s of the orbits I_2, ⋯, I_7 in the $u-v$-representation. A striking feature is that, after the initial sharp rise following the onset of instability of each orbit, the values of λ_s rapidly converge to a common limiting curve. This indicates, that the rather large spread of the Liapunov exponents λ_k in the $\tilde{\rho}-\tilde{z}$-representation (see Fig. III-13) is related to the singular nature of the Coulomb potential.

*) There is an unpublished conjecture[118)] by Robnik from 1985 that generalizes Benettin's result in the following way: The square root scaling applies to the Liapunov exponent λ on every stochastic component, when a certain natural nondegenerate parametrization of the perturbation is chosen. One such natural nondegenerate parametrization p is defined by the requirement that at least one periodic orbit's period deviates linearly with p from its value at $p=0$ for small p. (Benettin has considered the systems that instantly become ergodic—there is only one stochastic component— upon an arbitrarily small perturbation $p \neq 0$. A generic KAM-system on the other hand has many stochastic components.)

The conjecture can be easily understood in terms of area preserving maps. The eigenvalues of the linear part of the iterated map near a periodic point are given by

$$\sigma = \frac{1}{2}\{\mathrm{Tr}M \pm \sqrt{(\mathrm{Tr}M)^2-4}\},$$

where M is the linear part of the iterated map. Recall that the longest periodic orbits, which are dense in a stochastic component, approximate the chaotic orbits asymptotically. Therefore we look at the behaviour of σ as a function of the perturbation parameter p. Assuming analyticity of M, specifically $\mathrm{Tr}M = 2+p+\text{h.o.t.}$, we find from the above equation that $\sigma = 1 \pm \sqrt{p} + \text{h.o.t.}$, so that

$$\lambda = \ln(1 \pm \sqrt{p}) \propto \sqrt{p},$$

which completes Robnik's demonstration. The numerical evidence in support of that was given by J. J. Burnett in 1986 in his unpublished Project Work[123)] on heart-shaped billiards.[124)]

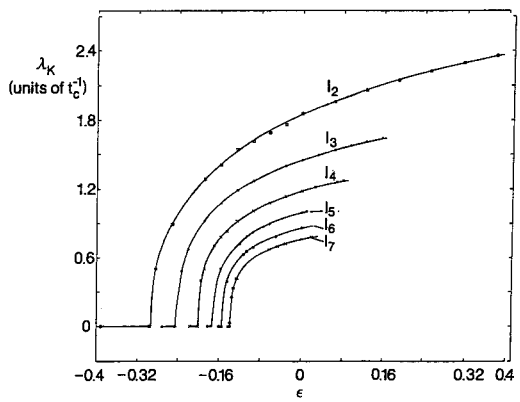

Fig. III-13. Liapunov exponents λ_k of the orbits I_2, I_3, ⋯, I_7 as functions of scaled energy.

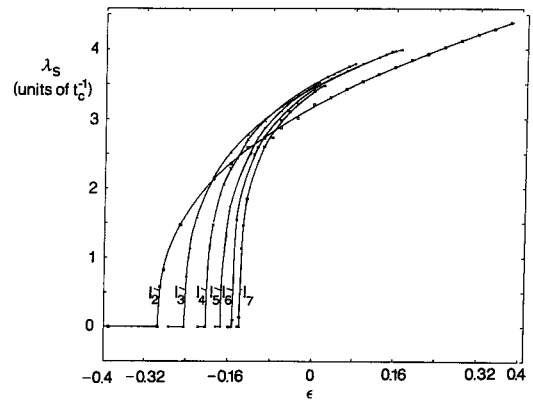

Fig. III-14. Liapunov exponents λ_s (obtained in the semi-parabolic representation with rescaled time) of the orbits I_2, I_3, ⋯, I_7 as functions of scaled energy.

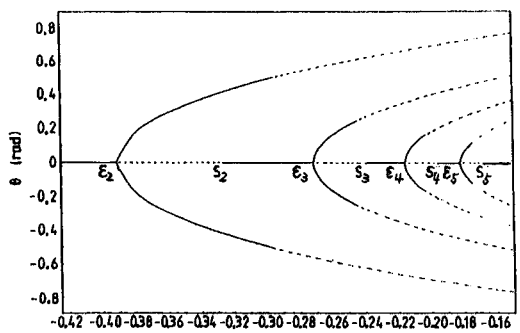

Fig. III-15. Bifurcation of the periodic orbit I_∞ into I_2 at ε_2, then regaining the stability at s_2, and into I_3 at ε_3, then regaining stability at s_3, etc. (from Al-Laithy and Farmer[112]).

The present result is now supplemented by an independent work by Al-Laithy and Farmer,[112] who did not use the concept of Liapunov exponents but still considered the behaviour of the stability matrix M by means of the *residue*,[113] $R=(1/4)(2-\mathrm{Tr}M)$, to investigate the instability of the I_∞-orbit (birth of the others) and its recovery. Their result relevant here for presenting the bifurcation can be shown most conveniently by the initial angle θ (in the cylindrical coordinates) of the orbit with respect to the B-axis, i.e., $\theta=\arctan(d\rho/dz)_{t=0}=\arctan(p_\rho/p_z)_0$, and is illustrated in Fig. III-15 with the present notation ε_ν and s_ν. For more details see Ref. 111) which is closely connected to the Bielefeld experiment discussed in § V.2.

Appendix to III.2: *The elliptic cylindrical coordinate*[66),69)]

A three-dimensional sphere of unit radius S^3 embedded in the four-dimensional coordinate space R^4 (u_1, u_2, u_3, u_4) satisfying

$$u_1^2+u_2^2+u_3^2+u_4^2=1 \qquad \text{(III·A1)}$$

can be described by the elliptic cylindrical coordinate (α, β, ϕ)−type I :[68]

$$u_1=\mathrm{sn}(\alpha, k)\mathrm{dn}(\beta, k')\cos\phi\,, \qquad u_2=\mathrm{sn}(\alpha, k)\mathrm{dn}(\beta, k')\sin\phi\,,$$
$$u_3=\mathrm{dn}(\alpha, k)\mathrm{sn}(\beta, k')\,, \qquad u_4=\mathrm{cn}(\alpha, k)\mathrm{cn}(\beta, k')\,, \qquad \text{(III·A2)}$$

where Jacobi's elliptic function for the α-variable has the modulus k $(0\leq k\leq 1)$ and

that for the β-variable has the modulus k', which is the *complementary modulus* of that for the α-variable, i.e., $k'=\sqrt{1-k^2}$. The elementary relations for these elliptic functions, $\mathrm{sn}^2(\alpha, k)+\mathrm{cn}^2(\alpha, k)=1$, $k^2\mathrm{sn}^2(\alpha, k)+\mathrm{dn}^2(\alpha, k)=1$, etc., are shown to satisfy the condition (III·A1). The following association of the u-variables with the ordinary phase space $(\boldsymbol{p}, \boldsymbol{r})=R^3\times R^3$, i.e.,

$$\boldsymbol{p}(p_x, p_y, p_z)=\frac{n}{r}(u_1, u_2, u_3), \qquad r(=\sqrt{x^2+y^2+z^2})=n^2(1-u_4),$$

$$\text{where} \qquad n=(-2E)^{-1/2}, \tag{III·A3}$$

establishes that the unit sphere condition (III·A1) is equivalent to the stationary bound Kepler motion $(1/2)\boldsymbol{p}^2-1/r=E(<0)$: This is the origin of the name *Fock hypersphere* for (III-A1).

The classical equations of Kepler motion, $\dot{\boldsymbol{r}}=\boldsymbol{p}$ and $\dot{\boldsymbol{p}}=-\boldsymbol{r}/r^3$, can be expressed in terms of the equations for the u-variables, in particular, in the canonical form, if the conjugate momenta p_u are defined by

$$\boldsymbol{p}_u(p_1, p_2, p_3, p_4)=n^2r(\dot{u}_1, \dot{u}_2, \dot{u}_3, \dot{u}_4), \tag{III·A4}$$

which also enable one to represent the angular momentum $\boldsymbol{L}$ and the Runge-Lenz vector $\boldsymbol{A}$ as (subscripts $i=1, 2, 3$ meaning the first three components)

$$\boldsymbol{L}(=\boldsymbol{r}\times\boldsymbol{p})=(\boldsymbol{u}\times\boldsymbol{p}_u)_{i=1,2,3}; \qquad \boldsymbol{A}=\frac{1}{n}(\boldsymbol{u}p_{u_4}-u_4\boldsymbol{p}_u)_{i=1,2,3}. \tag{III·A5}$$

The equations of the Kepler motion are thus formally written as

$$\dot{\boldsymbol{u}}=\frac{1}{n^2r}\boldsymbol{p}_u, \qquad \dot{\boldsymbol{p}}_u=-\frac{1}{r}\boldsymbol{u}, \tag{III·A6}$$

but under a certain condition that should reduce them to the original set.

Lakshmanan and Hasegawa[69] have shown that the elliptic cylindrical coordinate introduced by (III·A2) can be enlarged to a phase space equivalent canonically to the original $R^3\times R^3$. Namely, the following definition:

$$\begin{aligned} &p_{\alpha,\beta}=n^2r(k^2\mathrm{cn}^2\alpha+k'^2\mathrm{cn}^2\beta)(\dot{\alpha}, \dot{\beta}), \\ &p_\phi=n^2r\mathrm{sn}^2\alpha\mathrm{dn}^2\beta\dot{\phi} \end{aligned} \tag{III·A7}$$

yields the canonical momenta of (α, β, ϕ) by means of which the map $R^3\times R^3\to(S^3\times R^3)$ is a canonical transformation associated with the (bound) Kepler motion, where the three independent constants of motion can be given by $p_\phi=m$ (the angular momentum z-component) plus

$$\frac{p_\alpha{}^2+p_\beta{}^2}{k^2\mathrm{cn}^2\alpha+k'^2\mathrm{cn}^2\beta}+\frac{p_\phi{}^2}{\mathrm{sn}^2\alpha\mathrm{dn}^2\beta}=n^2, \tag{III·A8}$$

$$\frac{k'^2\mathrm{cn}^2\beta p_\alpha{}^2-k^2\mathrm{cn}^2\alpha p_\beta{}^2}{k^2\mathrm{cn}^2\alpha+k'^2\mathrm{cn}^2\beta}+\frac{k'^2\mathrm{cn}^2\alpha\mathrm{cn}^2\beta p_\phi{}^2}{\mathrm{sn}^2\alpha\mathrm{dn}^2\beta}=k^2n^2\Lambda. \tag{III·A9}$$

(III-A8) is the eccentricity relation $\boldsymbol{A}^2+n^{-2}\boldsymbol{L}^2=1$ whereas (III·A9) is shown to be the Runge-Lenz hyperboloidal relation (III·31) so that the choice $k=1/\sqrt{5}$ is adapted to

surviving the weak diamagnetic perturbation upon the motion.

It can be checked easily that both left-hand sides of (III·8, 9) are mutually involutive and that these two constants of motion reduce to two independent relations

$$p_\alpha{}^2=k^2n^2(1+\Lambda)+m^2-k^2n^2\mathrm{sn}^2(\alpha, k)-m^2/\mathrm{sn}^2(\alpha, k)\,,$$

$$p_\beta{}^2=-k^2n^2(1+\Lambda)-m^2+n^2\mathrm{dn}^2(\beta, k')+k^2m^2/\mathrm{dn}^2(\beta, k')\,.$$

But they can be singled out into one complex-analytic function

$$p_\zeta{}^2=k^2n^2(1+\Lambda)+m^2-k^2n^2\mathrm{sn}^2\zeta-m^2/\mathrm{sn}^2\zeta\,, \qquad \text{(III·A10)}$$

if $\zeta=\alpha$ on the real axis and $\zeta=i\beta+K+K'$ on the shifted imaginary axis.

This constitutes our basic recognition that the two-dimensional map on the Fock hypersphere $(\alpha, \beta)\to(p_\alpha, p_\beta)$ can be regarded as a complex analytic map: This fact assures that the action integration is described as the Cauchy integration (III·38b) from which all the important properties such as the sum rule can be deduced.

§ IV. Transition from regular to chaotic spectra

One of the positive contributions to knowledge of spectral fluctuations in the random-matrix theoretical framework[19),84)] from the investigation of the diamagnetic Kepler system is a direct observation that the regular spectrum (quadratic Zeeman spectrum) undergoes a smooth transition to a chaotic spectrum. In 1986, three groups of investigators[85)~87)] reported a result of comparison between the computed frequency histogram of the energy level nearest-neighbour spacing (NNS) and theoretical formulas of the distribution for the spacing, all in agreement with the so-called *Wigner surmise*[84)] in the fully developed chaotic regime (see Fig. IV-6). The concept of the *spectral rigidity*[19)] expressed by the quantity $\bar{\Delta}_3$ (Dyson-Mehta statistics[84)]) was also considered as an important indicator of the correlation properties of the spacings, and was found in general agreement with the prediction by the Gaussian Orthogonal Ensemble (GOE) theory[19),84)] in such a chaotic regime. However, more detailed comparisons have revealed that an appropriate theoretical formula which interpolates between the regular and the chaotic limits is lacking. In particular, Wintgen and Friedrich[41)] reported an explicit evidence that, near the regular limit, the computed frequency histogram does not fit the prediction by Berry and Robnik[37)] whose formula was devised on a sound basis of probability theory. Robnik,[40)] also Hasegawa, Mikeska and Frahm,[42)] argued a possible reason of this discrepancy. In particular, the latter authors proposed a remedy of the Berry-Robnik formula, which provided a considerable improvement of the fit to the computed histograms. This section is devoted to an account of the story with the aim towards a possible further development.

IV.1. *Some concepts from random matrix theory*

We consider a sequence of real numbers $\{x_1, x_2, \cdots, x_n, \cdots\}$ consecutively labelled, $x_n\leq x_{n+1}\leq\cdots$, which has the physical meaning of the eigenvalue energy sequence of a quantum system. All the x_n's are regarded as random variables, that is, they appear

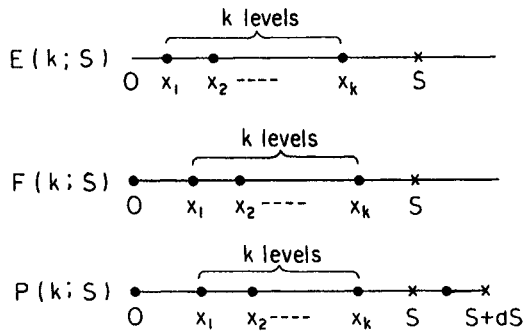

Fig. IV-1. Schematics to show the meaning of the three kinds of probabilities (or probability densities) $E(k;S)$, $F(k;S)$ and $P(k;S)$.

by chance so that for any subset of the sequence a probability $P(\{x_{n_i}\})dx_{n_1}\cdots dx_{n_r}$ is supposed to exist. It can be regarded also as a stochastic process with the discrete index set $\{n\in N\}$, and we assume that it is stationary with unit mean of the adjacent level-spacing

(a) $P(\{x_{n_i}\})=P(\{x_{n_i+m}\})$

(b) $\langle(x_{n+1}-x_n)\rangle=\int SP(S)dS=1$ with $\int P(S)dS=1$, where

$$\int P(\{x_{n_i}\})dx_1\cdots dx_{n-1}dx_{n+1}\cdots dx_N=\text{constant independent of } x_n$$

and $$\int P(\{x_{n_i}\})dx_1\cdots dx_{n-1}dx_{n+2}\cdots dx_N=\text{function of } (x_{n+1}-x_n)\equiv P(S),$$

$$S=x_{n+1}-x_n\,.$$

A typical class of such probability densities (or, in a respect, probabilities) is of those deduced from a fixed distribution of the Gaussian Ensembles, specifically, the GOE distribution.*) Mehta and des Cloizeaux[88] investigated a set of probabilities denoted by $E(k;S)(k=0,1,2\cdots)$, also two other related probabilities (and probability densities) $F(k;S)$ and $P(k;S)$, which have the following meaning:

$E(k;S)$: probability that an interval of length S contains k levels of the sequence $\{x_n\}$ (a level means any such x_n).

$F(k;S\}$: probability that an interval of length S *which starts at a level* contains k levels.

$P(k;S)$ (density of a spacing distribution): $P(k;S)dS$ represents the probability that an interval of length S which starts at a level contains k levels and, further, *the $(k+1)$th level lies in the interval* $(S, S+dS)$.

These definitions are illustrated in Fig. VI-1. We note that, once the definitions are fixed, these three probability sets are not necessarily restricted to those of the GOE origin. In general, the three sets are related to one another as follows (note that all these probabilities vanish for $S\to\infty$):

*) Some artifices are necessary for the deduction, because the GOE distribution by itself does not satisfy (a) and (b). For example, the "unfolding map" of the sequence is introduced to assure the constancy of $\int P(\{x_{n_i}\})dx_1\cdots dx_{n-1}dx_{n+1}\cdots dx_N$ (see Ref. 19)).

$$F(k\,;S)=\int_S^\infty [P(k\,;x)-P(k-1\,;x)]dx\,,\qquad k=1,2,\cdots,\tag{IV·1}$$

$$E(k\,;S)=\int_S^\infty [F(k\,;x)-F(k-1\,;x)]dx\,,\qquad k=1,2,\cdots,\tag{IV·2}$$

which can be extended to $k=0$ by defining $P(k\,;x)=F(k\,;x)\equiv 0$ for $k<0$. Or, conversely,

$$P(k\,;S)=-\frac{d}{dS}\sum_{j=0}^{k}F(j,S)\,,\qquad F(k\,;S)=-\frac{d}{dS}\sum_{j=0}^{k}E(j,S)\tag{IV·3}$$

and hence

$$P(k\,;S)=\frac{d^2}{dS^2}\sum_{j=0}^{k}(k-j+1)E(j\,;S)\,.\tag{IV·4}$$

If we specialize to the nearest-neighbour spacing, $k=0$, we have

$$P(0\,;S)=\frac{d^2}{dS^2}E(0,S)$$

or

$$E(0\,;S)=\int_S^\infty dx\int_x^\infty d\xi P(0\,;\xi)=\int_S^\infty xdxP(0\,;x)\left(1-\frac{S}{x}\right),\tag{IV·5}$$

the second representation yielding a simple probabilistic interpretation.[37]

In the beginning stage of the random matrix theories[84] the NNS distribution was expressed in the form

$$P(0\,;S)=[e^{-\int_0^S\mu(x)dx}]\cdot\mu(S)\,,\tag{IV·6}$$

where $\mu(S)$ has a probability assignment such that

$$\mu(s)ds=\text{prob. [a level lies in } (S,\,S+dS)\text{, given one at 0]}\,.\tag{IV·7}$$

Assuming that $\mu(S)$ satisfies $\lim_{S\to\infty}\int_0^\infty\mu(x)dx=\infty$, we also have

$$\int_S^\infty P(0\,;x)dx(=F(0\,;S))=e^{-\int_0^S\mu(x)dx}$$

$$=\text{prob. [there is no level in } (0,\,S)\text{, given one at 0]}\tag{IV·8}$$

so that a functional equation can be set up for $P(0,S)$[19] as

$$P(0\,;S)=\mu(S)\cdot\int_S^\infty P(0\,;x)dx\,.\tag{IV·9}$$

This says that the probability of the *NN*-spacing is the product of two probabilities: prob. [a level in $(S,\,S+dS)$]$\times$prob. [no level in $(0,\,S)$] under the condition of one level given at 0. Two typical examples are (hereafter, the number 0 will be omitted for the indication of *NN*):

$$\text{Possion distribution}\qquad P(S)=e^{-S}\,,\qquad \mu(S)=1\tag{IV·10}$$

and Wigner surmise $$P(S)=\frac{\pi}{2}Se^{-(\pi/4)S^2}, \qquad \mu(S)=\frac{\pi}{2}S. \tag{IV·11}$$

These satisfy two kinds of normalization as

$$\langle 1\rangle=1, \quad \langle S\rangle=1. \quad \text{(spacing normalization)} \tag{IV·12}$$

For each, the two related probabilities $F(0, S)$ and $E(0, S)$ are given by

Poisson distribution: $$F(S)=E(S)=e^{-S}, \tag{IV·13}$$

Wigner surmise: $$F(S)=e^{-(\pi/4)S^2}, \qquad E(S)=\mathrm{erfc}\left(\frac{\sqrt{\pi}}{2}S\right), \tag{IV·14}$$

where $$\mathrm{erfc}(x)=\frac{2}{\sqrt{\pi}}\int_x^\infty e^{-t^2}dt. \tag{IV·14a}$$

Berry and Robnik[37] introduced an ansatz concerning $E(S)$ to investigate intermediate situations between the two typical cases (IV·10) and (IV·11).

Consider that the phase space of a dynamical system (say, with two degrees of freedom) is partially filled by invariant tori and the rest by a chaotic domain, i.e., those situations we have seen in preceding sections, so that it is divided into two regimes, denoted by 1 (regular regime) and 2 (chaotic regime).

Ansatz. A sequence of (semiclassical) levels $\{x_n\}_1$ (computed from regular orbits) and a sequence of those $\{x_n\}_2$ (from chaotic orbits) are *statistically independent* of each other so that any sequence of mixed levels has a probability $E(S)$ of no level in $(0, S)$ given by

$$E(S)=E_1(S)E_2(S), \tag{IV·15}$$

where

$$E_1(S)=\frac{1}{\rho_1}e^{-\rho_1 S} \quad (P_1(S)=\rho_1 e^{-\rho_1 S}) \tag{IV·15a}$$

and

$$E_2(S)=\frac{1}{\rho_2}\mathrm{erfc}\left(\frac{\sqrt{\pi}}{2}\rho_2\right) \quad \left(P_2(S)=\frac{\pi}{2}\rho_2 Se^{-(\pi/4)\rho_2 S^2}\right), \tag{IV·15b}$$

in which the two constants ρ_i $(i=1, 2)$ measure the weight of the respective regime of the phase space ($\rho_1=0$ corresponds to fully chaotic).

Thus the ansatz provides us with an interpolation formula of $P(S)$ by

$$P(S)=\frac{d^2}{dS^2}(E_1(S)E_2(S)), \qquad \rho_1+\rho_2=1 \quad \text{from} \quad \langle S\rangle=1, \tag{IV·16}$$

as a one-parameter family of densities with the parameter $\rho_1(0\leq\rho_1\leq 1)$. This is shown in Fig. IV-2. The characteristic feature of this family lies in the probability density at 0-spacing $P(0)=\rho_1(2-\rho_1)$,[37] which shows that the level repulsion occurs only for the limit of the full chaos. This is in contradiction to the intuitive understanding that no matter how small a perturbation causes a level repulsion: What one

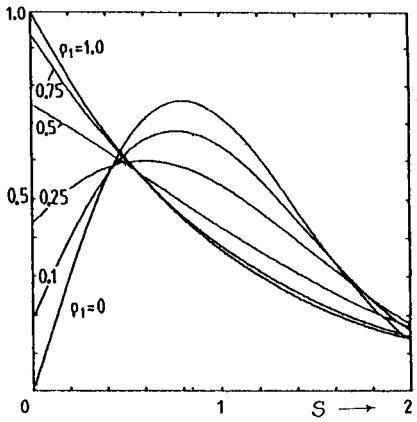

Fig. IV-2. One-parameter family of the nearest-neighbour spacing distribution according to the formula due to Berry and Robnik[37] for an interpolation between the Poisson ($\rho_1=1$) and the Wigner ($\rho_1=0$) distribution.

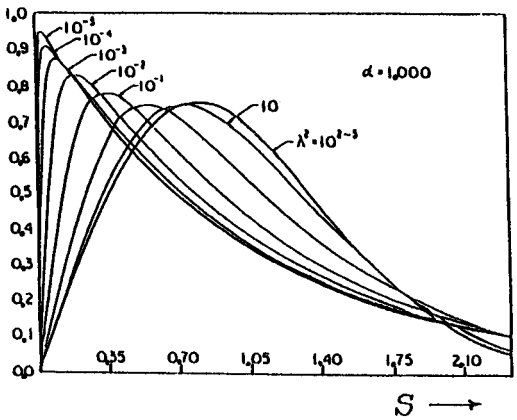

Fig. IV-3. One-parameter family of the nearest-neighbour spacing distribution according to the formula due to Hasegawa et al.[42] for an interpolation between the Poisson ($\lambda=0$) and the Wigner ($\lambda\gg1$) distributions. Still another parameter exists, α, which is fixed to be unity.

really expects is that $P(0)\neq0$ only for the regular limit $\rho_1=1$, and any deviation from this value makes $P(0)=0$ as shown in Fig. IV-3, and that the transition from the regular to chaotic spectra is nonanalytic in distribution at $S=0$. This must be the consequence of an appropriate inclusion of level fluctuations into the Berry-Robnik formulation.

IV.2. *Effect of level fluctuations on the spacing distribution*

Our starting point is the equation which relates the NNS distribution to the (conditional) level density $\mu(S)$, i.e., (IV·6), which we rewrite as

$$P(S)dS=[e^{-\int_0^S\mu(x)dx}]\mu(S)dS\,. \qquad \text{(IV·17)}$$

We consider the spacing variable S as a stochastic process with a continuous index set which is denoted by t as if it were a time variable, and the right-hand side of the above equation is equated to a random force just like writing a Langevin equation for a Brownian motion.[89] In the form of stochastic differential equations (SDE),[90] therefore

$$[e^{-\int_0^{S_t}\mu(x)dx}]\mu(S_t)dS_t=\sigma B(t)\,, \qquad \text{(IV·18)}$$

where $B(t)$ stands for the Brownian motion of unit strength (the strength is represented by a constant σ) defined by the expectation properties

$$\langle B(t)\rangle=0\,, \qquad \langle(B(t+dt)-B(t))^2\rangle=dt\,. \qquad \text{(IV·18a)}$$

We show two results about the stationary distribution of such a stochastic process defined by SDE: $f(S_t)dS_t=\sigma dB(t)$.

1st result. The SDE $f(S_t)dS_t=\sigma dB(t)$ can be converted into the standard form, i.e., $dS_t=[f(S_t)]^{-1}\sigma dB(t)$, if the multiplication of the differentials dS_t and $dB(t)$ by

any function of S_t (so-called multiplicative noise) is interpreted as in the Stratonovich sense (sometimes denoted as $\circ dS_t$, etc.).[91]

2nd result. The standard SDE $dS_t=a(S_t)\sigma dB(t)$ (Stratonovich), when rewritten in the equivalent Itô SDE $dS_t=(\sigma^2/2)a'adt+a\sigma dB(t)$, $a'(S)\equiv(d/dS)a$, has the stationary distribution of S_t (the stationary solution of the resulting Fokker-Planck equation), $P(S)\propto|a(S)|^{-1}$.

If the above results are applied to (IV·18) in the Stratonovich sense, the stationary distribution for S_t is just the originally assumed distribution for NNS, i.e., $P(S)=[e^{-\int_0^S\mu(x)dx}]\mu(S)$. This implies the fact that the NNS distribution, when affected by a single Gaussian white noise, remains unchanged on the average. The purely regular regime, or purely chaotic regime, can be regarded as this situation. Hence, for an intermediate situation of both regimes to coexist, we are led to the following:

Ansatz for fluctuations: Two Brownian motions $\sigma_1B_1(t)$ and $\sigma_2B_2(t)$, independent of each other, are associated to the regular regime with Poisson distribution (IV·15a) and to the chaotic regime with Wigner surmise (IV·15b), respectively, which affect the process S_t *additively*.

By this ansatz we now write a new form of SDE for the process S_t as

$$dS_t=\frac{\sigma_1}{P_1(S_t)}dB_1(t)+\frac{\sigma_2}{P_2(S_t)}dB_2(t)\,, \tag{IV·19}$$

where $P_i(S)=[e^{-\int_0^{S_t}\mu_i(x)dx}]\mu_i(S)\,,\quad i=1,2\,,$

i.e., $$P_1(S)=\rho_1e^{-\rho_1S}\,,\qquad P_2(S)=\frac{\pi}{2}\rho_2Se^{-(\pi/4)\rho_2{}^2S^2}\,. \tag{IV·19a}$$

(Again, each multiplicative noise is understood as Stratonovich.)

The stationary solution of the resulting Fokker-Planck equation is shown to be given by

$$P_\lambda(S)=N'\{\sigma_1{}^2\{P_1(S)\}^{-2}+\sigma_2{}^2\{P_2(S)\}^{-2}]^{-1/2}\,, \tag{IV·20}$$

$$=\frac{N}{\sqrt{\{P_2(S)\}^2+\lambda^2\{P_1(S)\}^2}}P_1(S)P_2(S) \tag{IV·20a}$$

with $\lambda=\sigma_2/\sigma_1\,.$

We note that the right-hand side expression of (IV·20) for the stationary solution is the inverse square-root of the diffusion coefficient D of the Fokker-Planck equation where $D=D_1+D_2$ of the constituent coefficients D_i associated with the respective noise $dB_i(t)$, $i=1, 2$.

It can be observed in the above formula that an important correlation property arises between the two regimes through the inverse square-root in (IV·20) in spite of the assumed independence of the two noises. Thus, for the two limiting cases: $P_{\lambda=0}(S)=P_1(S)$ and $P_{\lambda=\infty}(S)=P_2(S)$. The feature of this correlation is that it is capable of exhibiting the expected discontinuity at the 0-spacing which Fig. IV-3 in fact demonstrates.

Detailed analyses of the formula applied to the hydrogen atom in a magnetic field

are discussed in the next subsection. Here we only mention that $P_\lambda(S)$ is actually a two-parameter family of the NNS distributions: Besides $\lambda=\sigma_2/\sigma_1$, it depends on the ratio $\alpha=\rho_2/\rho_1$, i.e., the ratio of the average spacings, but our emphasis is that the key parameter to govern the regular-to-chaotic transition is λ which measures the *relative strength of the noises,* not of the spacings as was considered to be the case in the Berry-Robnik formulation. Some further remarks on the result relevant at the present stage are now in order.

(a) First, one may well ask if the regular regime of the diamagnetic Kepler system would really be subject to the Poisson statistics. The question should be examined in the context of Berry and Tabor's theory[92] because this predicts some important non-generic examples for which the NNS distribution differs from the Poisson, or even it does not exist. Indeed, the pure classical Kepler system must be precisely their non-generic case of non-existing statistics (equivalent to three harmonic oscillators of a common frequency). In order to assure the generic Poisson statistics it is necessary to examine the scaled level-density which includes the quadratic Zeeman spectra: A convincing answer to this question must be postponed.

(b) Interpolations between the regular to chaotic spectra for the correlation properties of the spacings (i.e., $\bar{\Delta}_3$-statistics) have to be deferred also, because it is necessary first to establish a reliable asymptotic form of the function $\mu(x)$ for $x\to\infty$ for the long-range correlation, which has been well studied by the GOE theory (the Wigner surmise, $\mu(x)\propto x$ is irrelevant since it only concerns a small x). We note that the recently developed dynamical theory by Pechukas,[30] Yukawa,[31] Nakamura and Lakshmanan[93] which succeeds to Dyson's Brownian motion model[29a] is promising for this purpose.*) The stochastic formulation[94),95] by which the result (IV·20) has been obtained is actually a consequence of the context of Yukawa's formulation; his equation of 'motion' on the same time-axis as Dyson first introduced. An important point is that the transition parameter $\lambda=\sigma_2/\sigma_1$ in the formula (IV·20) can be identified with Yukawa's temperature ratio[31] β/γ so that $\lambda^2=\beta/\gamma$ holds.

(c) The Gaussian ensemble theory covers not just the GOE: Another important category is GUE (Gaussian unitary ensembles) which applies to quantum systems without time reversal. In principle, diamagnetic Kepler systems must belong to such only because of the presence of the linear Zeeman term, but this commutes with the rest part of the Hamiltonian implying that the regular-to-chaotic transition occurs to GOE not to GUE. For these topics, the readers are referred to the description by Robnik.[33] The stochastic formulation should, however, be considered on an equal footing of both categories. It must be important when the statistics is extended to that of transition strengths for which the Porter-Thomas distribution[84] is a new subject of investigations.

IV.3. *Tests from the quantal diamagnetic Kepler problem*

In this subsection we discuss the quantum aspects of the transition from regularity to irregularity for the diamagnetic Kepler problem, or synonymously, the hydrogen atom in a strong magnetic field. We will present computed spectra of highly

*) Yukawa's theory[31] suggests that $\mu(x)=x[\lambda^2+x^2]^{-1/2}$ which has the asymptotic property $\mu(x)\xrightarrow{x\to\infty}1$. This is shown to yield the GOE characteristic of $\Delta_3(L)$ for a large spacing L.

excited states in strong laboratory fields (a few Tesla) and use them to search for symptoms of "quantum" chaos in the classically chaotic regime. In doing so, we will also test the concepts developed in the foregoing subsection. This will highlight the fact that the hydrogen atom in a strong magnetic field is indeed an ideal example of a simple but real physical system displaying all the features which are currently causing so much excitement in the classical and quantum mechanical study of nonintegrable systems.

The basic difficulty in solving the Schrödinger equation belonging to the Hamiltonian of the diamagnetic Kepler problem for *arbitrary* diamagnetic strength lies in the fact that the spherical symmetry of the Coulomb potential, on the one hand, and the cylindrical symmetry of the magnetic field on the other, prevent a separation of variables so that closed-form analytical solutions are not possible in general. One is therefore forced, in the complete quantum theoretical treatment of the problem, to resort to numerical methods. To obtain "exact" (as opposed to variational) solutions it is suggestive to invoke basis function expansions which are inspired by the symmetries of the limiting cases $B\to 0$ and $B\to\infty$. These are, in the first case, expansions in terms of oscillator functions in semi-parabolic coordinates (adapted to the $SO(2,2)=SO(2,1)\oplus SO(2,1)$ dynamical symmetry of the Coulomb problem, cf. Englefield,[96] or expansions in terms of spherical harmonics and a set of complete radial functions (ordinary $SO(3)$ symmetry), while the case $B\to\infty$ suggests expansions in terms of Landau functions with a complete longitudinal basis. The different expansions are employed depending on whether one approaches the intermediate-field regime from the side of low or intense fields, and overlapping results are expected in the transitional region.

Except at very high fields ($\gamma\geq 0.05$),[97] calculations using the Landau function expansion have confined themselves so far to low-lying states. The longitudinal parts of the wavefunctions were determined by direct integration of the system of coupled differential equations that follow from Schrödinger's equation.[98] By contrast, calculations using expansions based on the field-free group properties have been performed for both low-lying and highly excited states, and in this case energies and wavefunctions were obtained by either direct integration, or diagonalization of the Hamiltonian matrix in large basis sets. In our own computations in this regime we expanded the wavefunctions in terms of spherical harmonics, $\psi_m=\sum h_l(r)\,Y_{l,m}(\theta,\phi)$ (m is the magnetic quantum number), and the radial functions in the complete, orthonormal set of functions

$$G_{nl}^{(\zeta)}(r)=\zeta^{3/2}\left[\frac{n!}{(n+2l+2)!}\right]^{1/2}\exp[-\zeta r/2](\zeta r)^l L_n^{(2l+2)}(\zeta r)\,, \qquad \text{(IV·21)}$$

where ζ denotes an inverse-length parameter, and the $L_n^{(2l+2)}$ are generalized Laguerre polynomials. Matrix elements with respect to this basis can be expressed in closed analytical form and give rise to a banded Hamiltonian matrix which can be diagonalized by efficient standard algorithms. Our choice of basis bears some resemblance with the Sturmian basis used previously by Edmonds[15] and Clark and Taylor[14] but avoids the difficulties associated with the nonorthogonality of the latter. As compared to the oscillator basis in semi-parabolic coordinates (used, e.g., by Delande and

Gay,[99] and, extensively, by Wintgen and Friedrich[100]), where the diagonalization produces eigenstates each of which belongs to a different value of the magnetic field strength (solutions are obtained in the E-B plane along straight lines E/B=const), in our basis one diagonalization procedure yields the spectrum at *fixed* B, in accordance with most experimental situations. In our calculations we used basis sizes of up to 220000 for determining both eigenvalues and eigenvectors of all states up to the ~950th excited state in given m-parity subspaces in the strong-field regime. Convergence was established by varying the size of the basis and the scale parameter ζ.

As a result of our efforts we are able to calculate the energies and oscillator strengths of Rydberg states in laboratory fields of a few Tesla up to the field-free ionization threshold $E=0$. To demonstrate the quality of our computations we present, in Fig. IV-4, a comparison, in different energy intervals, between the experimental spectrum of $\Delta m=0$ Balmer transitions to $m=0$, even-parity Rydberg states of deuterium taken by the Bielefeld group (Holle et al.[18]) at $B=5.96$ Tesla, and the corresponding theoretical spectrum computed by us. The interval considered in Fig. IV-4 covers a range of energy where one lies deeply in the n-mixing regime. The agreement between theory and experiment can be considered excellent; moreover, theory reveals where neighbouring lines were no longer resolved in the experiment. We note that the comparison of relative intensities is slightly marred by the fact that saturation effects occurred in the experiment in strong lines. As one moves further up in energy in Fig. IV-4, the line density clearly grows and the structure of the spectrum becomes increasingly complicated. Nevertheless it is also here that we find practically complete agreement between theory and experiment, with the experiment being limited, as regards the number of detectable lines, by the finite resolution. This is particularly evident from Fig. IV-5, which shows a direct comparison between the experimental and theoretical spectra in the range $-24\,\mathrm{cm}^{-1}$ to $-12\,\mathrm{cm}^{-1}$ at 6 Tesla. The broad experimental feature around $-13\,\mathrm{cm}^{-1}$, e.g., is found to be composed of ~10 lines of different intensities.

All in all we have compared successfully more than 1800 lines so far in the π and σ spectra in the strong-field regime, and this certainly can be considered a hallmark of modern quantitative spectroscopy in magnetic fields.

Taking a look at Fig. III-8 one recognizes that in the ranges of energy covered by Figs. IV-4 and IV-5 the classical counterpart of the quantum system under investigation undergoes the transition from regularity to chaos. It is suggestive, then, to ask whether or not fingerprints of this transition are visible in the quantal spectra. Evidently, the oscillator strength spectra convey a *qualitative* impression of the increasing complexity of the quantal spectrum as one penetrates into ranges of energy where classical motion becomes more and more chaotic.

To put the notion of increasing complexity of the quantal spectrum in the classically chaotic region on a more *quantitative* footing, however, it is useful to undertake a statistical analysis, in the spirit of Bohigas et al.[28] of the level fluctuations of the sequence shown in Fig. IV-4. Our results for the distribution of the spacings of adjacent energy levels, and the results of the Dyson-Mehta $\bar{\Delta}_3$ statistics for the nearest-neighbour spacings, in three successive energy intervals have been presented elsewhere (Wunner et al.[87]). The histograms of the nearest-neighbour

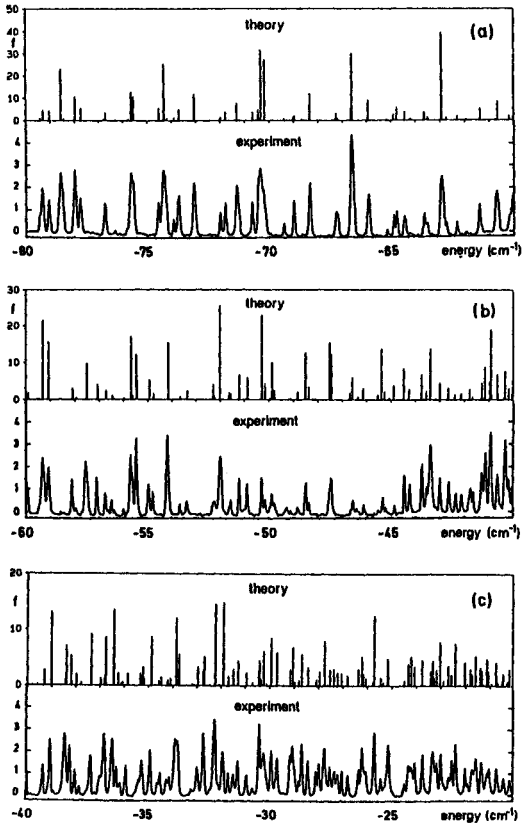

Fig. IV-4. Deuterium Rydberg atoms in a magnetic field of 5.96 Tesla : comparison between the theoretical oscillator strength spectrum and the experimental photoabsorption spectrum (Holle et al.[19]) for $\Delta m=0$ Balmer transitions to $m=0$, even-parity final states, over the range of energy from $-80\,\mathrm{cm}^{-1}$ to $-20\,\mathrm{cm}^{-1}$. The oscillator strengths are given in units of 10^{-6}, the experimental intensity scale is in arbitrary units. A total of 267 theoretical lines contributes to the spectrum shown. Note that at the end of the energy range classical motion becomes completely irregular (cf. Fig. III-8). (The exact value of γ for which the theoretical calculation was performed is $\gamma=2.5350\cdot10^{-5}$, and the mass scaling for deuterium is taken into account.)

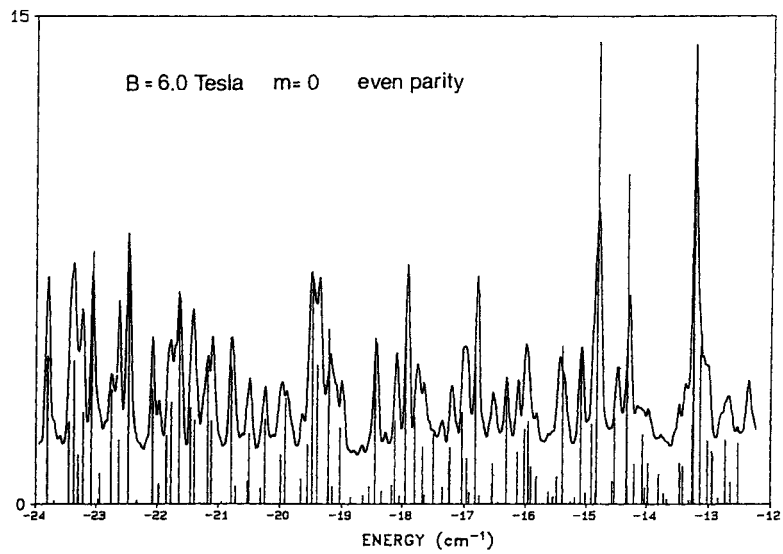

Fig. IV-5. Comparison between the experimental spectrum and the theoretical photoabsorption spectrum of $\Delta m=0$ transitions from $2p_0$ to even parity final Rydberg states with energies between $-12\,\mathrm{cm}^{-1}$ and $-24\,\mathrm{cm}^{-1}$ in a magnetic field of 6 Tesla. For the theoretical results (straight lines) the ordinate respresents the oscillator strength in units of 10^{-6}. The experimental results have kindly been provided by the Bielefeld group[70]. Note that the wealth of theoretical spectral structure can no longer be resolved by the experiment. The range of energy shown lies in the domain of chaotic motion of the corresponding classical system.

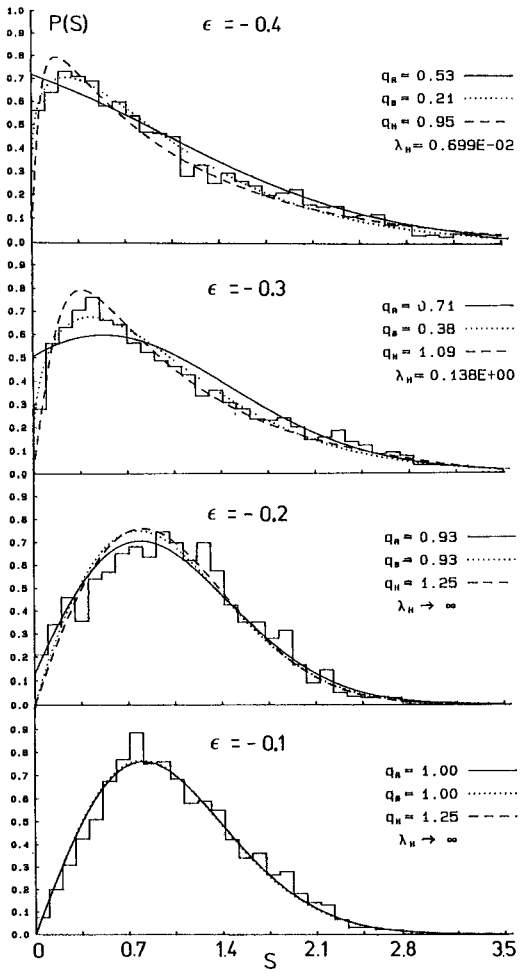

Fig. IV-6. Nearest neighbour energy spacing histograms for hydrogen Rydberg levels calculated at different values of the scaled energy ε. The smooth curves show the results of least-squares fits to the histograms using different fit formulae (solid line: Berry and Robnik formula, dotted line: Brody formula, dashed line: Hasegawa's stochastic formula, evaluated for α=1). The q and λ values denote the corresponding best fit parameters.

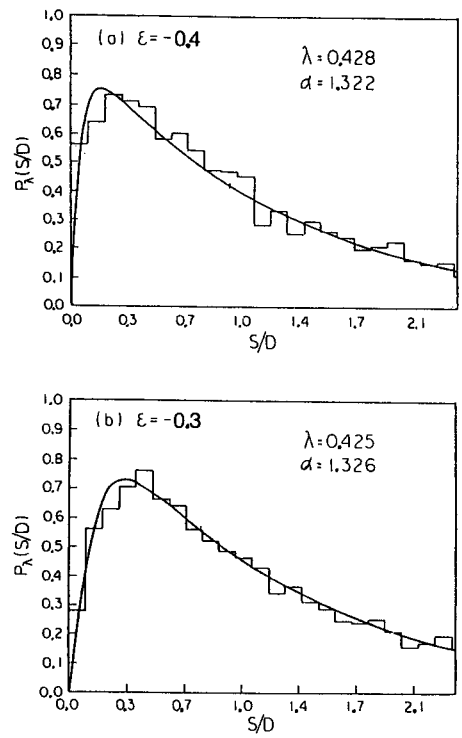

Fig. IV-7. Same as Fig. IV-6, but with the results of the stochastic fit formula obtained by varying both λ and α. Note that the overshooting near maximum is slightly mitigated by additionally varying α.

distributions exhibit a clear transition from a Poisson-like to a Wigner-like distribution as one proceeds to intervals of energies where classical motion becomes increasingly irregular. In an analogous manner the $\bar{\Delta}_3$ statistics display a transition from the Poisson case to that characteristic of the predictions of random-matrix-theory (Gaussian orthogonal ensemble, GOE). A Poisson form of the nearest-neighbour histogram implies maximum probability, and a Wigner form zero probability, for finding two levels at the same energy value. Therefore level *clustering* (~ uncor-

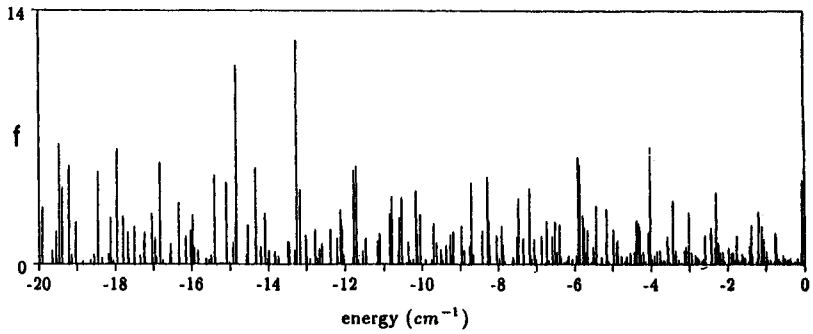

Fig. IV-8. Oscillator strength spectrum of $\Delta m=0$ Balmer transition from $2p_0$ to evenparity Rydberg states with energies between $-20\,\mathrm{cm}^{-1}$ and the field-free ionization limit at a field strength of 5.96 Tesla (oscillator strengths in units of 10^{-6}). In our computations convergence of the f values is obtained to within a few percent. The range of energy shown lies in the domain of chaotic motion of the classical hydrogen atom.

related energy levels) proves characteristic of quantum systems in the classically regular regime, while level *repulsion* (~correlated levels) proves typical of quantum systems in the classically chaotic regime. The universality of the characterization of the onset of "quantum" stochasticity by these level fluctuation rules, which had before only been found in model systems such as the stadium problem or the Sinai billiard, is thus reinforced also in magnetic Rydberg atoms. This finding was confirmed by independent work of Wintgen and Friedrich[85] and Delande and Gay.[86]

Here we will concentrate on the test of the fit formula for nearest-neighbour spacing histograms derived in the foregoing subsection adopting a stochastic differential equations approach (see (IV·19a, 20a)). The normalisation constant, N, and ρ_1 can be eliminated from (IV·19a, 20a) by the conditions $\langle 1\rangle=1$, $\langle S\rangle=1$ (S is the level distance). Limiting forms of the stochastic formula are the Poisson distribution ($\lambda=0$) and the Wigner distribution ($\lambda\to\infty$). The formula does contain the desired nonanalytic behaviour at $S=0$: $P_\lambda(0)$ is finite for $\lambda=0$, while $P_\lambda(0)=0$ for any $\lambda\neq 0$. The parameter $\alpha(=\rho_2/\rho_1)$ can be interpreted as representative of the nonuniversal behaviour of the specific system under consideration in the transition region between complete regularity and irregularity.

We have tested the usefulness of the stochastic formula by performing least-squares fits to the histograms for the nearest neighbour-distributions of the energy levels of the hydrogen atom in a magnetic field at fixed scaled energies $\varepsilon=-0.4$, -0.3, -0.2, and -0.1 as given by Wintgen and Friedrich.[41] Figure IV-6 shows the results obtained choosing $\alpha=1$. It is seen that the stochastic formula is indeed able to produce reasonable fits to the histograms also in the near-regular regime. Also shown in Fig. IV-6 are the results which we obtained using the Berry-Robnik[37] formula, and the empirical Brody[101] formula. The "overshooting" effect of the stochastic formula near maximum is mitigated if in addition to λ we also vary α in the fitting process. The results obtained in this way are shown in Fig. IV-7, and reveal the potential of the stochastic formula. Further tests involving larger data sets are under way.

As a final point we want to report results of the search for a signature of classical

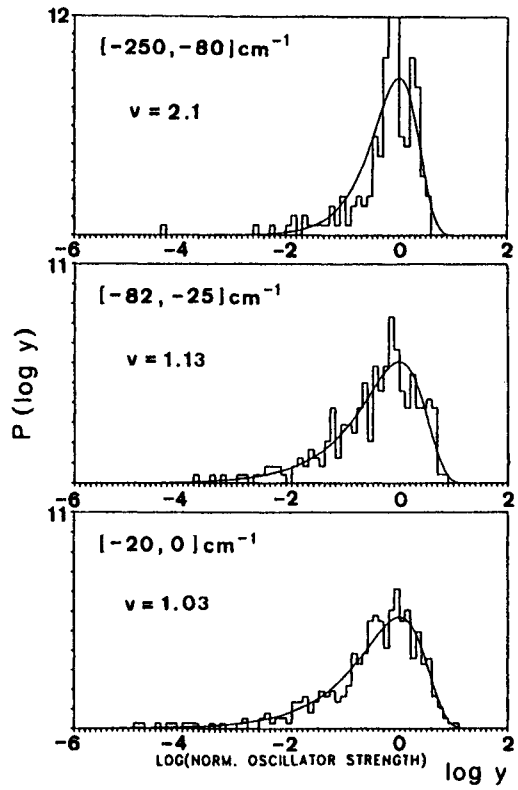

Fig. IV-9. Three histograms of computed Balmer transition strengths at 5.96 Tesla and their fits (continuous curves) by the Alhassid-Levine form of $P(y)$. Each panel gives the energy range of the final Rydberg states. In the classical system, motion changes from near-regular over near- irregular to irregular, as one passes through these intervals. In the quantum system we find a decrease of ν towards a value close to 1 (the Porter-Thomas limit). Oscillator strengths have been scaled by the secular variation prior to binning and normalized in such a way that $\bar{y}=1$. On the vertical axis, $P(\log y)$ is given in units of 10^{-2}.

chaos in the statistical properties of *transition strength spectra* of hydrogen atoms in strong magnetic fields in the chaotic regime, that is we go beyond investigating energy level sequences and look at quantities that are related to wavefunctions in a sensitive way.

Figure IV-8 shows, for a magnetic field strength of 5.96 Tesla, our computed oscillator strength spectrum of the $\Delta m=0$ dipole transitions from $2p_0$ to even-parity Rydberg states with energies from $-20\,\mathrm{cm}^{-1}$ up to the field-free ionization limit. Remember that at this field strength, classical motion becomes irregular around -25 cm^{-1}. In quest of further manifestations of chaos in quantal spectra we have analyzed the fluctuations of oscillator strengths of Balmer transitions to Rydberg states in the near-regular, near-irregular, and irregular regime. Following Alhassid and Levine[102] we consider the probability $P(y)dy$ of finding a value y of the strength of an allowed transition from a given state to an arbitrary final state between y and $y+dy$. For a structureless spectrum the maximum-entropy principle, together with the completeness relation of the states and the normalization condition, implies the Porter-Thomas form*) for $P(y)$, viz., $P(y)\propto\exp(-y/2\bar{y})/\sqrt{y}$. For situations where structures in the spectrum impose additional constraints we adopt the form $P(y)\propto y^{(\nu-1)/2}\exp(-\nu y/2\bar{y})/\sqrt{y}$. Here ν denotes a parameter characterizing the deviance of

*) This is cited from the paper by C. E. Porter and R. G. Thomas, Phys. Rev. **104** (1956), 483 given in Ref. 84).

y from its averaged value $\bar{y}$ (see Ref. 102) for details). Figure IV-9 shows three histograms of computed oscillator strengths of Balmer transitions to Rydberg states in a magnetic field of 5.96 Tesla and their fits by this functional form. In the three energy ranges of the final states covered in Fig. IV-9 classical motion changes from almost completely regular to irregular. The results presented in Fig. IV-9 reveal an increase in the spreading of the fluctuations of the quantal oscillator strengths as this change takes place in the classical system. Correspondingly ν decreases from top to bottom in Fig. IV-9, and in particular, we find that the fluctuations in the spectrum shown in Fig. IV-8 are best fitted by a value of $\nu=1.03$, that is a value very close to the Porter-Thomas limit for the GOE chaotic spectra. The characteristic differences in the distributions of transition strength fluctuations between classically regular and chaotic parameter ranges evident from Fig. IV-9 confirm findings[102] for transition strengths in a Hénon-Heiles-type model system. Our results thus point to another universal signature of classical chaos in the spectra of quantal systems.

§ V. Current topics

V.1. *Aspects of recent experiments——regular spectra* ——Problem of Semiclassical Quantization——

Experimental and theoretical investigations of the diamagnetic Stark spectra (parallel fields) on Li atoms have been performed and reported by the Orsay group (Cacciani, Luc-Koenig, Pinard, Thomas and Liberman),[103),104] which are one of the finest spectroscopy at present relevant to the 'pre-chaos' diamagnetic Kepler (DK) problem. In the pure diamagnetic case, the reported experiments revealed the existence of the two regions of the DK motion first predicted by Solov'ev[12] in terms of the Runge-Lenz hyperboloid. The underlying semiclassical quantization by which the authors obtain a theoretical tool for analyses is Solov'ev's formula (III-38c), which should be clarified from the analytic viewpoint in § III : There was a puzzling feature of this formula in that the action integral contains a *discontinuity* at $\Lambda=0$, i.e., at the hyperbolic point of the unique separatrix line to separate the two regions. Consequently, the above authors adopted a special device of modifying the formula so that a unique, continuous universal relationship can be constructed between the normalized action variable x and the hyperboloidal value, Λ, i.e., $\Lambda=\Lambda(x)$. This matter is discussed here with a view of possible necessity of consolidating the theory of Maslov indices.

Solov'ev's action integral is recited with an indication of the integration ranges, which consist of three ; I, II and III (following Cacciani et al.[104]), denoted by j_{I}, j_{II} and j_{III}, respectively. In the absence of an electric field, $j_{\mathrm{I}}=j_{\mathrm{II}}$ and

$$j_{\mathrm{I}}(\Lambda)=\frac{1}{\pi}\int_{\vartheta_1}^{\vartheta_2} L_\perp(\vartheta\,;\Lambda)d\vartheta \qquad \text{and} \qquad j_{\mathrm{III}}(\Lambda)=\frac{1}{\pi}\int_{\vartheta_3}^{\vartheta_4} L_\perp(\vartheta\,;\Lambda)d\vartheta\,, \tag{V·1}$$

where

$$L_\perp(\vartheta\,;\Lambda)=\left[n^2\left(1+\frac{\Lambda}{1-5\sin^2\vartheta}\right)-\frac{m^2}{\sin^2\vartheta}\right]^{1/2}$$

with $k^2=1/5$ in (III·38c). See Fig. V-1.
For $m=0$, $j_{\rm I}$ reduces to an integral over the range $\vartheta\in[0, \vartheta_2]$. Then,

$$\frac{1}{n}j_{\rm I}(\Lambda)=\frac{1}{\pi}\int_0^{\vartheta_2}\sqrt{1+\frac{\Lambda}{1-5\sin^2\vartheta}}\,d\vartheta\,, \qquad 0<\vartheta_2\leq\sin^{-1}\frac{1}{\sqrt{5}} \tag{V·2a}$$

[non-zero, real value only for $\Lambda\leq 0$, with $\vartheta_2=\sin^{-1}\sqrt{(1+\Lambda)/5}$]

and

$$\frac{1}{n}j_{\rm III}(\Lambda)=\frac{1}{\pi}\int_{\vartheta_3}^{\pi-\vartheta_3}\sqrt{1+\frac{\Lambda}{1-5\sin^2\vartheta}}\,d\vartheta\,, \qquad \sin^{-1}\frac{1}{\sqrt{5}}\leq\vartheta_3<\frac{\pi}{2} \tag{V·2b}$$

[non-zero, real value only for $\Lambda\geq 0$, with $\vartheta_3=\sin^{-1}\sqrt{(1+\Lambda)/5}$].

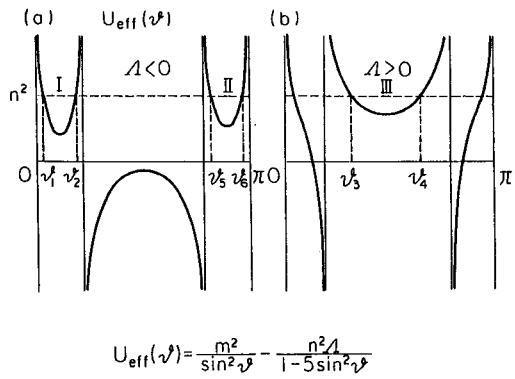

Fig. V-1. Indication of the ranges of Solov'ev's integration (V·1) in terms of the effective potential $U_{\rm eff}(\vartheta)$: $L_\perp(\vartheta)=\sqrt{n^2-U_{\rm eff}(\vartheta)}$.

Twice of $2j_{\rm I}(\Lambda)(=j_{\rm I}+j_{\rm II})$ and $j_{\rm III}(\Lambda)$ are drawn in Fig. V-2(a) in the range $-1\leq\Lambda\leq 4$, which exhibits a conspicuous discontinuity at $\Lambda=0$. Since Λ is the quantity proportional to the diamagnetic energy shift to first order (in γ^2), the discontinuity of the action variable vs Λ could be regarded as spurious, i.e., a relabelling of the energy terms versus a parameter of an otherwise smooth variation of the energy. A simple remedy of this situation which Cacciani et al.[104] devised is to replace $2j_{\rm I}(\Lambda)$ by its *complement*: $2j_{\rm I}(\Lambda)\mapsto n-2j_{\rm I}(\Lambda)$. This makes the gap between the two integrals (V-2a) and (V-2b) vanishing at $\Lambda=0$, in view of

$$\frac{1}{n}j_{\rm I}(0)=\frac{\vartheta_0}{\pi}=\frac{1}{\pi}\sin^{-1}\left(\frac{1}{\sqrt{5}}\right) \quad \text{and}$$

$$\frac{1}{n}j_{\rm III}(0)=\frac{2}{\pi}\sin^{-1}\left(\frac{2}{\sqrt{5}}\right). \tag{V·3}$$

Consequently, a smooth, continuous curve is obtained of the function $x=x(\Lambda)$, $-1\leq\Lambda\leq 4$, as in Fig. V-2(b) which, upon interchange of the abscissa and ordinate, could be regarded as a consecutive relabelling of the energy terms against the variable x. The crosses plotted associated to the resulting curve show, as a matter of fact, a good agreement of the observed peaks ($n=32$, odd parity manifold of Li given in Fig. V-3) with the curve thus obtained.

We now show that the modified relation between the action x and the diamagnetic energy shift Λ which the Orsay group has adopted, aiming at the unique universal DK structure in any Rydberg multiplet, can be put in a single, analytic formula in § III, i.e.,

$$x=\frac{j_\xi}{n}=\frac{2}{\pi}\int_0^{\theta_0^*}\sqrt{\frac{4-\Lambda-4\sin^2\theta^*}{5-4\sin^2\theta^*}}d\theta^*, \tag{V·4}$$

where $\theta_0^*=\frac{\pi}{2}$ for $-1<\Lambda\leq 0$, (V·4a)

$=\sin^{-1}\sqrt{1-\frac{1}{4}\Lambda}$ for $0\leq\Lambda<4$. (V·4b)

Or, by the sum rule presented in (III·49) and proved successively,

$$1-x=\frac{j_z}{n}=\frac{2}{\pi}\int_0^{\theta_0}\sqrt{\frac{1+\Lambda-\sin^2\theta}{5-\sin^2\theta}}d\theta, \tag{V·5}$$

where $\theta_0=\sin^{-1}\sqrt{1+\Lambda}$ for $-1<\Lambda\leq 0$, (V·5a)

$=\frac{\pi}{2}$ for $0\leq\Lambda<1$. (V·5b)

This shows that the unique, universal DK structure of the energy vs action (here the universality referring to the irrespectiveness of the principal quantum number of each multiplet) is fully expressed in the integral along one elementary cycle (either γ_α or γ_β in Fig. III-4) for any allowed value of Λ. If conversely speaking, Solov'ev's action integral can be regarded as exhibiting a *transfer* from the integral along one cycle to the other by a change of the sign of Λ, then, what characterizes this transfer? The answer is: It always retains a contour-integration type with two *caustics*. Namely, both $j_{\rm I}$- and $j_{\rm III}$-integrations involve two caustics where the integrand vanishes and its derivative with respect to Λ becomes singular, as can be seen in Fig. V-1. However,

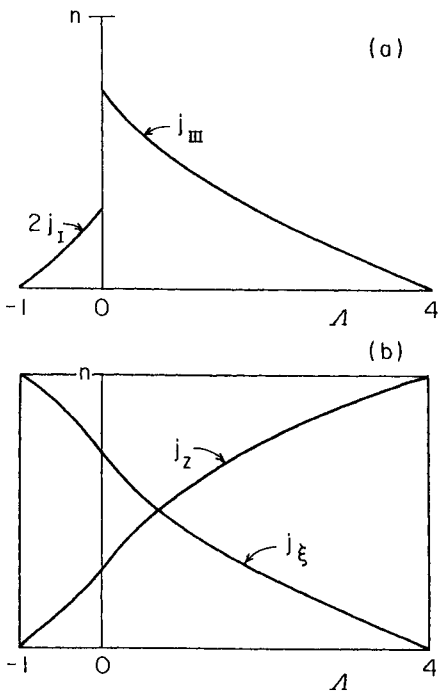

Fig. V-2. Relation between Solov'ev's action integral (V·1) and the analytic action integral (V·4a) (or V·4b). (a) Solov'ev's one given piecewise for $-1<\Lambda\leq 0$ and for $0\leq\Lambda<4$ with a discontinuity at $\Lambda=0$. (b) Analytic action integrals $j_\xi(\Lambda)$ and $j_z(\Lambda)=n-j_\xi(\Lambda)$. It is customary to associate Λ with the third quantum number K defined consecutively from the top value of the diamagnetic splitting energy (i.e., $\Lambda_{\rm max}=4$) downwards, which amounts to the identification $K=j_\xi$.

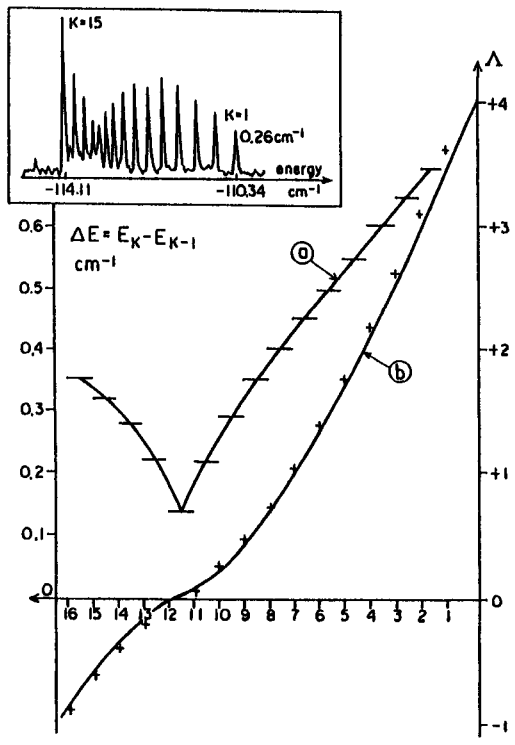

Fig. V-3. Comparison of the observed energy terms of Li ($n=32$, odd parity multiplet) with the universal diamagnetic-Kepler relation between $\Lambda=\Lambda(x)$ (after Cacciani et al.[103]). Curve (a) shows a spacing between the consecutive energy terms which exhibits a cusp-like minimum at $\Lambda=0$ to be compared with a theoretical prediction from (V·4, 5). Curve (b) shows the direct comparison of the plot Λ, experimentally deduced, with the predicted curve $\Lambda=\Lambda(x)$ with $nx=j_\ell$. The spectral profile cited is in the same reference, but $n=31$.

this raises a rather difficult question about the theory of Maslov indices as discussed below.

The Maslov index α for a given action integral is defined by the number of (directed) caustics along the closed trajectories by which the integration is carried out, and $\alpha=2$ means that the motion involved is *libration*-like while $\alpha=0$ *rotation*-like, which gives the distinction between a half-integer quantum number and a full integer one in the associated semiclassical quantization rule.[105] The question about which characteristic the regular DK motion does possess has been discussed with a view that the motion of the Runge-Lenz vector $\boldsymbol{A}$ is libration-like for $\Lambda<0$ and rotation-like for $\Lambda>0$ (along the $\boldsymbol{B}$-axis—see, for example, the review article by Gay[11]). This view must be modified now to say more precisely that

the major component z shows a libration, but associated with it exists

a rotation of the minor component ρ *for* $-1<\Lambda<0$

and

the major component ρ shows a libration, but associated with it exists

a rotation of the minor component z for $0<\Lambda<4$.

One can state the situation rigorously for the special case $m=0$ (then, ρ is replaced by the full-plane coordinate ξ) by profiting the $z-\xi$ duality in § III which extends to the libration-rotation characteristic.

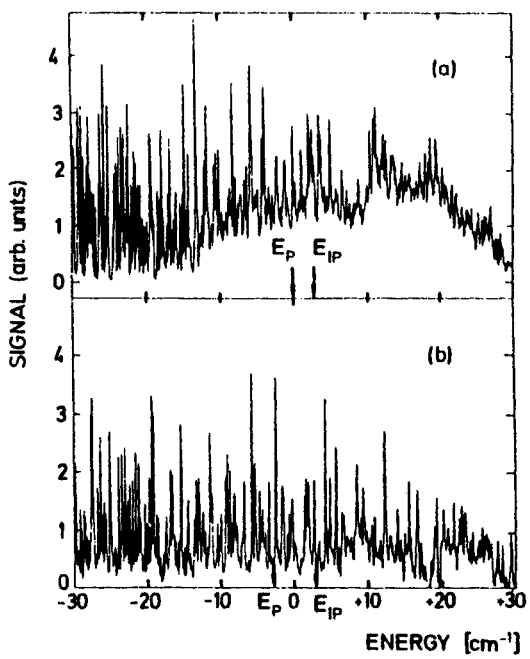

Fig. V-4. Photoabsorption spectra of $\Delta m=0$ Balmer transitions from $2p_0$ (a) and $2p_{-1}$ (b) to even-parity Rydberg states of the hydrogen atom in a magnetic field of 5.96 Tesla. Note that classical motion is practically fully chaotic in the energy range covered (cf. Fig. III-8). $E=0$ is the field-free ionization limit, E_{IP} is the actual ionization potential including the Landau zero-point energy, E_P gives the size of the (paramagenetic) linear Zeeman shift. (From Main et al.[70])

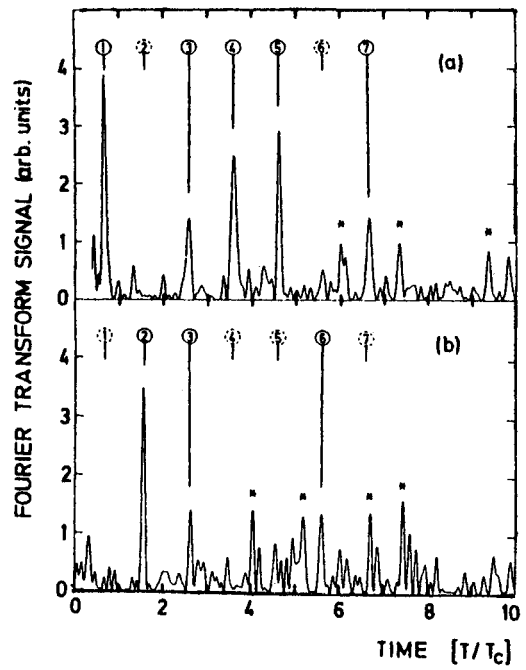

Fig. V-5. Fourier transforms (squared) of the spectra (a) and (b) of Fig. V-4. The labels $\nu=1, 2, \cdots$ correspond to the recurrence times of the classical orbits I_ν. (From Main et al.[70])

The nature of the rotation or libration in the regular DK motion has been discussed in a series of papers by Delos et al.[106] with a conclusion[107] that the Maslov index α should be 2 irrespective of the presence of the rotation component, and the same conclusion has been reached by other authors.[108] We agree with it. However, then there should be a remark about action integrals like (V·4, 5) which involve a libration-rotation transition. There must exist a rule by which such a transition can be judged as real or spurious, and at present the answer is lacking.

V.2. *Aspects of recent experiments—resonances in chaos*

The most challenging problem of the diamagnetic Rydberg atoms for the past two decades—since Garton and Tomkins[7]—has been to establish a satisfactory understanding of the resonances of photoabsorption spectra in a range near the ionization limit which belongs, as is clear now from the foregoing analyses, to the full classical-chaos regime. Latest progress of laser spectroscopy has attained a revision of the original Garton-Tomkins experiment on Ba I such that the ultra-high excited states with principal quantum numbers ~500 can be resolved on which up to 180 quasi-

Landau resonances are measurable for a weak field of 0.0736 Tesla : Rinneberg and coworkers[109] reported this result, confirming the almost equal resonance-spacing $\Delta E \sim 1.5\hbar\omega_c$ around $E=0$ associated with the typical periodic orbit. Prior to this report, however, an essential progress in the understanding of the nature of such quasi-Landau resonances has been provided by the Bielefeld group :[18),70)] Namely, the periodic orbits are not restricted to the Garton-Tomkins type, instead essentially an infinite set of those exist which correspond to I_1, I_2, $\cdots$, I_∞ of the discussion in § III·4 and possibly more, where I_1 of the planar periodic one is associated with the Garton-Tomkins resonance (see Fig. III-6). Such an additional resonance has been observed in Ba I also by Rinneberg et al.[109] Hence we will discuss this subject here and in the next subsection.

Welge and coworkers[18),70)] excited *hydrogen* (or *deuterium*) Rydberg states by resonant two-photon absorption (vuv, vacuum ultraviolet; uv, ultraviolet), $H(n=1)+\text{vuv}\rightarrow H(n=2)+\text{uv}\rightarrow H^*$, in magnetic fields from ~4 to 6 Tesla. Figure V-4 shows π excitation spectra of H-atom Balmer transitions to Rydberg states around $E=0$ taken at $B=5.96$ Tesla. The additional quasi-Landau resonances become visible in the Fourier transforms of the photoabsorption spectra as obvious peaks (see Fig. V-5). The peak denoted by 1 corresponds to the Garton-Tomkins resonance ($\Delta E=1.5\hbar\omega_c$) while the spacings of the new resonances are found to be given by 0.64, 0.39, 0.28, 0.22, 0.18 $\hbar\omega_c$, respectively.

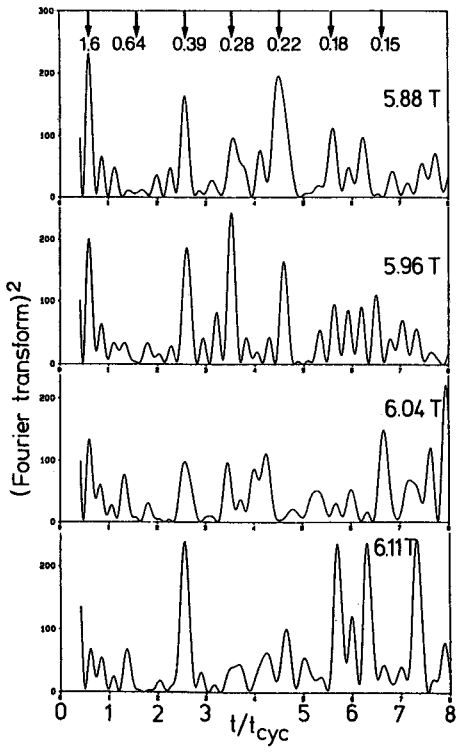

Fig. V-6. Fourier spectra of the theoretical photoabsorption spectra with $m=0$ in the range $-35\,\text{cm}^{-1}$ to $-13\,\text{cm}^{-1}$ for four slightly different magnetic field strengths around 6 Tesla. Peaks are indicative of corresponding quasi-periodic classical orbits with different frequencies (given in units of the cyclotron frequency in the top frame). Note the structural change in the transforms at small variations of the magnetic field strength.

The resonances were first rationalized in terms of a model by Reinhardt[110] who proposed an interpretation of the Garton-Tomkins oscillatory behaviour of the photoabsorption cross section in Heller's linear-response formula of the dipole μ,

$$\sigma(\omega)\propto\frac{\omega}{2\pi}\int_{-\infty}^{\infty}e^{i\omega t}\langle 0|\mu(0)\mu(t)|0\rangle dt\,, \tag{V·6}$$

by considering the recurrent peak-off of the autocorrelation function of μ whose Fourier transform yields $\sigma(\omega)$: The physical process of the atomic electron initially localized in the low-lying orbital in response to the optical excitation into the near-ionization regime would be

a constant repetition of tracing a large orbit ejected from the core returning again to it whose period, designated as a *recurrent time* T, just characterizes the resonance: $\omega=2\pi/T$. Reinhardt demonstrated in his simplified calculation of the autocorrelation function (assuming that it is zero after the first recurrence), and hence the cross section, that the proposed picture really holds.

The important result now is that, being motivated by the model, the Bielefeld group extended the idea to non-planar orbits, which in the present notation correspond to I_2, I_3, $\cdots$ up to I_7 for interpreting the observed additional resonances. The Bielefeld group then constructed[61] both by means of numerical integration and of a simple analytic model the expected orbits and their quantization to deduce several characteristic numbers which are to be compared with the observed data. A significant point in connection with Reinhardt's idea is that the initial condition of the integration they chose was $\rho=0$, $z=0$ for the coordinate (i.e., the atomic electron initially located at the atomic core) together with their momenta on which the condition of recurrence was imposed, thus expressing the actual physical situation. The same model to predict additional resonances was proposed also by Al-Laithy et al.[111),112)]

One should bear in mind that according to Fig. III-13, the classical orbits I_1, I_2, $\cdots$ assume nonvanishing Liapunov exponents in the range of parameters used in the experiment. That is, *unstable* classical periodic orbits present in the otherwise completely irregular regime are found to give rise to modulations in the quantal spectra with frequencies equal to their classical orbital frequencies. The peaks are of course also present in the Fourier transforms of the computed theoretical spectra. Moreover, the Fourier spectra of the theoretical photoabsorption spectra shown in Fig. V-6 for four slightly different magnetic field strengths reveal a strong sensitivity of the strengths of the peaks to small variations of the magnetic field, indicative of the fact that the photoabsorption spectra themselves are highly sensitive to small variations of an external parameter (here the magnetic field strength) in the classically near-irregular and chaotic regime. The point is related to a highly important issue concerning the difference between classical and quantal chaos involving the *break time*, as discussed in § II, and to the question whether the observed spectra are to be classified into the quasi-periodic spectra or something beyond it of the 'intrinsic' chaos.

At this time, however, we have to postpone a relevant judgement after more clarification of the information from experiment, and we outline in the next subsection the analytic model of the periodic orbits: We aim to substantiate many matters in § III in terms of the observational reality.

V.3. *A simple model of periodic and quasi-periodic orbits*

The model is based on a truncation of the Hamiltonian (III·18) by the expansion of the Coulomb potential

$$-\frac{1}{\sqrt{\rho^2+z^2}}=-\frac{1}{|z|}+\frac{\rho^2}{2|z|^3}+O(\rho^4/z^5) \tag{V·7}$$

valid for $|\rho/z|<1$. (V·7a)

The discussion to follow stems from Main, Holle, Wiebusch and Welge[61] supplemented by the present authors (Hasegawa and Kuwata).[114] The first term of the expansion in (V·7) yields the truncation into two fully separate dynamics consisting of a (2-dimensional) harmonic oscillation and a 1-dimensional Kepler motion: For $p_\varphi=0$, $H=H_\rho+H_z$ with

$$H_\rho\equiv\frac{1}{2}p_\rho{}^2+\frac{1}{2}\left(\frac{\gamma}{2}\right)^2\rho^2=E_\rho\,, \tag{V·8}$$

$$H_z\equiv\frac{1}{2}p_z{}^2-\frac{1}{|z|}=E_z\,. \tag{V·9}$$

If one goes to the next higher-order term in the expansion, H_ρ in (V·8) is replaced by

$$H_\rho=\frac{1}{2}p_\rho{}^2+\frac{1}{2}\left(\left(\frac{\gamma}{2}\right)^2+\frac{1}{|z^3|}\right)\rho^2\,, \tag{V·8′}$$

which amounts to a modulation of the harmonic-oscillator frequency $\gamma/2$ by the time-dependent perturbation, $1/|z|^3$, of the z-motion: The effect makes the frequency $\gamma/2$ tend always to increase. We will take into account this effect by an adiabatic approximation later, and before doing so first let us examine the possible periodic orbits under the aforementioned initial condition, i.e., starting at the origin at $t=0$, assuming the full separation.

For the harmonic oscillation, one simply has

$$\rho=\rho_0\sin\left(\frac{\gamma}{2}t\right),\qquad p_\rho=\frac{\gamma}{2}\rho_0\cos\left(\frac{\gamma}{2}t\right);\qquad \rho_0=\left(\frac{2}{\gamma}p_\rho\right)_{t=0}, \tag{V·10}$$

which can be reorganized by the action J_ρ and the energy E_ρ as

$$J_\rho=\frac{1}{2\pi}\oint_{\rho>0\ \text{half plane}}p_\rho d\rho=E_\rho/\gamma\,;\qquad E_\rho=\frac{\gamma^2}{8}\rho_0{}^2\,. \tag{V·10a}$$

(Note that the allowed phase space consists of the positive half ρ-p_ρ plane.) For the Kepler motion, one can exploit a parameter representation of the coordinate vs time by means of an angle ψ (the so-called eccentric anomaly with eccentricity unity) such that

$$z=z_0\sin^2\frac{\psi}{2}\,,\qquad p_z=\left(\frac{2}{z_0}\right)^{1/2}\cot\frac{\psi}{2}\,;\qquad z_0 \text{ is related to the energy } E_z \text{ by}$$

$$E_z\left(=\frac{1}{2}p_z{}^2-\frac{1}{|z|}\right)=\frac{-1}{z_0}\qquad (z_0>0 \text{ assumed})\ <0\,. \tag{V·11}$$

Here, the time variable t is related to ψ via $dt=(z_0/2)^{3/2}2\sin^2\psi/2\ d\psi$ by

$$t=\left(\frac{z_0}{2}\right)^{3/2}(\psi-\sin\psi)$$

$$=J_z{}^3(\psi-\sin\psi)\,, \tag{V·11a}$$

this second representation being a consequence of the action J_z as

$$J_z=\frac{1}{2\pi}\oint_{(z<0 \text{ half plane})} p_z dz=(z_0/2)^{1/2}=(-2E_z)^{-1/2} \quad \text{or}$$

$$E_z=-\frac{1}{2J_z^2}. \tag{V·11b}$$

Thus, by virtue of (V·11a), one can show the orbit in the ψ-representation:

$$\rho=\rho_0\sin\left[\frac{\gamma}{2}J_z^3(\psi-\sin\psi)\right], \qquad z=z_0\sin^2\frac{\psi}{2}, \tag{V·12}$$

which provides us with a means to express the condition of recurrence. Namely, let the electron be ejected at $\psi=0$. Then, the first recurrence of z occurs at $\psi=2\pi$ on which $\rho=0$ is imposed. This results in all the simplest recurrent orbits characterized by an integer ν so that

$$\gamma J_z^3=\nu, \qquad \nu=1, 2, \cdots \quad \text{which is designated as "}\nu\text{-type".} \tag{V·13}$$

By this is meant that, during the completion of one Kepler orbit along z, the motion of ρ executes ν-times oscillation, for which the total action must be defined by

$$J=\nu J_\rho+J_z. \tag{V·14}$$

It can be seen that Eqs. (V·13, 14) together with the individual energy vs action relation are sufficient, in principle, to find the answer to the condition of resonance. We need, however, to take into account the ρ-z coupling by adopting the Hamiltonian (V·8′) for improving purpose.

Our approach is the "adiabatic perturbation", so to speak. By the adiabatic approximation we mean that the effect of the z-motion on the ρ-oscillation will be treated by regarding $z(t)$ as a slowly-varying external field, and by the perturbation that the coupling, $(1/2)|z|^{-3}\rho^2$ in (V·8′), is weak: This latter condition is clearly not true for $|z|\lesssim\rho$, but we think it still worthwhile to investigate this approach.

Consider the action integral (V·10a), and the effect of such an adiabatic modulation of the frequency γ involved. The adiabaticity implies that the effect is expressed entirely as a change of energy $E_\rho(\gamma)\to E_\rho(\gamma+\delta_\gamma)$ without modifying J_ρ (just the adiabatic invariance of the action!), thus

$$E_\rho=(\gamma+\delta_\gamma)J_\rho=\frac{1}{8}(\gamma+\delta_\gamma)^2\rho_0^2. \tag{V·15}$$

We compute the correction of energy $\delta_\gamma J_\rho$ by the perturbation theory in classical mechanics,[49] obtaining

$$\delta_\gamma=\frac{1}{J_\rho}\left\langle\frac{1}{2}|z(t)|^{-3}\rho^2(t)\right\rangle_{T_\rho}, \tag{V·16}$$

where $\langle\ \rangle_{T_\rho}$ is an average over the trajectory of ρ-oscillation in an appropriate period T_ρ. This period T_ρ is generally different from the minimum unperturbed period $4\pi\gamma^{-1}$ of the oscillation because of the presence of $|z(t)|^{-3}$ which is not periodic with this period: The appropriate period can be selected from the condition (V·13) of the ν-type periodic orbit to be given by

$$T_\rho=2\pi\nu\gamma^{-1} \quad \text{(consistently to } T_\phi=2\pi \text{ for } z(\phi) \text{ in (V·12))}. \tag{V·17}$$

Apart from the change (V·15) and (V·17), the foregoing analysis to deduce the resonance condition is unchanged, which is now summarized:

$$\text{total energy} \quad E=(\gamma+\delta_\gamma)J_\rho-\frac{1}{2}J_z^{-2}, \tag{V·18a}$$

$$\text{total action} \quad J=\nu J_\rho+J_z, \tag{V·18b}$$

$$\text{condition of recurrence} \quad (\gamma+\delta_\gamma)J_z^3=\nu; \quad \nu=(1)^*, 2, 3, \cdots. \tag{V·18c}$$

(*Case $\nu=1$ must be replaced by the *two-dimensional model* in § III.1.)

We introduce the "ν-th defect parameter", δ_ν following Main et al.,[61] to represent the condition for "ν-type resonance": δ_ν is a negative shift of the integer $\nu(=2, 3, \cdots)$ which is regarded as induced by the positive frequency shift δ_γ, and we define it as

$$\delta_\nu=J_z^3\delta_\gamma. \tag{V·19}$$

Then, from (V·18c)

$$\gamma J_z^3=\nu-\delta_\nu, \quad \text{and hence} \quad \frac{\gamma+\delta_\gamma}{\gamma}=\frac{\nu}{\nu-\delta_\nu}, \tag{V·20}$$

which enables us to dispose J_z and hence J_ρ from (V·18b) to get the E vs J relation as follows:

$$E=\frac{J\gamma}{\nu-\delta_\nu}-\frac{3}{2}\left(\frac{\gamma}{\nu-\delta_\nu}\right)^{2/3}.$$

We have two equivalent ways of representing the above result, namely,

$$I_\nu \quad \begin{cases} \text{(a)} \quad J\gamma^{1/3}=(\nu-\delta_\nu)E\gamma^{-2/3}+\frac{3}{2}(\nu-\delta_\nu)^{1/3}, & \text{(V·21a)} \\ \text{(b)} \quad J^2E=\frac{J^3\gamma}{\nu-\delta_\nu}-\frac{3}{2}\left(\frac{J^3\gamma}{\nu-\delta_\nu}\right)^{2/3}. & \text{(V·21b)} \end{cases}$$

The second version is just the *extended scaling law of Feneuille,* i.e., (III·13) with the universal function f defined for each ν-type resonance as

$$\epsilon=f_\nu(\beta), \quad \epsilon\equiv J^2E \quad \text{and} \quad \beta=J^3\gamma \quad \text{with} \quad f_\nu(\beta)=\frac{\beta}{\nu-\delta_\nu}-\frac{3}{2}\left(\frac{\beta}{\nu-\delta_\nu}\right)^{2/3}. \tag{V·21b′}$$

Graphs of these representations are shown in Fig. V-7 from Ref. 61). Note that the $\nu=1$ Feneuille function is given exactly in terms of the Φ-function in § III.1.

An important aspect of Fig. V-7 is the ability of the two formulas (V·21a, b) to indicate the "birth" of the ν-th periodic orbit I_ν as a consequence of the instability of the special orbit I_∞, as discussed in § III. 4 (Fig. III-15[112] and Eq. (III·69)):

$$I_\infty \to I_\nu \quad (\nu=2, 3, \cdots) \tag{V·22}$$

$$\text{which occurs at the scaled cut-off energy} \quad \varepsilon_c^{(\nu)}=-\frac{1}{2}(\nu-\delta_\nu)^{-2/3}. \tag{V·22a}$$

Table V-1. The "defect parameter" α_ν (or δ_ν[61]) from experiment and computations.

ν	α_ν(exp)	α_ν(calc)[a]	α_ν(calc)[b]	α_ν(calc)[c]
2	0.43	0.56	0.56	0.35
3	0.42	0.49	0.52	0.33
4	0.40	0.46	0.48	0.31
5	0.38	0.44	0.45	0.30
6	0.39	0.43	0.48	0.29
7	0.34	0.42	0.39	0.28

α_ν(exp) from Ref. 70): It is related to the cut-off energy $\varepsilon_c^{(\nu)} = -1/2(\nu-\alpha_\nu)^{-2/3}$. α_ν(calc), a) from Ref. 80), b) from Table III-1, c) from (V·23).[114]

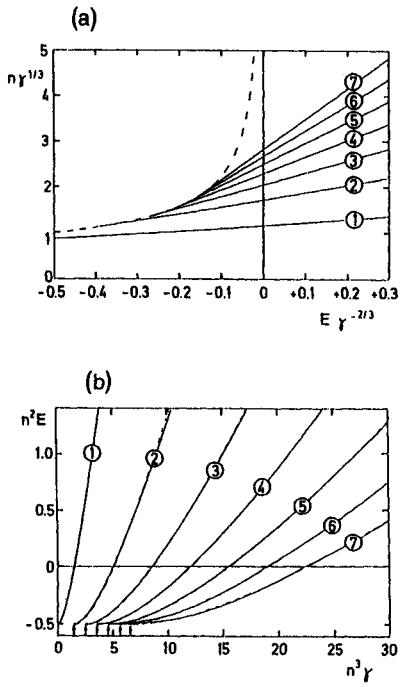

Fig. V-7. Two ways of representing the relation between the total energy E and the total action J for the "ν-type" resonance after Main et al.[61] ($J=n$ in the present notation). (a) The encircled number represents the lines for $\nu=1, 2, \cdots, 7$, fitted by (V·21a) with δ_ν computed from the EBK quantization. The dashed line shows the pure Rydberg relation $n\gamma^{1/3}=(-2E\gamma^{-2/3})^{-1/2}$. (b) The same fit by (V·21b) (dashed lines). Arrows indicate the cut-off point $\beta_c^{(\nu)}=\nu-\delta_\nu$. Case $\nu=1$ is based on the Feneuille function (ad hoc) in the "2-dimensional model".

In Fig. V-7(a), the J vs E relation for the pure Kepler orbit along the B-axis, $J_z=(-2E)^{-1/2}$, appears as the envelope of the straight tangent-lines of (V·21a) showing that a change of orbit takes place along each tangent line, while Fig. V-7(b) shows that this occurs at the cut-off energy (V·22a) as the minimum of each Feneuille function f_ν against β at $\beta_c^{(\nu)}=\nu-\delta_\nu$, where I_ν is "born". In this connection, we present an analytic formula[114] for δ_ν based on (V·16, 19, 20):

$$\delta_\nu=\frac{1}{2\nu\pi}\int_0^{2\pi}\frac{\sin^2[\nu(\phi-\sin\phi)/2]}{\sin^4(\phi/2)}d\phi\,. \qquad \text{(V·23)}$$

Table V-1 summarizes their numerical values together with those in the literature.

The present discussion suggests an extended construction of more complex

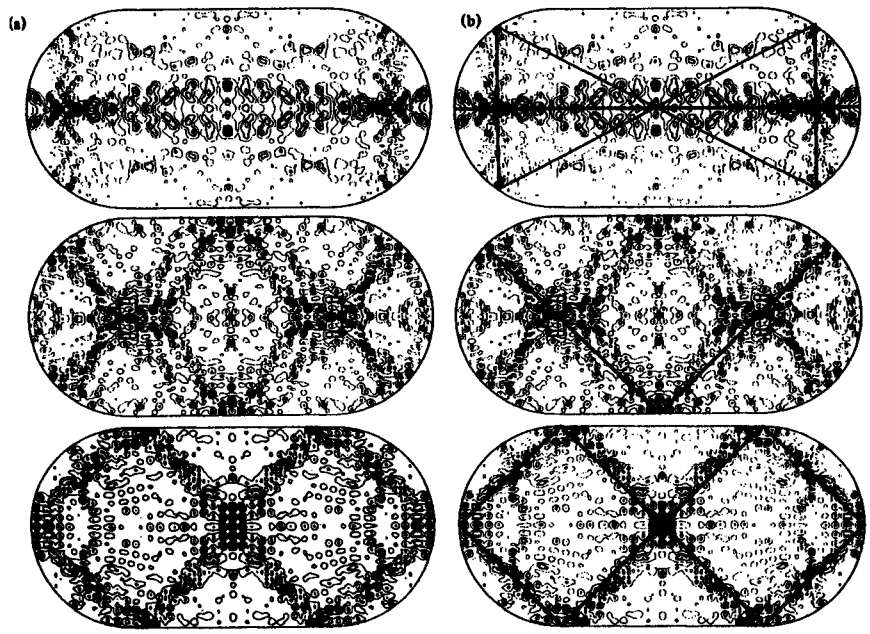

Fig. V-8. Examples of scars in the stadium. (Taken from Heller.[43])

periodic orbits or quasi-periodic*) orbits in which, e.g., the first recurrence of the z-Kepler motion does not allow the recurrence of the ρ-oscillation but the l-th z-recurrence meets the m-th ρ-one with l and m being *incommensurate*. Studies in this direction have been undertaken,[75),115)] not just for imagination, but for assigning purpose[115)] of the actual peaks in the spectra. These must lend themselves to a future description, and we will turn to the subject of eigenfunctions next.

V.4. *The eigenfunctions of the classically chaotic systems*

The bound state eigenfunctions of classically ergodic Hamilton systems possess a much less organized structure than those of the classically integrable systems. In fact they have been predicted to be random such that according to Voros[116)] the corresponding mean probability density is determined by the microcanonical Wigner (phase space) function in the semiclassical limit when $\hbar \to 0$.

It is easy to extract the essential information from the semi-classical eigenfunctions of the integrable systems (II·34). It must be recalled that the actual eigenfunction is a sum of finite numbers of contributions of the form (II·34), each contribution being associated with a projection of the given quantized torus onto the configuration space. It follows (when the action $S(\boldsymbol{q}, \boldsymbol{I})$ is locally Taylor expanded) that the semiclassical eigenfunction of an integrable system locally is a superposition of a finite number of plane waves, which is the origin of the ordered structure. There are as many contributing plane waves as there are projection leaves of the corresponding torus.

This picture is changed in an ergodic system in so far that now any conceivable

*) A "quasi-periodic" function is a special "almost-periodic" function in that, when Fourier decomposed, only a finite number of linear-independent frequencies arise.

nonisolating integral of motion has infinitely many projection leaves. In other words in almost every point in the configuration space of an ergodic system there are infinitely many possible velocity directions for classical trajectories passing through that point. The correspondence principle then suggests that in the semiclassical limit the eigenfunctions can be *locally* represented as a superposition of infinitely many plane waves propagating along the rays—the classical trajectories. If their phases are random (Berry's assumption[117]) then one has a random superposition of infinitely many plane waves, giving rise to a Gaussian random function by the central limit theorem.

However, Robnik[118] has argued that Berry's random phase hypothesis breaks down on dynamical grounds, a result of the analysis of the quantum integrability and of its consequences. He has demonstrated, using the arguments from the perturbation theory, that "almost every quantum Hamilton system with purely discrete spectrum is quantum integrable, but its quantum integrals of motion generically do not have a classical limit when $\hbar \to 0$". Further, as a consequence of the quantum integrability at any non-zero $\hbar$ there would be correlation between the phases on dynamical grounds. Such correlations would give rise to deviations from the Gaussian randomness of the eigenfunctions of the classically ergodic (and nevertheless quantum integrable) systems.

The early numerical evidence by McDonalds and Kaufman[119] seemed to agree with the property of Gaussian randomness. But then came the important discovery by Heller[43] of the scars (of the classically periodic orbits) in the eigenfunctions of the stadium. It became clear that scars exist in the eigenfunctions of arbitrarily highly-ing states, although the counting measure of scarred states might vanish with increasing energy in consistency with the results of Shnirelman[120] (see Fig. V-8). By a scar we mean a region of enhanced probability density in the neighbourhood of a classical periodic orbit. Heller[42] has elaborated on a theory of scars based on the consideration of wave packet dynamics propagating along the classical periodic orbit, and obtained the following result for the probability density on the scar in the phase space,

$$\frac{|\psi|^2_{\mathrm{SCAR}}}{\langle|\psi|^2\rangle} = \frac{2\pi}{\lambda\tau}, \tag{V·24}$$

where $\langle|\psi|^2\rangle$ is the microcanonical mean probability density, λ is the instability exponent (Liapunov exponent) and τ is the period of the orbit. Thus the shorter and the less unstable the periodic orbit, the more pronounced is its scar.

A similar result has very recently been derived also by Robnik[118] in a different theory based on the semiclassical calculation of the Green function in terms of classical periodic orbits. For two degrees of freedom the result is (in configuration space)

$$\frac{|\psi|^2_{\mathrm{SCAR}}}{\langle|\psi|^2\rangle} = \nu \sum_{n=1}^{\infty} \frac{\sin\frac{nS_1}{\hbar}}{\sinh\frac{n\lambda\tau}{2}}, \tag{V·25}$$

Table V-2. Orbital frequencies and Liapunov exponents of the periodic orbits I_ν at energy $\varepsilon=0$.

ν	$\omega_{\mathrm{orb}}/\omega_c$	$\lambda\tau_c/\pi$	$\lambda\tau_{\mathrm{orb}}$
1	1.50	0.63	1.32
2	0.64	0.59	2.90
3	0.39	0.46	3.70
4	0.28	0.38	4.26
5	0.22	0.32	4.57
6	0.18	0.27	4.71

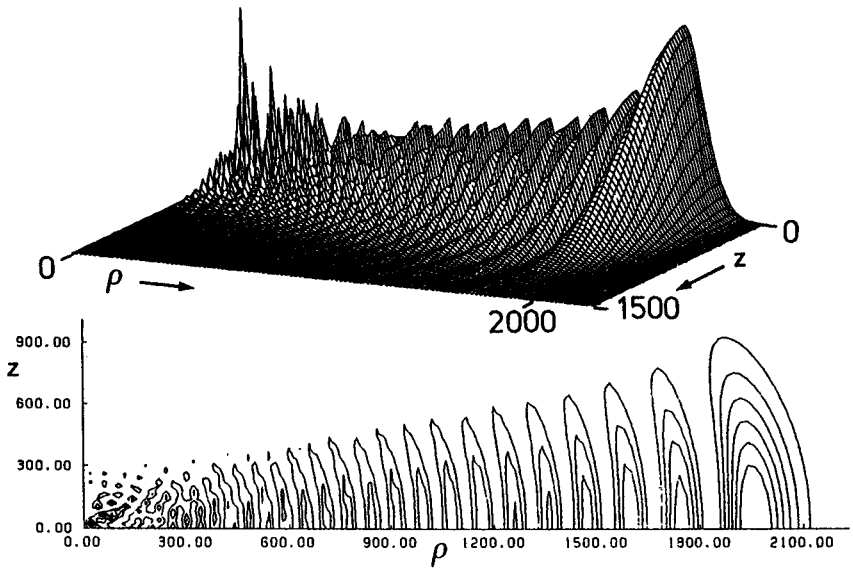

Fig. V-9. 3d-plot and contour plot of $\rho\psi^*\psi$ of the state that can diabatically be traced back to the state $n=36$, $K=0$ in the low-B limit at a magnetic field strength of $B=5.96$ Tesla ($E\sim-32\,\mathrm{cm}^{-1}$). Length scales are in Bohr radii. Evidently the wavefunction of this strate is strongly concentrated along the periodic orbit that runs perpendicular to the direction of the magnetic field, which is still stable at this energy.

where S_1 is the classical (Maupertuis) action of the underlying periodic orbit, and ν is the effective number of contributing orbits. It is now clear that the quantization condition for the classical action of the scar orbit

$$S_1=\left(2m+\frac{1}{2}\right)\pi\hbar\,,\qquad m=0,\,1,\,2,\cdots \tag{V·26}$$

is important especially at very small values of $\lambda\tau$, because a departure from the quantization condition would result in a certain averaging away of the terms contributing to the sum (V·25).

With the numerical wavefunctions of the hydrogen atom in strong magnetic fields at hand it is an obvious task to also take a look at their spatial structure. A motivation is of course the theory of scars discussed above. At small $\lambda\tau$ the intensity ratio for a scar that must satisfy the quantization condition (V·26) is according to (V·25) reduced to

$$\frac{|\psi|^2_{\mathrm{SCAR}}}{\langle|\psi|^2\rangle}=\frac{\pi\nu}{2\lambda\tau}\,,\qquad \lambda\tau\ll 1\,. \tag{V·27}$$

This result is in agreement with the original scaling by Heller as given by (V·24), when projected onto the configuration space. (His result is the average of the intensity ratio, due to the assumption of the uniform scar intensities over an energy range.) For details see Ref.118)

In Table V-2 we present explicit sample results for the size of Liapunov exponents of the first 6 periodic orbits of the series I_ν (characterized by their orbital

frequency) at $E=0$. Surprisingly the orbit running in the plane perpendicular to the direction of the field is found to be most unstable at this energy, while the degree of instability decreases as one goes up the series. On the other hand, the "discrepancy per period", $\lambda\tau$, is seen to be smallest for the planar orbit and to increase for the longer-periodic orbits. Thus if scarring occurs in these states around $E=0$, one would expect that the orbit running in the plane perpendicular to the direction of the magnetic field (which is associated with the quasi-Landau resonance of $\sim 1.5\omega_c$ around $E=0$) should most prominently scar the wavefunctions, while the scarring should become less pronounced for the longer-periodic orbits.

Wavefunctions around $E=0$ in this problem have not yet been fully analyzed with respect to the presence or absence of scars, but we can present results of our analyses of wavefunctions below this limit. Figure V-9 shows the wavefunction of the state which can diabatically be traced back to the state $n=36$, $K=0$ in the low-B limit at a magnetic field strength of 5.96 Tesla (the energy of the state at this field strength is $E\sim -32\,\mathrm{cm}^{-1}$, corresponding to a scaled energy of $\varepsilon\sim -0.15$, and thus lies in the near-irregular regime, cf. Fig. III-8). This state can be associated with the periodic orbit in the plane perpendicular to the direction of the magnetic field, although the neigbourhood of the classical orbit also contributes to the wavefunction of course. Even though most of classical phase space has become irregular at this energy, the Liapunov exponent of the planar orbit is still found to vanish (stable orbit), and hence the very pronounced concentration of the wavefunction along the classical periodic orbit is the expected correspondence familiar from situations where WKB (or EBK) quantization is still applicable. In the light of scar theory this correspondence can be considered the limiting ($\lambda\to 0$) case of scarring. Figure V-10 gives an example of a wavefunction in the completely irregular regime ($E\sim -15\,\mathrm{cm}^{-1}$). The contour plot shows vague indications of enhanced probability of presence along both the planar orbit and the first nonplanar orbit, which are both found to be *unstable* at this energy. Obviously the instability has grown so large as to wash out the precise tracks of the periodic orbits over a extended fraction of space in the wavefunction.

We have also represented *pictorially* hydrogen atoms in strong magnetic fields using the graphics display media available today. The starting point is of course the quantum mechanical interpretation of the squared modulus of the wavefunction as the spatial probability of presence of the electron. Imagining the equivalence of this scalar field to an optically thin self-radiating gaseous nebula, that is, assuming that the scalar field emits "light" with an intensity proportional to the local numerical value of the scalar field, and which propagates without absorption, the intensity a distant observer receives from such an object out of a specific direction is simply the integral along the line-of-sight of the intensities emitted towards the observer. By scanning the whole object with the line-of-sight moving across it in a fine grid, a raster image can be computed which is a good approximation to what the observer actually sees. The raster image is mapped onto the bit planes of a raster graphics display using an intensity or a colour-coding scheme to yield a true picture of the self-radiating object. In our computations we employed a raster of 575×575 lines-of-sight and 256 intensity levels.

In Fig. V-11 we present first examples of pictures of hydrogen Rydberg states with

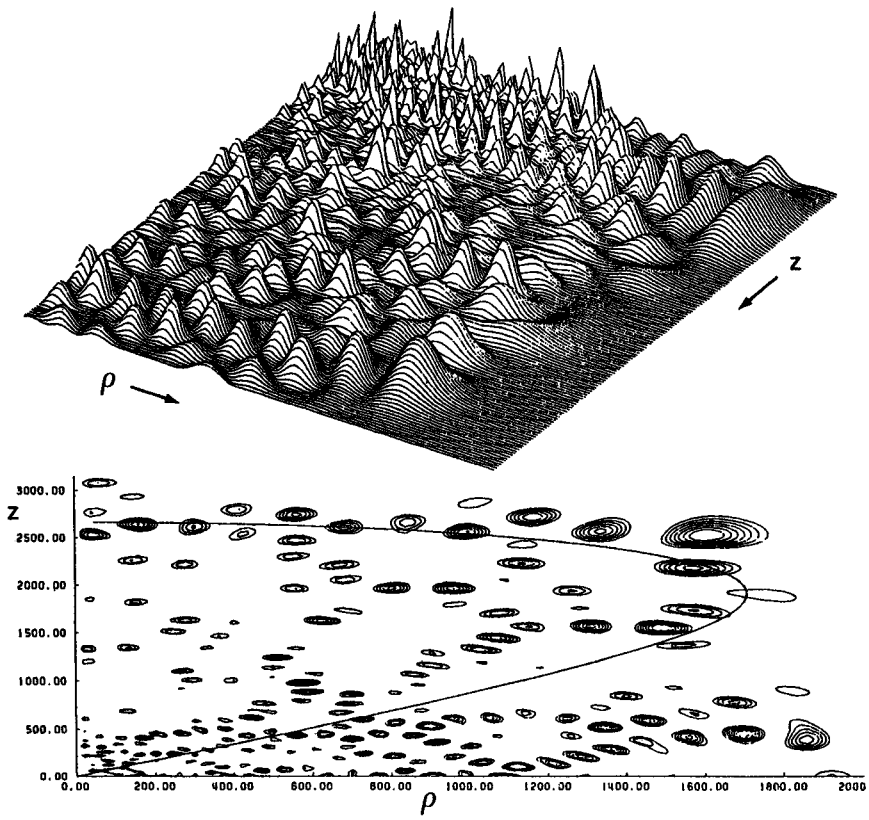

Fig. V-10. Same as Fig. V-9 for a state in the completely irregular regime (B=5.96 Tesla, $E\sim-15$ cm^{-1}). The contour plot reveals vague scars caused by both the planar and the first nonplanar periodic orbit (solid curve), which are unstable at this energy.

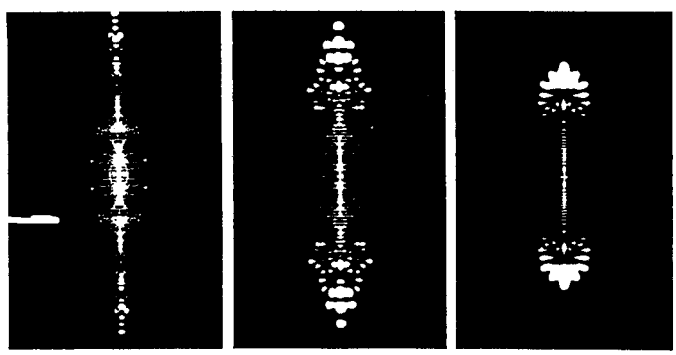

Fig. V-11. Pictures of the probabilities of presence of the electron in different highly excited $m=0$ states, with energies in the classically chaotic regime, of the hydrogen atom in a magnetic field of 5.96 Tesla. The spatial extent of the bizarre atomic structures shown is on the order of 10^{-3} mm.

$m=0$ in a magnetic field of 5.96 Tesla. The energies of the states lie in the range between -30 and -10 cm^{-1}, and thus in the classically chaotic regime. The pictures demonstrate that the atoms have become extended objects along the direction of the magnetic field (linear dimensions $\sim$10000 Bohr radii), and are more or less delocal-

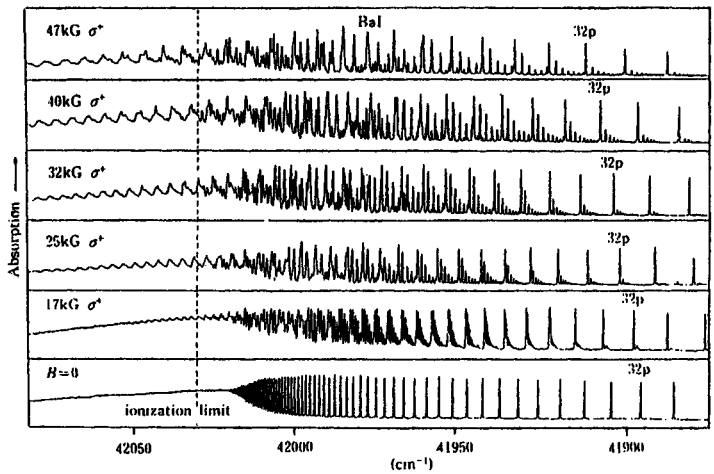

Fig. V-12. Magnetic field dependence of the absorption spectrum of the barium atom near the first ionization threshold reported in 1978 (after Lu, Tomkins and Garton[7a]).

ized, in the sense that they fill most of the configuration space available on account of the remaining conservation laws. Patterns in the shape of the atoms are caused by the nodal structures of the wavefunctions. We have not yet analyzed the pictures with respect to the presence or absence of "scars" along classical periodic orbits, but evidently an analysis of this type is an obvious application of the optical visualization of the states.

Figure V-11 demonstrates that hydrogen atoms in strong magnetic fields contain, in addition to both chaos and order, a high element of beauty.

V.5. *Concluding remarks*

We may emphasize that the hydrogen atom in a strong magnetic field is an elementary and generic system exhibiting all the important features of the *stationary problem* in quantum chaos. Since it is not an artificial model but a real system, having applications in astrophysics (strongly magnetic white dwarfs) and being studied in laboratory spectroscopic experiments, we can regard it as a paradigm of quantum chaos, especially, as it is so fundamental. This is well demonstrated by the number of profound results reported in the past two or three years,[48] and thus confirms the predictions and the line of thoughts proposed in 1982.[2] Among the results the most striking are the rôle of unstable periodic orbits in the resonance spectra and the statistical aspects of the energy levels in classically regular vs chaotic regimes. Actually, these two aspects are the very questions in quantum chaos which are apparently interfering with each other. Thus, in concluding the present review, we wish to remark on the issue for clarifying the questions in a unified context of quantum chaos.

5.1. A brief survey on the understanding of the quasi-Landau resonances

The first theoretical attempt to understand the discovery of Garton and Tomkins[7] (see Fig. V-12) was the semiclassical quantization of the planar orbits by

Edmonds[8] and followed by Starace[58] (its explicit demonstration), Rau[58a] (an intuitive model in terms of "strong-field mixing"), Feneuille[55] (the adiabatic hypothesis of the orbit which results in the possible scaling law) and Hasegawa et al.[54] (establishing the scaling law). The question of why and how such a two-dimensional model could give stable quantum eigenstates was raised and investigated first by Fano[121] who discussed the problem in terms of the concept of *standing-wave formation on the potential ridge* (the diamagnetic binding superimposed upon the Coulomb attraction results in a "ridge" of the potential down to the magnetic field direction). This was apparently the first motivation to investigate the problem from the stability viewpoint and stimulated Clark and Taylor's numerical work[14] to test the idea.

Fano's question of the standing-wave formation can be regarded as solved at least for the regular regime, i.e., the regime of no inter-n-mixing, where the well-defined KAM tori yield the exact EBK (torus) quantization with the uppermost quantized level that provides the answer. What should be explored as remaining unsolved is that such a formation of the standing wave holds even in the classical full-chaos regime, and moreover, the formation is not restricted to such a series of the planar orbits but extends, though less prominently, to systematic groups of non-planar orbits.

It has now been recognized that those periodic orbits with the simpler structure and the shorter period play the more decisive rôle in the quasi-Landau resonance phenomena as predicted from the theory of scars. Surely,[46] if the scars of classically periodic orbits exist in the bound state eigenfunctions of classically ergodic Hamilton system, and if their structure is correlated over a sufficiently large number of states, then firstly, their existence implies clustering of the energy levels, and secondly, for an appropriate polarization of the photons the dipole matrix elements are enhanced so that the modulations show up in the photoabsorption cross section: This is the quasi-Landau resonances below the ionization threshold. However, our understanding in this context is still in a qualitative stage waiting for a more precise analysis. Its importance cannot be stressed too much in view of the exponentially growing number of the periodic trajectories contributing to the semiclassical quantization in the full-chaos regime.

To date, the most elaborate theoretical work on the quasi-Landau resonances reported has been the series of papers by Delos and his colleague,[126] who examined some sixty periodic orbits of the recurrent type (in the sense of § V.3) which may contribute to the Green's function formula of the optical spectra, i.e., the linear response formula (V·6). Being unable to go into details, we here make two possible comments: (1) These authors do not refer to the concept of scars, and therefore it would be highly desirable to examine these orbits with respect to their stability index (i.e., the Liapunov exponent) to see the relative importance. (2) They introduce a special averaging procedure of the Green's function to cut the time scale by a maximum period, or, to restrict the frequency by a *minimum resolution* (of the exciting laser frequency). This seems to ensure the stability of their calculation of the spectra, which should be enlightened from the fundamental aspect of "quantum chaos" whose controversial point will be discussed to an extent.

We note that very recently the photoabsorption cross section for the quasi-Landau resonances has been calculated semiclassically in terms of classical periodic

orbits by Bogomolny.[126a)]

5.2. The dynamic vs stationary dual aspect of the optical spectra

We have so far been retaining the standpoint that the diamagnetic Kepler system is the paradigm of quantum chaos in the stationary aspect. There exists another aspect of the quantum-chaos disciplines, i.e., the *dynamical aspect*, its present status being seemingly not transparent. We argue here that the optical spectra —specifically, the ones involving the quasi-Landau resonances—cannot be free from such a dynamical aspect. This is because the optical absorption belongs typically to those irreversible phenomena for which the applicability of the linear-response formula depends crucially on the decay property of the autocorrelation function $\Phi(t)=\langle\mu(0)\mu(t)\rangle$: If the time evolution of the dipole, $\mu(t)$, is either according to an integrable classical Hamilton dynamics or to the Heisenberg motion with a Hamiltonian of a discrete spectrum (a bounded system), then $\Phi(t)$ must be an almost-periodic function which never exhibits an asymptotic decay behaviour.

The question about a possible 'imitation' of a classical-chaos dynamics by its bounded quantum analogue in a finite transient period was initiated by studies of the kicked rotator model by Casati et al.[127)] (see a review by Chirikov et al.[128)]) and expounded by a number of investigators (see a recent review by Toda et al.[129)]). Two characteristic times of scaling are accepted to exist, i.e. the random time T_r (the quantum dynamics simulates the classical one for $t<T_r$) and the discrete time T_d (it attains the stationarity of almost periodicity for $t>T_d$), the latter being identified with the 'break time' mentioned in § II.2. We will not inquire further their true meanings, but we wish to point out that the optical spectra of the diamagnetic hydrogen atom in the classical full chaos apparently acquire both the characteristics.

On the one hand, the quantum mechanical autocorrelation function $\Phi_{\rm qm}(t)$ (for which the average bracket means $\langle 0|\ |0\rangle$) should exhibit a typical oscillation reflecting the recurrence in the sense of Reinhardt :[110)] If it were computed according to the classical-chaos dynamics, the classical $\Phi_{\rm cl}(t)$ (for which $\langle\ \rangle$ means the average over the classical density) would never show the recurrence without decay.

On the other hand, the $\Phi_{\rm qm}(t)$ is also expected to possess an asymptotic decay whose mathematical description should be sought in a kind of the *mixing* of the underlying quantum dynamics. This is because, otherwise, the beautiful correspondence between the classical chaos and the GOE statistics elucidated actually in our system must be impossible (recall an extended study of the kicked rotator where the quantum integrable regime—*in a variation of the Planck constant*—actually leads to the Poisson statistics[130)]). We expect that the precise correspondence between the classical chaos and the GOE statistics verified in a number of examples would be a manifestation of the *potential mixing* proposed by Adachi et al.[131)] This would yield a promising possibility of combining the dynamical and statistical aspects of the theory of small quantum systems[132)] by the name of quantum chaos.

Acknowledgements

H. H. thanks E. Luc-Koenig and M. Kuwata for providing him with a number of

clarifying points. G. W. is grateful to his coworkers who have been instrumental in obtaining part of the results presented in this work, in particular to G. Zeller, W. Schweizer, R. Niemeier, and to H. Ruder and H. Friedrich. His part of this work was supported by the Deutsche Forschungsgemeinchaft. H. H. and M. R. acknowledge the financial support in part by the National Science Foundation under Grant No. PHY82-17853, supplemented by funds from the National Aeronautics and Space Administration.

We thank Mrs. Irmgard Stumpf and Miss Julia Wunner for their help in typing and editing the manuscript.

References

1) A. R. Edmonds and R. A. Pullen, Preprint Imperial College (1980) (unpublished).
2) M. Robnik, J. Phys. Colloque C2, **43** (1982), 45.
2 a) M. Robnik, J. of Phys. **A14** (1981), 3195.
3) W. P. Reinhardt and D. Farrelly, J. Phys. Colloque C2, **43** (1982), 29.
4) A. Harada and H. Hasegawa, J. of Phys. **A16** (1983), L259.
5) M. Hénon and C. Heiles, Astron. J. **69** (1964), 73.
6) A. J. Lichtenberg and M. A. Lieberman, *Regular and Stochastic Motion* (Springer-Verlag, New York, Heidelberg, Berlin, 1983).
7) W. R. S. Garton and F. S. Tomkins, Astrophys. J. **158** (1969), 839.
7 a) K. T. Lu, F. S. Tomkins and W. R. S. Garton, Proc. R. Soc. London **362** (1978), 421.
8) A. R. Edmonds, J. Phys. Colloque C4, **31** (1970), 71.
9) H. Hasegawa, in *Physics of Solids in Intense Magnetic Fields,* ed. E. D. Heidemenakis (Plenum, 1969), Chapter 10.
10) D. Kleppner, M. C. Littman and M. L. Zimmerman, in *Rydberg States of Atoms and Molecules,* ed. R. F. Stebbings and F. B. Dunning (Cambridge University Press, 1983).
11) J. C. Gay, in *Photophysics and Photochemistry in the Vacuum Ultraviolet,* ed. S. P. McGlynn, G. L. Findley and R. H. Huebner (Reidel Dordrecht, 1985).
12) E. A. Solov'ev, Sov. Phys. -JETP Lett. **34** (1981), 265 ; **55** (1982), 1017.
13) M. Robnik, J. of Phys. **A17** (1984), 109.
14) C. W. Clark and K. T. Taylor, J. of Phys. **B13** (1980), L737 ; **15** (1982), 1175.
14 a) C. W. Clark and K. T. Taylor, J. Phys. Colloque C2, **43** (1982), 127.
15) A. R. Edmonds, J. of Phys. **B6** (1973), 1603.
16) G. Wunner and H. Ruder, Physica Scripta **36** (1987), 291.
G. Wunner, W. Schweizer and H. Ruder, Book of Invited Papers : *The Hydrogen Atom Symposium,* Pisa, Italy (Springer Verlag, 1988).
17) G. Wunner, W. Rösner, H. Herold and H. Ruder, Astron. Astrophys. **149** (1985), 102.
18) A. Holle, G. Wiebusch, J. Main, B. Hager, H. Rottke and K. H. Welge, Phys. Rev. Lett. **56** (1986), 2594.
19) O. Bohigas and M. -J. Giannoni, Lecture Notes in Physics **209** (1984), 1.
20) F. Rannou, Astron. Astrophys. **31** (1974), 289.
20 a) M. Hénon, in *Chaotic Behaviour of Deterministic Systems, Proc. of the Les Houches Summer School,* ed. G. Iooss, R. H. G. Helleman and R. Stora (North-Holland, Amsterdam, 1983).
21) J. Guckenheimer, Lecture in Applied Mathematics **17** (1979), 187.
22) M. Robnik, "Vorlesungen über das klassische Chaos und das Quantenchaos," Preprint Heidelberg MPIfK ; (in German), (1988) ; the English version is to appear.
23) F. Gustavson, Astron. J. **21** (1966), 670.
24) M. V. Berry, Ann. of Phys. **131** (1981), 163; also, Review in *Chaotic Behaviour of Deterministic Systems,* ed. G. Iooss, R. H. G. Helleman and R. Stora (North-Holland, Amsterdam, 1983).
25) M. Robnik, in *Photophysics and Photochemistry in the Vacuum Ultraviolet,* ed. S. P. McGlynn, G. L. Findley and R. H. Huebner (Reided, Dordrecht, 1985).

26) G. Casati, B. V. Chirikov, D. L. Shepelyansky and I. Guarneri, Phys. Rep. **154** (1981), 77.
27) O. Bohigas and H. A. Weidemüller, *Aspects of Chaos in Nuclear Physics,* Ann. Rev. Nucl. Part. Sci. **38** (1988), 421.
28) O. Bohigas, M. J. Giannoni and C. Schmit, Phys. Rev. Lett. **52** (1984), 1.
29) F. J. Dyson, J. Math. Phys. **3** (1962), 140.
29 a) F. J. Dyson, J. Math. Phys. **3** (1962), 1191.
30) P. Pechukas, Phys. Rev. Lett. **51** (1983), 943.
31) T. Yukawa, Phys. Rev. Lett. **54** (1985), 1883; Phys Lett. **116** (1986), 227.
32) M Wilkinson, J. of Phys. **A21** (1988), 1173.
33) M. Robnik, Lecture Notes in Physics **263** (1986), 120.
34) T. U. Seligman and J. J. M. Verbaarschot, Phys. Lett. **108A** (1985), 183.
35) M. V. Berry and M. Robnik, J. of Phys **A19** (1986), 649.
36) M. Robnik, J. of Phys. **A17** (1984), 1049.
37) M. V. Berry and M. Robnik, J. of Phys. **A17** (1984), 2413.
38) T. H. Seligman, J. J. M. Verbaarschot and M. R. Zirnbauer, Phys. Rev. Lett. **53** (1984), 215.
39) T. H. Seligman, J. J. M. Verbaarschot and M. R. Zirnbauer, J. of Phys. **A18** (1985), 2751.
40) M. Robnik, J. of Phys. **A20** (1987), L495.
41) D. Wintgen and H. Friedrich, Phys. Rev. **A35** (1987), 1464.
42) H. Hasegawa, H. J. Mikeska and H. Frahm, Phys. Rev. **A38** (1988), 395.
43) E. J. Heller, Phys. Rev. Lett. **53** (1984), 1515.
44) E. J. Heller, P. O'Connor and J. Gehlen, Phys. Rev. Lett. **58** (1987), 1296.
45) E. J. Heller, Lecture Notes in Physics **263** (1986), 162.
46) M. Robnik, in *Proceedings of the Conference "Atomic Spectra and Collisions in External Fields", Egham, Surrey, England, 1987,* ed. by K. T. Taylor, M. H. Nayfeh and C. W. Clark to appear in *the Series Physics of Atoms and Molecules* (Plenum, 1988).
47) M. Robnik, J. of Phys. **A19** (1986), L841.
48) K. T. Taylor, *Proceedings of the Conference "Atomic Spectra and Collisions in External Fields", Egham, Surrey, 1987* ; in *the Series Physics of Atoms and Molecules* (Plenum, 1989).
49) V. I. Arnold, *Mathematical Methods of Classical Mechanics* (Springer, New York, 1978).
50) A. Einstein, Verh. Deutsch. Phys. Ges. Berlin **19** (1917), 82.
51) V. P. Maslov and M. V. Fedoryuk, *Quasiclassical Approximation for the Equations of Quantum Mechanics* (Nauka, Moscow, 1976) (in Russian) [English translation (Reidel Dondrecht, 1981)].
52) M. Robnik and E. Schrüfer, J. of Phys. **A18** (1985), L853.
53) R. Gajewski, Physica **47** (1970), 575.
54) H. Hasegawa, S. Adachi and A. Harada, J. of Phys. **A16** (1983), L503.
55) S. Feneuille, Phys. Rev. **A26** (1982), 673.
56) G. L. Surmelian and R. F. O'Connell, Astrophys. J. **190** (1974), 741.
57) G. Wunner and H. Ruder, J. Phys. Colloque C2, **43** (1982), 137.
58) A. F. Starace, J. of Phys. **B6** (1973), 585.
58 a) A. R. P. Rau, Phys. Rev. **A16** (1977), 613.
59) J. A. C. Gallas and R. F. O'Connell, J. of Phys. **B15** (1982), L75, L593.
60) J. C. Gay, D. Delande and F. Biraben, J. of Phys. **B13** (1980), L729.
60 a) D. Delande, C. Chardonnet, F. Biraben and J. C. Gay, J. Phys. Colloque C2, **43** (1982), 97.
61) J. Main, A. Holle, G. Wiebusch and K. H. Welge, Z. Phys. **D6** (1987), 295.
62) W. P. Reinhardt and D. Farrelly, J. Phys. Colloque C2, **43** (1982), 29.
M. A. Al-Laithy and C. M. Farmer, J. of Phys. **B20** (1987), L747.
63) M. L. Zimmerman, M. M. Kash and D. Kleppner, Phys. Rev. Lett. **45** (1980), 1092.
C. W. Clark and K. T. Taylor, J. of Phys. **B13** (1980), 1737.
C. W. Clark, Phys. Rev. **A24** (1981), 605.
M. Robnik, J. of Phys. **A14** (1981), 3195.
64) H. Hasegawa, in *Fundamental Aspects of Quantum Theory,* ed. V. Gorini and A. Frigerio (Plenum, 1986), p. 193.
65) H. Hasegawa, A. Harada and Y. Okazaki, J. of Phys. **A17** (1984), L883.

66) H. Hasegawa and S. Adachi, J. Phys. Soc. Jpn. **57** (1988), 80.
67) M. Kuwata, A. Harada and H. Hasegawa, J. of Phys. **A**, submitted (1989).
68) E. G. Kalnins, J. W. Miller and P. Winternitz, SIAM J. App. Math. **30** (1976), 630.
69) M. Lakshmanan and H. Hasegawa, J. of Phys. **A17** (1984), L889; cf. Ref. 12) and D. R. Herrick, Phys. Rev. **A26** (1982), 323.
70) J. Main, G. Wiebusch, A. Holle and K. H. Welge, Phys. Rev. Lett. **57** (1986), 2789.
71) D. Wintgen, Phys. Rev. Lett. **58** (1987), 1589.
72) J. B. Delos, S. K. Knudson and D. W. Noid, Phys. Rev. **A30** (1984), 1208.
73) W. Schweizer, R. Niemeier, H. Friedrich, G. Wunner and H. Ruder, Phys. Rev. **A38** (1988), 1724.
74) D. Wintgen and H. Friedrich, Phys. Rev. **A36** (1987), 131.
75) M. L. Du and J. B. Delos, Phys. Rev. Lett. **58** (1987), 1731.
76) V. I. Oseledec, Trans. Moscow Math. Soc. **19** (1969), 197.
77) H. D. Meyer, J. Chem. Phys. **84** (1968), 3147.
78) R. A. Horn and C. A. Johnson, *Matrix Analysis* (Cambridge University Press, Cambridge U. K., 1985).
79) M. Yu. Sumetskii, Sov. Phys. -JETP **56** (1982), 959.
80) D. Wintgen, J. of Phys. **B20** (1987), L511.
81) G. Benettin, L. Galgani and J.-M. Strelcyn, Phys. Rev. **A14** (1976), 2338.
82) G. Benettin and J. -M. Strelcyn, Phys. Rev. **A17** (1978), 773.
83) G. Benettin, Physica **13D** (1984), 211.
84) For an earlier development, see *Statistiscal Theories of Spectra*: *Fluctuations,* ed. C. E. Porter (A cademic Press, New York, 1965).
85) D. Wintgen and H. Friedrich, Phys. Rev. Lett. **57** (1986), 571.
86) D. Delande and J. C. Gay, Phys. Rev. Lett. **57** (1986), 2006.
87) G. Wunner, U. Woelk, I. Zech, G. Zeller, T. Ertl, F. Geyer, W. Schweizer and H. Ruder, Phys. Rev. Lett. **57** (1986), 3261.
88) M. L. Mehta and J. des Cloizeaux, Ind. J. Pure App. Math. **3** (1972), 329.
89) R. Kubo, M. Toda and N.Hashitsume, *Statistical Physics II* (Springer-Verlag, Berlin, Heidelberg, New York, Tokyo, 1985), p. 1.
90) K. Itô and S. Watanabe, *"Introduction to Stochastic Differential Equations", Proc. Intern. Symp. SDE Kyoto, 1976,* ed. K Itô (Kinokuniya, Tokyo, 1978).
91) H. Hasegawa and H. Ezawa, Prog. Theor. Phys. Suppl. No. 69 (1980), 41.
92) M. V. Berry and M. Tabor, Proc. R. Soc. London **A356** (1977), 375.
93) K. Nakamura and M. Lakshmanan, Phys. Rev. Lett. **57** (1986), 1661.
94) H. Hasegawa, in *Proceedings of the Conference "Atomic Spectra and Collisions in External Fields", Egham, Surrey, England, 1987,* ed. by K. T. Taylor, M. H. Nayfeh and C. W. Clark in *the Series Physics of Atoms and Molecules* (Plenum, 1988).
95) H. Hasegawa, *"Complete Integrability and Stochastization of Yukawa's Equation for Quantum Chaos" Proceedings of Nonlinear Evolution Equations, 1988 Como workshop,* ed. A Fordy (Manchester University Press).
96) M. J. Englefield, *Group Theory and the Coulomb Problem* (Wiley, New York, 1971).
97) H. Friedrich and M. Chu, Phys. Rev. **A28** (1983), 1423.
98) W. Rösner, G. Wunner, H. Herold and H. Ruder, J. of Phys. **B17** (1984), 29.
99) D. Delande and J. C. Gay, J. of Phys. **B16** (1984), L335; **19** (1987), L173.
100) D. Wintgen and H. Friedrich, J. of Phys. **B19** (1986), L99, 991; Phys. Rev. Lett. **57** (1986), 571.
101) T. A. Brody, Lett. Nuovo Cim. **7** (1973), 482.
102) Y. Alhassid and R. D. Levine, Phys. Rev. Lett. **57** (1986), 2879.
103) P. Cacciani, E. Luc-Koenig, J. Pinard, C. Thomas and S. Liberman, Phys. Rev. Lett. **56** (1986), 1124; J. of Phys. **B19** (1986), L519.
104) P. Cacciani, S. Liberman, E. Luc-Koenig, J. Pinard and C. Thomas, J. of Phys. **B21** (1988), 3473. Also, a private communication from E. Luc-Koenig.
105) I. C. Percival, Adv. Chem. Phys. **36** (1977), 1.
106) J. B. Delos, S. K. Knudson and D. W. Noid, Phys. Rev. **A28** (1983), 7; **30** (1984), 1208. J. B. Delos, R. L. Waterland and M. L. Du, Phys. Rev. **A37** (1988), 1185.

107) R. L. Waterland, J. B. Delos and M. L. Du, Phys. Rev. **A35** (1987), 5064.
108) Ref. 104).
P. A. Braun, Sov. Phys. -JETP **57** (1983), 492.
E. A. Solov'ev, private communication.
109) J. Neukammer, H. Rinneberg, K. Vietzke, A. König, H. Hieronymus, M. Kohl, H. J. Grabka and G. Wunner, Phys. Rev. Lett. **59** (1987), 2947.
110) W. P. Reinhardt, J. of Phys. **B16** (1983), L635.
111) M. A. Al-Laithy, R. F. O'Mahony and K. T. Taylor, J. of Phys **B19** (1986), L773.
112) M. A. Al-Laithy and C. M. Farmer, J. of Phys. **B20** (1987), L747.
113) J. M. Green, J. Math. Phys. **9** (1968), 760.
114) H. Hasegawa, M. Kuwata and P. Davis, presented at 1987 Meeting Kyoto (M. Kuwata master thesis 1989).
115) A. Holle, G. Wiebusch, H. Rottke and K. H. Welge, Phys. Rev. Lett. **61** (1988), 161.
116) A. Voros, Lecture Notes in Physics **93** (1979), 326.
117) M. V. Berry, J. of Phys. **A12** (1977), 2083.
118) M. Robnik, submitted to Phys. Rev. Lett.
119) S. W. McDonald and A. N. Kaufman, Phys. Rev. Lett. **42** (1979), 1189.
120) A. L. Shnirelman, Uspekhi Matem. Nauk **29** (1979), 181.
121) R. S. MacKay, J. D. Meiss and I. C. Percival, Physica **D13** (1984), 55.
122) M. Robnik, (1985) unpublished.
123) J. J. Burnett, Project Work H. H. Wills Physics Laboratory (Bristol University, 1986).
124) M. Robnik, J. of Phys. **A16** (1983), 3971.
A. Hayli, T. Dumont, J. Moulin-Ollagier and J.-M. Strelcyn, J. of Phys. **A20** (1987), 3237.
125) U. Fano, Phys. Rev. **A22** (1980), 2660.
126) J. B. Delos and M. L. Du, IEEE J. Quant. El. **24** (1988), 1445.
M. L. Du and J. B. Delos, Phys. Rev. **A38** (1988), 1986, 1913.
126 a) E. G. Bogomolny, JETP Lett. **47** (1988), 527; JETP (1989), submitted.
127) G. Casati, B. V. Chirikov, F. M. Izrailev and J. Ford, Lecture Notes in Physics **93** (1979), 334.
128) B. V. Chirikov, F. M. Izrailev and D. L. Shepelyansky, Sov. Sci. Rev. Sec. **C2** (1981), 209.
129) M. Toda, S. Adachi and K. Ikeda, this issue, p. 323.
130) H. Frahm and M. J. Mikeska, Phys. Rev. Lett. **60** (1988), 3.
131) S. Adachi, M. Toda and K. Ikeda, Phys. Rev. Lett. **61** (1988), 655.
132) B. Eckhardt, Phys. Rep. **163** (1988), 205.